



UNIVERSITÀ DEGLI STUDI DI SALERNO



UNIVERSITÀ DEGLI STUDI DI SALERNO
Dipartimento di Farmacia

Dottorato di ricerca
in Scienze Farmaceutiche
Ciclo XII NS — Anno di discussione 2014

Coordinatore: Chiar.mo Prof. *Gianluca Sbardella*

***IN VITRO AND IN CELL FUNCTIONAL
PROTEOMICS ON NATURAL COMPOUNDS***

settore scientifico disciplinare di afferenza: CHIM/06

Dottorando

Dott. *Chiara Cassiano
Casapullo*

Tutore

Chiar.mo Prof. *Agostino*

Co-tutore

Chiar.mo Prof. *Angela
Zampella*

Chiar.mo Prof.
Alessandra Tosco

Table of Contents

Abstract	I
	Page
Introduction	1-34
Chapter 1 Mass spectrometry-based chemical proteomics: an overview	3
Results and Discussion	35-97
Chapter 2 Chemical Proteomics Reveals Heat Shock Protein 60 as the Main Cellular Target of the Marine Bioactive Sesterterpene Suvanine.....	37
Chapter 3 Heteronemin, a marine sponge terpenoid, targets TDP-43, a key factor in several neurodegenerative disorders.....	56
Chapter 4 In cell chemical proteomics by copper-catalyzed Huisgen 1,3 dipolar cycloaddition.....	71
Chapter 5 New insights in the cCMP interaction profile by chemical proteomics.....	93
Conclusions	103-108
Chapter 6 Conclusions.....	105
Experimental Section	109-141

Table of Contents

Chapter 7 In vitro and in cell chemical proteomics on marine compounds target discovery : Experimental procedures.....	111
Chapter 8 New insights in cCMP interaction profile by chemical proteomics: Experimental procedures.....	135
Bibliography	141-156
List of Abbreviations	157-159

Abstract

Chemical proteomics has acquired a pivotal role in chemical biology because of its peculiar capability to deeply analyze the proteome from many points of view. Proteins identification, characterization and quantification provide a detailed portrait of a biological system. In particular, pharmaceutical research is looking with interest at chemical proteomics because the mechanism of action of bioactive molecules remains one of the main challenge^[1]. Particularly, the identification of target proteins and investigation of ligand-receptor interactions are today considered essential steps in the drug discovery and development process. Affinity purification-based mass spectrometry approaches (AP-MS) have emerged as a valuable mean to link bioactive compounds to their cellular targets^[2]. In recent years, the application of such techniques led to successful results in determining the macromolecular partners of many interesting bioactive molecules^[3,4]. These techniques require the chemical modifications of the molecule of interest onto a solid matrix, in order to allow the bioactive compound to “fish out” its specific interactors from a cell lysate or a tissue extract. Once eluted, these cellular targets are identified by MS and bioinformatics analysis^[5,6]. Later on, the biological profile of the selected compound toward its cellular interactors is investigated by *in vitro* and/or *in vivo* assays.

The application of this strategy to the cases of suvanine (SUV)^[7], heteronemin (HET)^[8,9] and scalaradial (SLD)^[10,11] led to the identification of their main cellular targets. The identified interactions were then validated by means of surface plasmon resonance, whereas their biological relevance was established through *in vitro* and *in vivo* assays.

An *in cell fishing for partners* procedure was also developed and applied to the case of SLD and Oleochantal (OLC)^[12].

Abstract

Eventually, a competition variant of the standard AP-MS approach was also performed to analyze the interactome of the endogenous metabolite, 3'-5'-cyclic cytidine monophosphate (cCMP).

HSP60 has been identified as the main biological target of SUV in HeLa cells, and its ability in inhibiting the HSP60 activity was demonstrated *in vitro*, evaluating the reduction of HSP60 mediated refolding of citrate synthase.

HET was found to bind TDP43, a nucleic acid-binding protein involved in some neurodegenerative diseases. A marked effect of HET in lowering the binding affinity between TDP43 and the TAR32 oligonucleotide has been established by alpha screen technology. Moreover, a high tendency of TDP43 to aggregate upon HET treatment was demonstrated *in vitro*, by using recombinant TDP43, and in cell, through western blot and immunofluorescence analyses.

Peroxiredoxin 1 and 14-3-3 ϵ were recognized as main cellular partners of SLD, by applying the described AP-MS approach.

Later on, SLD was chosen as a probe for the development of an *in cell fishing for partners* experiment based on bio-orthogonal chemistry^[13,14]. SLD was first decorated with an azide-containing linker and then a living cell sample was treated with the tagged molecule. The SLD interactors, selected in the cellular environment, were then fished out by promoting an azide-alkyne cycloaddition between the tagged SLD and an acetylenic functionalized matrix. Peroxiredoxin 1 and 14-3-3 ϵ , along with proteasome, were recovered as specific and main SLD partners. The effectiveness of bio-orthogonal chemistry in affinity-based target discovery experiments was further confirmed assessing the ability of Oleocanthal to select HSP90, its already known target^[15].

The cCMP interactome was deeply analyzed by means of AP-MS and competition experiments showing, along with the known partners PKA and

PKG^[16], the heterogeneous nuclear ribonucleoproteins as a new class of potential cCMP effectors.

[1] Ziegler S., Pries V., Hedberg C., Waldmann H., *Angew. Chem. Int. Ed.*, (2013), **52**, 2744-92

[2] Rix U., Superti-Furga G., *Nat. Chem. Biol.*, (2009), **5**, 616-24

[3] Margarucci L., Monti M.C., Tosco A., Riccio R., Casapullo A., *Angew. Chem. Int. Ed.*, (2010), **49**, 3960-63

[4] Margarucci L., Monti M.C., Mencarelli A., Cassiano C., Fiorucci S., Riccio R., Zampella A., Casapullo A., *Mol. BioSyst.*, (2012), **8**, 1412-17

[5] Jeffery D.A., Bogyo M., *Curr. Opin. Biotechnol.*, (2003), **14**, 87-95

[6] Godl K., Grüss O.J., Eickhoff J., Wissing J., Blencke S., Weber M., Degen H., Brehmer D., Örfi L., Horváth Z., Kéri G., Müller S., Cotten M., Ullrich A., Daub H., *Cancer Res.*, (2005), **65**, 6919-25

[7] De Marino S., Festa C., D'Auria M.V., Bourguet-Kondracki M.L., Petek S., Debitus C., Andrs R.M., Terencio M.C., Pay M., Zampella A., *Tetrahedron*, (2009), **65**, 2905-9.

[8] Kamel H.N., Kim Y.B., Rimoldi J.M., Fronczek F.R., Ferreira D., *J Nat Prod.*, (2009), **72**, 1492-6

[9] Schumacher M., Cerella C., Eifes S., Chateauvieux S., Morceau F., Jaspars M., Dicato M., Diederich M., *Biochem. Pharm.*, (2010), **79**, 610-22

[10] Cimino G., De Stefano S., Minale L., *Experientia*, (1974), **30**, 846-7

[11] G. Cimino, S. De Stefano, L. Minale, E. Trivellane, *J Chem Soc Perkin I.*, (1977), 1587-93

[12] Beauchamp G.K., Keast R.S., Morel D., Lin J., Pika J., Han Q., Lee C.H., Smith A.B., Breslin P.A., *Nature*, (2005), **7055**, 45-6

[13] Vila A., Tallman K.A., Jacobs A.T., Liebler D.C., Porter N.A., Marnett L.J., *Chem. Res. Toxicol.*, (2008), **21**, 432-44

Abstract

[14] Prescher J.A., Bertozzi C.R., *Nat. Chem. Biol.*, (2005), **1**, 13-21

[15] Margarucci L., Monti M.C., Cassiano C., Mozzicafreddo M., Angeletti M., Riccio R., Tosco A., Casapullo A., (2013), *Chem. Commun. (Camb.)*, **49**, 5844-46

[16] Hammerschmidt A., Chatterji B., Zeiser J., Schröder A., Genieser H.G., Pich A., Kaefer V., Schwede F., Wolter S, Seifert R., *PLoS One*, (2012), **7**, e39848

INTRODUCTION

-CHAPTER 1-

Mass spectrometry-based chemical proteomics: an overview

1. Introduction

In the post-genomic era, several “omics” sciences have been developed, aiming to depict the bio-functional effectors of genomic-encoded instructions. Particularly, proteomics is emerged as key technique because of its effectiveness in identification, characterization and quantification of proteins^[1,2].

The proteome is characterized by a high complexity because, in addition to the high amount of proteins expressed, is dynamically modulated during the time and by xenobiotics^[3]. Thus, mass-spectrometric based approaches have acquired a pivotal role in the proteomic field because of their peculiar capability to analyse thousands of proteins in a single-large-scale experiment, providing detailed portraits of biological systems^[4].

The growing impact of mass spectrometry in proteomics has driven a very rapid progress in terms of sensitivity, resolution, mass accuracy, and mass spectrometers scan rate^[5,6]. At the same time, new strategies for proteins/peptides separation have been developed to maximize mass spectrometers performance, whereas bio-informatics advances have made the data analysis process simpler and more exhaustive^[7]. Indeed, due to its comprehensiveness and versatility, mass spectrometry-based chemical proteomics is now considered one of the key techniques in many fields of chemical biology^[8]. In particular, pharmaceutical research is looking with interest at chemical proteomics because, even if the knowledge of the molecular mechanism of action is not essential for the discovery of new potential therapeutic agents, the identification of their cellular targets may facilitate the drug development. Moreover, these data are also useful to clarify the pharmacological and toxicological profile of a lead compound in a very early stage of D&D process.

Introduction

Definitely, the simplified concept of *one drug-one target* is currently losing credit, whereas the idea that drugs may simultaneously target several proteins is spreading around, opening the way to new approaches of investigation^[9].

Chemical proteomics is a multi-faced technique that encloses different disciplines such as chemical biology, organic chemistry and biochemistry, useful for the analysis of different aspects of proteins, such as their function, structures, interactions, expression alteration etc. Several chemical proteomic methodologies have been recently developed and, among them, three are considered particularly powerful, mainly in the field of pharmaceutical research: (a) *global proteomics* is useful to weigh the alterations in the proteins expression upon drug treatment, while (b) *compound centric chemical proteomics* (CCCP) matches bioactive compounds with their macromolecular targets, and (c) *activity based protein profiling* (ABPP) is applied to visualize the alteration of enzyme activities after external stimuli. The following chapters will focus on the main experimental aspects and recent developments of the above-mentioned approaches.

1.1 Mass spectrometry in proteomics: outlines

The informations about a protein identity can be retrieved by analysis of the intact macromolecule or its proteolytic peptides (**Figure 1**). The so called “top-down” approach is based on the LC-MSMS analysis of intact proteins^[10,11]. The handling of intact proteins is a crucial point in a MS experiment, first of all because of the solubility in MS friendly (detergent-free) buffers. Besides, the fractionation, ionization and fragmentation efficiency are more complicated in respect to peptides, and for these reasons top down approaches are not yet largely employed.

Peptide analysis, in the “bottom up” approach, is actually more feasible and, therefore, a huge number of experimental workflows have been introduced to maximize the information accessible from a single large-scale experiment^[12].

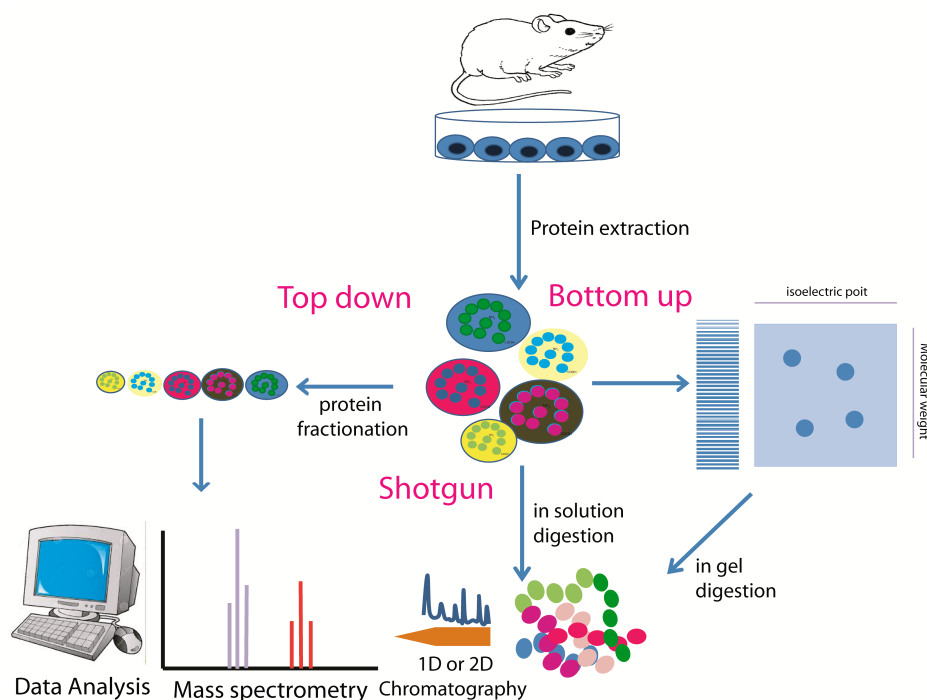


Figure 1. Representation of “top down”, “bottom up” and shotgun approaches

The analysis of a complex peptide sample is based on the selection of appropriate fractionation methods, required both at protein and peptide levels. One of the first strategies (still very popular) relies on the separation of protein sample by means of 2D or 1D gel electrophoresis^[13,14]. In a two-dimensional poly-acrylamide gel electrophoresis experiment (2D-PAGE), proteins are first separated on the basis of their isoelectric point (pI). During this step, named isoelectric focusing (IEF), proteins are loaded onto polyacrylamide gels (IEF gels) or immobilized pH gradient strips (IPG) and an electrical field is applied, allowing proteins to migrate through the pH gradient until they reach their pI. Later on, proteins are treated with sodium dodecyl sulphate (SDS), that confers them a charge roughly proportional to their molecular weight, and separated by application of an electric potential. Protein spots are detected by means of visible, such as silver and Coomassie, or fluorescent stains, such as

Introduction

Sypro Ruby and Deep Purple. Then, after excision from the gel, proteins are digested *in situ* with a proteolytic enzyme (mostly trypsin) to give the final peptides mixture. 2D-PAGE has an excellent resolving power and up to 10000 spots may be visualized on a large scale run^[15]. However, the procedure is time consuming and requires large sample amounts^[16]. For these reasons, 1D gel electrophoresis coupled to a liquid chromatography separation (Gel-LC-MS) step is largely preferred. In a 1D-PAGE, proteins are separated only according to their molecular weight^[17]. The entire gel lanes are then cut in small pieces and subjected to in-gel proteolysis^[18]. The peptide mixtures are finally separated and analysed through liquid chromatography coupled to mass-spectrometry. In order to improve sensitivity, the separation phase is usually performed in the nanoflow scale. Columns with a particle size in the order of 1 μm are directly interfaced with nano-electrospray sources, improving both peptide separation and sensitivity^[19].

Gel-based methods still suffer of some drawbacks, mainly the loss of sample due to an incomplete extraction from the gel. Therefore, during the last years, many efforts were oriented to build-up gel-free methods to analyse proteolytic mixtures without an upstream protein separation step. The analysis of complex peptide mixtures by means of HPLC-MS is known as “shotgun proteomics” or MuDPIT (Multi-Dimensional Protein Identification Technology)^[20]. The protein sample is directly subjected to proteolytic digestion, usually with two (or more) different enzymes (typically Lys-C and trypsin), and the obtained peptide mixture is subjected to a two-dimensional liquid chromatography separation (2D-LC)^[21,22]. 2D-LC exploits two serial orthogonal dimensions of separation to resolve complex peptide mixtures with high efficiency, thus improving the dynamic range of the MS identifications. The second dimension is usually a reversed-phase LC (RP-LC) step, because of its efficient separation power and the employment of salt-free MS compatible solvents^[23]. The first chromatographic dimension takes advantage of a different principle,

such as strong cation exchange (SCX)^[24,25], strong anion exchange (SAX)^[26], hydrophilic interaction liquid chromatography (HILIC)^[27,28], and in gel or in solution isoelectric focusing (Offgel)^[29,30].

Peptides are finally analysed by mean of mass spectrometry. The peptide identification comes in two different ways: the so called peptide mass fingerprint (PMF) and tandem MS profiling^[31,32]. Basically, in the former approach, the identity of unknown proteins is revealed by matching the measured peptide masses against a database of theoretical proteolytic fragments originated from *in silico* protein digestions. This approach is suitable for simple protein mixtures, such as digested spots coming from a 2D-PAGE. However, even though modern mass spectrometers have a ultra-high resolution and mass accuracy of a few ppm, the effectiveness of PMF analysis is inadequate because it is based only on the mass of the intact peptides. Therefore, the more informative tandem MS experiments are becoming widespread. Tandem MS relies on the employment of instruments equipped with an appropriate fragmentation source to record both the masses of the intact peptides and the originated fragments. The measurement of the *daughter ions* is useful to retrieve the true peptide sequence; indeed, depending on the fragmentation technique, the identity of the generated fragments is predictable. The most common and robust fragmentation technique is the so called collision induced dissociation (CID)^[33]; also electron transfer dissociation (ETD)^[34,35] and high collision dissociation (HCD) are very informative and can be employed alternatively to gain more informations on peptide sequences. More in details, CID exploits an inert gas such as nitrogen, argon or helium to induce the peptide fragmentation in a “mild” fashion, causing the amide bond (mostly y and b ions are produced) breakage^[36]. On the contrary, ECD/ETD induces random fragmentation along the peptide backbone, even if c and z ions are mostly formed employing thermal electrons or fluoranthene as source of energy^[37,38]. Finally, HCD^[39] is a beam based fragmentation

Introduction

technique mainly employed in the isobaric tag-based quantification (see global proteomics paragraph)^[40,41]. CID, ETD and HCD are considered as complementary techniques, since CID is well suited for the fragmentation of doubly and triply charged peptides, whereas ETD is preferred for the fragmentation of peptides with higher charge, with internal basic residues and for the analysis of post-translational modifications. Therefore, the application of a “decision tree” in which the fragmentation source is decided “on the fly” by the mass spectrometer, based on the precursor ion characteristics, has been demonstrated to be effective to improve the identification capabilities^[42].

Once the full MS and the MSMS spectra have been generated, the empirical fragmentation peptide profiles are matched with theoretical ones, contained in web accessible databases (SwissProt, NCBIInr), through a number of different search engines and algorithms, among which MASCOT^[43] and SEQUEST^[44] are the most used.

1.2 Global Proteomics

Mass spectrometry has emerged as one of the main tools for large-scale protein analysis, due to its unbiased nature and conceptual simplicity. Several cellular pathways can be modulated upon drug treatment, leading to a change in the level of specific subsets of proteins, so the drug-induced response is of central importance to understand the pathways involved in the final pharmacological and toxicological effects^[45-47].

Mass spectrometry-based proteomic analysis provides the possibility to estimate the entire proteome alterations in a single experiment^[48].

Many global proteomics strategies are today available to evaluate the response of a whole proteome to external stimuli and can be distinguished in gel-based and gel-free approaches (**Figure 2**).

Gel-based approaches are built on the evaluation of the intensities of the protein spots in a 2D-PAGE run, since they are directly proportional to the protein amounts. Proteins from two (or more) different samples (eg. chemically treated and un-treated cells) are separated on the basis of their pI and molecular weight and then stained as described in paragraph 1. The intensity of each spot is quantified and compared by means of a differential gel image analysis. Up- or down-regulated proteins are finally *in situ* digested and identified by MALDI-MS or LC-MSMS.

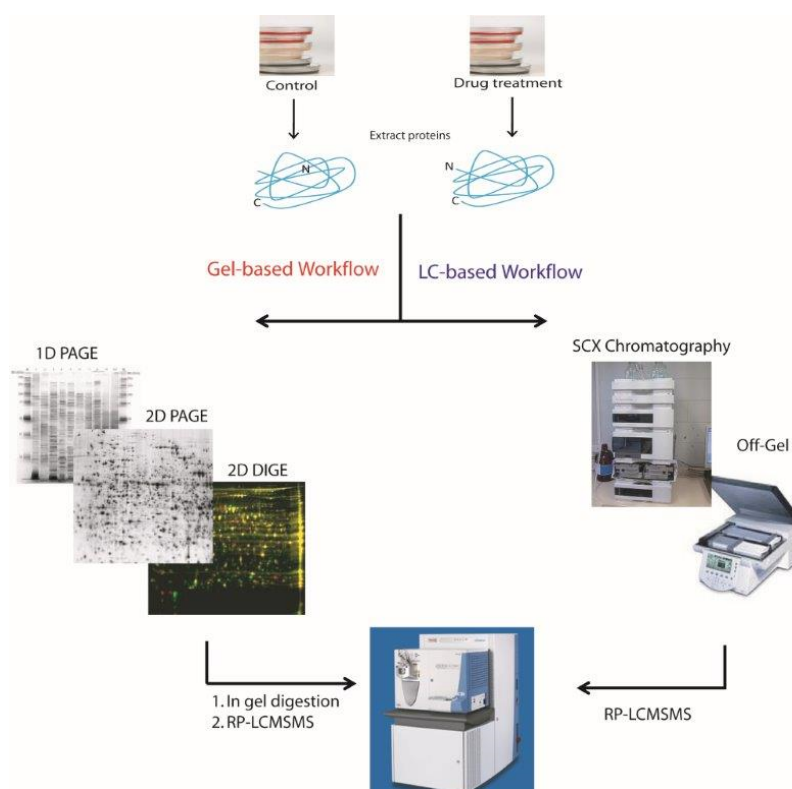


Figure 2. Schematic workflow of global proteomic experiments.

2D-PAGE, although suffering from some shortcomings, as discussed below, is a consolidate technique largely employed in global proteomics profiling, mainly due to its high resolving power^[49].

Introduction

To improve its efficiency, the so called two-dimensional differential in gel electrophoresis (2D-DIGE) is now routinely employed. In a 2D-DIGE experiment, samples are pre-labelled with fluorescent dyes (called Cy2, Cy3 and Cy5) and then mixed prior to isoelectric focusing, and therefore up to three samples can be run on the same gel^[50,51]. After completion of the electrophoresis run, the gel is scanned at the different excitation wavelengths of each dye, providing three gel images. Then, the images are superimposed, spot margins are defined and volumes are calculated and compared, giving the accurate protein expression levels for each sample. CyDye technology has a higher degree of linearity compared to silver and coomassie blue stains and is also quicker and more sensitive^[52].

Although the introduction of DIGE technique has overcome some of the shortcomings limiting the application of classical 2D-PAGE^[53], mainly due to “gel-to-gel” variations, both approaches are still affected by some restrictions imposed by the use of the gel procedure. First of all, the analysis is often complicated by co-migration of various proteins in a single spot or, on the contrary, by the presence of the same protein in multiple spots, due to isoforms and post-translational modifications. Furthermore, extremely acidic, basic or hydrophobic proteins (e.g. membrane-bound proteins)^[54], low and very high molecular weight or less abundant proteins^[55] are hardly monitored.

The drawbacks affecting gel-based approaches, together with the tremendous developments of mass-spectrometric performances and LC-based separation techniques, led to a rapid spread of gel-free approaches. Gel-free methods can be further divided in label-based and label-free approaches.

The label-based methodologies rely on the use of “labelled tags” to distinguish the same analyte in different samples within a single LC-MS experiment. During the last years, a number of labelling methods have been developed, grouped in metabolic and chemical labelling approaches (**Figure 3**).

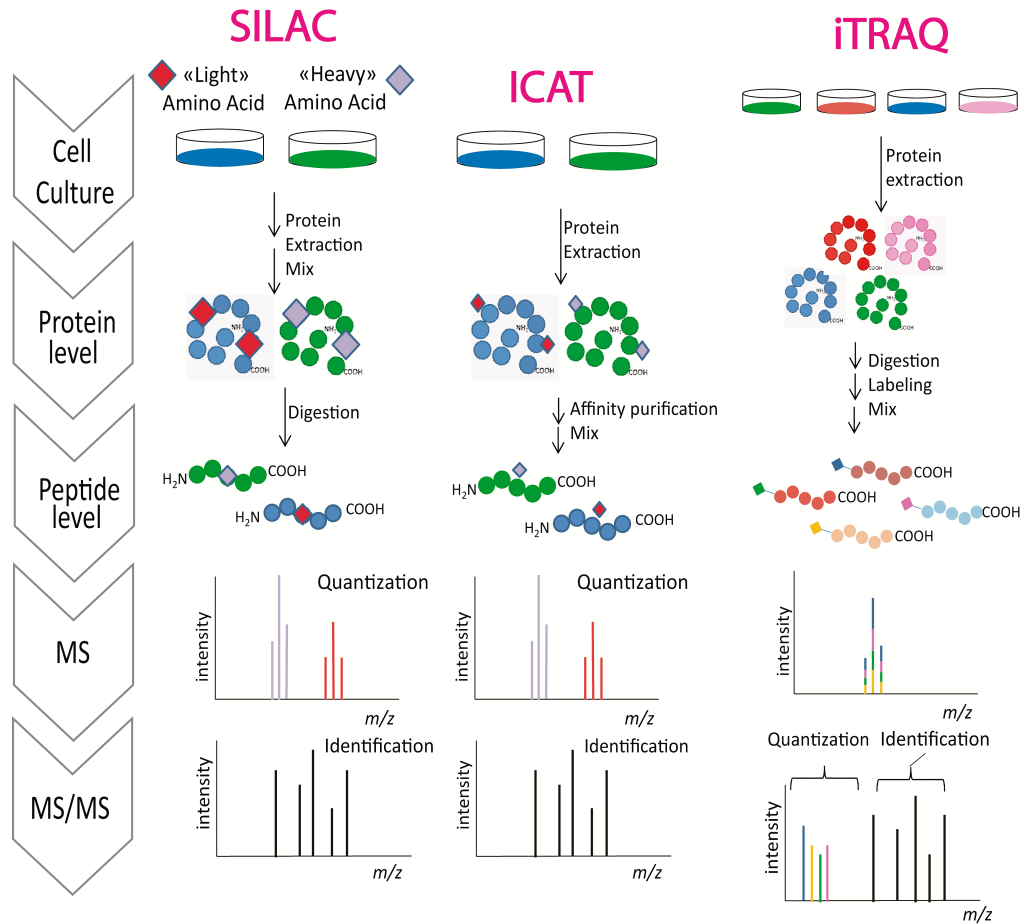


Figure 3. Most common label-based quantization techniques

In the metabolic approach, the label is introduced *in vivo* through auxotrophic amino acids^[56]. More in details, this labelling technique, known as Stable Isotope Labelling by Amino acids in Cell culture (SILAC), relies on the ability of cells fed with *heavy* amino acid to capture and incorporate them in the newly synthesized proteins^[57]. Therefore, two cell populations are cultivated either in presence of natural or isotopically (e.g. with deuterium, ^{13}C , ^{15}N)^[58,59] labelled amino acids and, after a number of cell divisions, one population is treated with the drug. Both the treated and un-treated cells are finally lysed and the extracted proteins are mixed prior to protein digestion. Due to the high complexity of the samples, usually the enzymatic digestion is performed by means of two different proteolytic enzymes, typically Lys-C and trypsin, and

Introduction

the mixture is subjected to a two-dimensional liquid chromatography separation (2D-LC). The following MS analysis allows the comparison of the peptides coming from the two samples connected by the mass-shift signature due to the incorporated tags and, through specific bioinformatics tools, the differentially expressed protein can be identified and quantified.

Chemical labelling approaches (**Table 1**) exploit chemical reaction to insert the tag portion either at protein or peptide level. The most common techniques are the isotope coated affinity tag (ICAT)^[60], iTRAQ^[61], and dimethyl labeling^[62].

The initial ICAT reagent has a iodoacetyl group tethered to a biotin tag via a deuterated or non-deuterated oxyethylene linker. The iodoacetyl moiety reacts with the cysteine side chain whereas the biotin portion is required for the affinity isolation step. Samples to be compared are treated either with the light probe (d0) or with the heavy one (d8). Once the two protein samples have been marked, they can be mixed and subjected to protein digestion. Prior to LC-MS analysis, tagged peptides are enriched by means of the biotin-avidin affinity (on coated column). The isolated peptides are finally analysed as already described for SILAC (**Figure 3**)^[60].

Both SILAC and ICAT allow the comparison of up to two samples in one experiment, whereas iTRAQ has been developed in a multiplexed fashion and allows the simultaneous analysis of up to eight samples.

The iTRAQ reagent consists of three fundamental building blocks: a quantification group (N-methylpiperazine), a balance group, and a hydroxyl succinimide ester group that reacts with the N-terminal amino groups and ϵ -side chain of lysines. The reactivity of iTRAQ reagents is conceptually more convenient than the ICAT reagent, since each ion selected for fragmentation contributes to the abundance estimation. Nevertheless, the most important difference between iTRAQ and the other techniques is that the quantification occurs at the MS/MS rather than MS level (**Figure 3**). This opportunity gives

a higher signal/noise ratio, due to the reduced chemical noise in MS², and a gain in sensitivity due to the isobaricity of the tags.

To date, eight iTRAQ reagents are commercially available, each having stable isotopes that are uniquely distributed between the reporter groups (m/z : 113, 114, 115, 116, 117, 118, 119, and 121) and the balance group. When iTRAQ-modified peptides are analysed by MS/MS, the signal intensity ratios of the reporter groups reflect the peptide quantities among different samples.

Nevertheless, precursor contamination results in under-estimation of small changes^[63,64] and, additionally, the cost of the iTRAQ reagents and the request of a mass spectrometer equipped with the opportune fragmentation source able to produce MS/MS fragments at low m/z , such as HCD, limit the use of this technique.

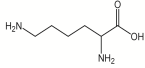
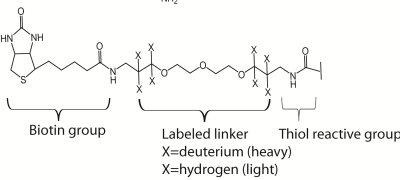
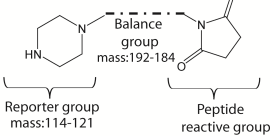
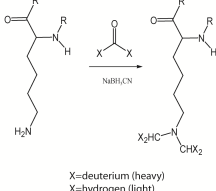
Label	Modification site	Structure
SILAC	In vivo incorporation of heavy lysine	 heavy lysine 6X ¹³ C
ICAT	Thiol group	 Biotin group Labeled linker X=deuterium (heavy) X=hydrogen (light) Thiol reactive group
iTRAQ	Peptide N-termini and ε-amino group of lysine	 Reporter group mass:114-121 Balance group mass:192-184 Peptide reactive group
Dimethyl labeling	Peptide N-termini and ε-amino group of lysine	 X=deuterium (heavy) X=hydrogen (light)

Table 1. Structures of isotopic labels for SILAC, ICAT, iTRAQ and dimethyl labeling.

Another label-based quantification technique that is worth to be mentioned, because of its low cost and massive applicability, is the so-called *stable*

Introduction

isotope dimethyl labeling^[65,66]. Peptide N-termini and lysine ϵ -amino groups quickly react with formaldehyde and cyanoborohydride producing N,N-dimethyl-amine peptides with a mass increment of 28 Da^[67]. Using deuterated formaldehyde, an isotopically marked peptide is obtained with a mass increment of 32 Da, whereas treating peptides with ^{13}C -(d2)-formaldehyde and cyanoborodeuteride, a mass increment of 36 Da is obtained (**Figure 4**). The quantification step is achieved comparing the intensities of the peptides matching the particular mass shift patterns due to the different labelling.

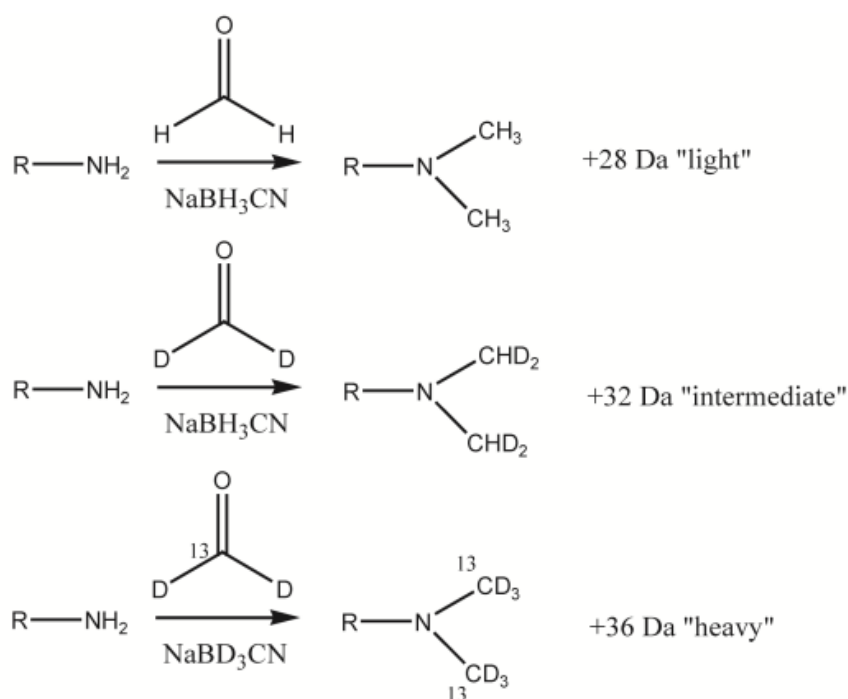


Figure 4. Triplex stable isotope dimethyl labeling

Isotopically and gel-based techniques are to date crucial tools to compare biological samples by mass spectrometry. Nonetheless, label-free methods are acquiring a growing importance in quantitative-MS field. The main advantages of label free methods are the virtual no-limit number of samples

that can be compared, and the higher dynamic range of quantification^[68,69]. In label-free quantification approaches, each sample is separately prepared and then subjected to LC-MS/MS^[70]. The relative or absolute protein quantity is then deduced either from the intensity of the intact proteolytic peptides, or by counting and comparing the number of MSMS spectra. The former method is based on the linear correlation between sample concentration and the signal response produced by electrospray ionization (ESI)^[71]. Peak area integration of a set of peptides per protein yields relative quantitative information among multiple samples. This method requires a fine tuning of chromatographic and mass spectrometric conditions. Indeed, the equivalent chromatographic profiles enable an easier alignment of two or more runs, that is needed to compare peptide intensities in different experiments. Finally, a right balance between acquisition of survey and fragment spectra (needed for peptide identification) is necessary to improve the peak area integration without compromise protein identification. Generally, this last issue is particularly difficult to accomplish and often a double run is required, in which the protein identification and quantification steps are performed in two consecutive steps. This procedure is tedious and sample-consuming, even if more accurate. The quantification procedure based on the count of MS/MS spectra is becoming more popular. In a data dependent scanning, the number of MS/MS spectra generated per peptide is actually connected to its abundance. The count and comparison of the generated MS² spectra allow the relative quantification of each identified protein.

1.3 Activity based protein profiling

Global proteomic methods record variations in the protein abundance, providing an indirect estimation of changes in protein activity. Actually,

Introduction

changes in protein abundance represent only a small part of the factors that influence the activity of enzymes: indeed, post-translational modifications, proteolytic processing, protein-protein interactions play a central role in enzyme activity regulation^[72]. Activity-based protein profiling (ABPP) has become an important tool in proteomics and, in turn, in chemical biology research due to its ability to monitor the active enzymes. On this basis, this technique is apart from the global proteomics approaches, whose first aim is profiling proteins on the basis of expression and abundance.

Activity based protein profiling (ABPP) uses active site-directed chemical probes to assess the functional state of specific subsets of enzymes in their native biological environment. ABPP probes are composed at least by three fundamental building blocks: (i) a reactive group, useful to bind and covalently label the active sites of a given enzyme class (warhead), (ii) a reporter tag, needed for the detection, enrichment and identification of probe labelled proteome and (iii) a linker spacer (**Figure 5**).

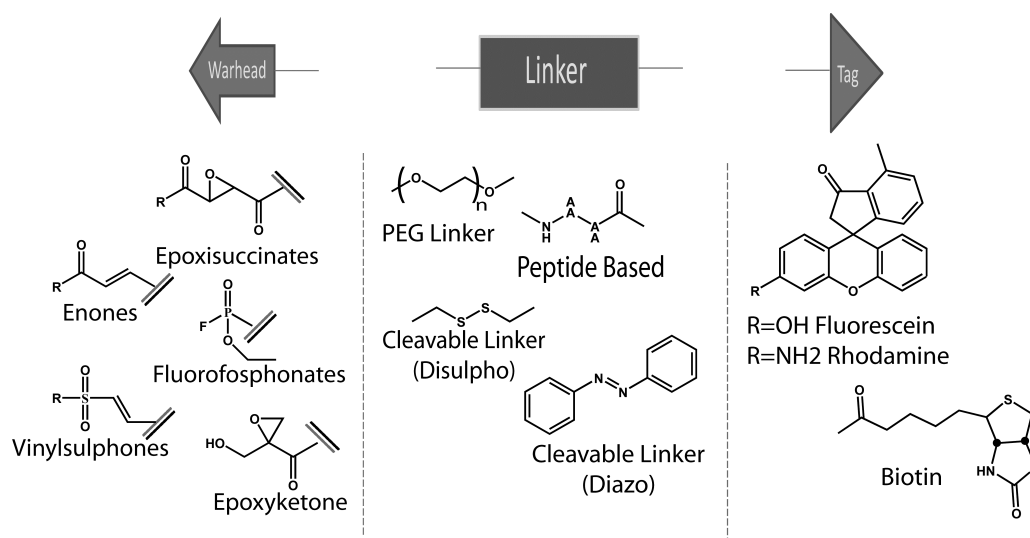


Figure 5. Schematic representation of probe key features with some representative examples.

ABPP probes are designed to monitor a large number of enzymes without cross-reaction with other proteins in the proteome, thus they take advantage from the structural features that characterize the active sites of different enzyme classes^[73]. On the basis of the labelling mode, three main classes of probes can be distinguished: (i) general alkylating probes, (ii) activity-based probes (ABPs) and (iii) affinity-based probes (AfBPs) (**Figure 6**). The first are based on the intrinsic capability of some functional groups to covalently label amino acids residues, such as cysteine, in a non-specific manner. On the contrary, ABPs are mechanism-based or suicide inhibitors tailored on the catalytic active site of the enzyme^[74]. The reaction mechanism responsible for the labelling event involves amino acid residues normally responsible for the binding of the natural substrates. Most of the functional reactive groups of the probe are represented by electrophilic traps such as epoxides or Michael acceptors (**Figure 5**). The reactive portion of the probe can be also “masked” in the original molecule and can be converted by the target enzyme in the reactive form. One of the main advantage of this kind of probes is their ability to bind the enzyme in a mechanism-based fashion enabling, as a consequence, only the visualization of enzymes in the active state. On the other hand, the ABPs design requires a deep knowledge of the catalytic mechanism of the active enzymes, precluding the investigation of less studied enzyme classes. Affinity-based probes greatly overcome this limitation recognizing the enzyme and performing a non-specific binding of a nearby protein functional group, not necessary involved in the catalytic mechanism. The bond formation can be a spontaneous event but is usually achieved by a photoreactive cross-linker, such as benzophenone or diazirine, that covalently binds the target enzymes upon UV irradiation^[75]. Although AfBPs have been successfully applied to label the metallo-protease enzyme family and the HDACs^[76-80], ABPs are still the most common probes in enzyme profiling.

Introduction

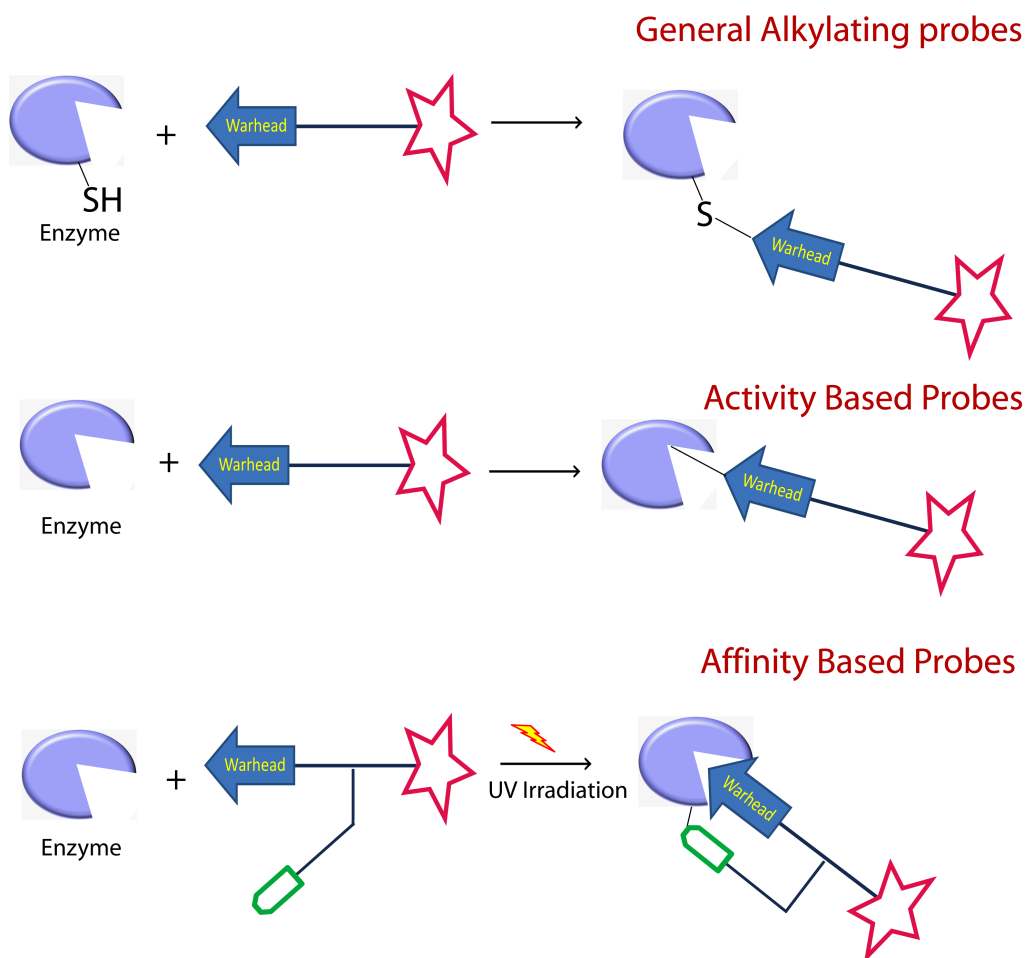


Figure 6. Three main classes of probes distinguishable on the basis of labelling mode

The tag portion of the probe allows the visualization and identification of the labelled proteins. The most commonly used tags are biotin, fluorophores, epitope or radioactive tags, that are compatible with the proteomic analysis systems such as SDS-PAGE, western blotting or liquid chromatography coupled to mass spectrometry. Gel-based approaches are preferred for a rapid comparative analysis of several proteomes. Probe-treated proteomes are first resolved by one or two-dimensional polyacrylamide gel electrophoresis (1D or 2D SDS-PAGE), and then visualized by either in-gel fluorescence scanning or avidin blotting^[81,82].

Currently, biotin probes are largely employed because biotinylated proteins can be easily enriched by avidin-beads. The biotin-avidin interaction is very strong, nearly irreversible ($K_D=10^{-15}$ M), thus also low abundant proteins can be efficiently isolated. Moreover, enriched proteins can be manipulated and identified by means of different proteomics techniques. Indeed, the bound proteins can be eluted by a denaturing buffer, separated by SDS-PAGE and subsequently subjected to in gel digestion for LC-MS/MS analysis^[83,84]. Alternatively, proteins can be directly subjected to on-beads digestion and analysed by multidimensional LC-MS/MS (ABPP-MudPIT). Taking into account parameters such as spectral counts or by means of other quantification strategies (SILAC or ICAT), it is also possible to compare the amount of active enzymes in two or more proteomes^[84-88]. Although the advantages of this technique, some shortcomings needs to be highlighted. Contamination by avidin and endogenously biotinylated proteins can be significant, and in many cases would prevent detection of low abundance targets. Furthermore, the on-bead digestion method leads to significant false positives, as a result of non-specific protein binding to the avidin resin.

Another LC-MS platform termed active-site peptide profiling (ASPP) is worth to be mentioned. The probe-labelled proteins can be digested in solution prior to an affinity enrichment, allowing the identification of modified peptides and, as a consequence, giving important information about the enzyme active site^[88,89].

The warhead is often linked to the tag region through a linker spacer that, providing enough space between the two components, facilitates both the reaction of the functional group with the enzyme and the purification step.

The linker region can range from an alkyl group to a PEG spacer or a peptide chain, and can incorporate a specific element to assist the recognition of the enzyme^[90].

Introduction

Additionally, linkers incorporating cleavable sites between the biotin and the bound biomolecule, such as proteolytic^[91] and chemically labile^[92-94] groups have been reported. These cleavable sites allow the release of the probe-labelled enzyme in mild conditions, enabling manipulation of the biomolecules in their native state.

To date, probes have been developed for more than a dozen of enzyme classes, including proteases, kinases, phosphatases, glycosidases, and oxidoreductases, and a wide range of chemical scaffold have been employed for probe design^[74]. The achievement of selectivity requires the tuning of both the probe affinity and reactivity. In fact, highly reactive warheads tend to be promiscuous, thus it is necessary to consider the enzyme chemistry or include a specificity element that directs the ABP to a particular class of enzymes or to a specific enzyme within a class. Chemical modification enables the reactivity to be confined and the probes optimized according to the requirements of specific target enzyme classes^[95]. Multiple biological methodologies for ABPP technology have emerged, and among them (i) comparative ABPP for target discovery, (ii) competitive ABPP for inhibitor discovery, and (ii) *in vivo* imaging. (**Figure 7**).

The first approach exploits the comparison of two or more proteomes in different physio-pathological conditions by ABPP to identify enzymes whose activity is regulated in response to external stimuli. Enzymes with unknown role can be visualized in a comparative experiments, thus they may be assigned to a specific mechanistic class on the basis of their ability to react with specific ABPs^[96].

The second major application of ABPP is the discovery of enzyme inhibitors. Inhibitor discovery by ABPP is possible because small molecules can compete with the activity-based probes for the binding to the enzyme active sites, thereby slowing the rate of probe labelling. The library of candidates inhibitors is pre-incubated with a cell or tissue-derived proteome and then the mixture is

treated with ABPs. Inhibitor-sensitive enzymes are detected by a reduction in probe labelling intensity.

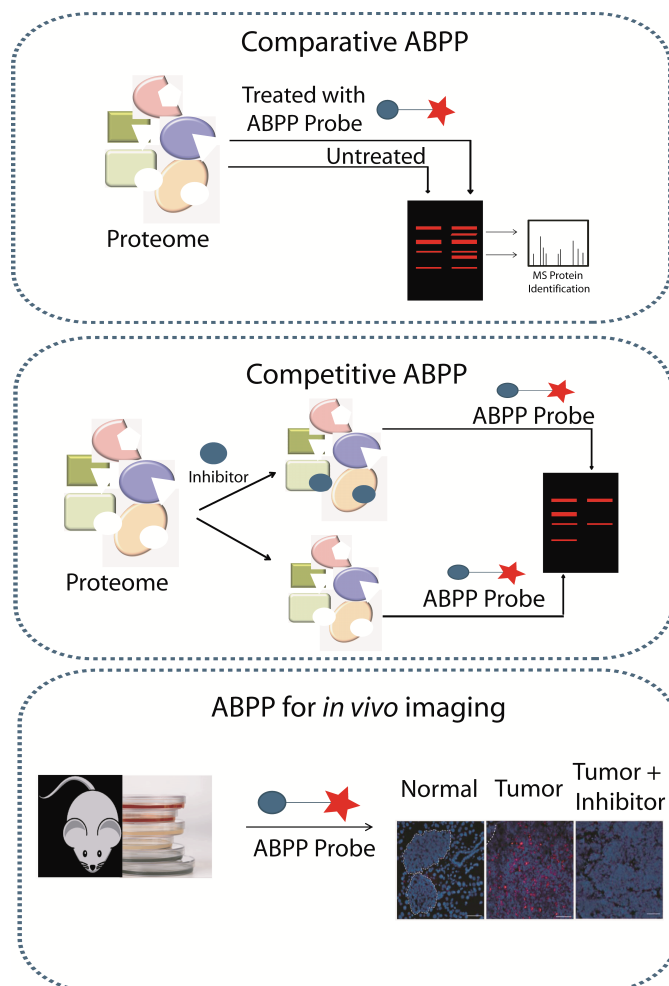


Figure 7. Main applications of ABPP in chemical biology research.

Competitive ABPP has several advantages over classical substrate assays for inhibitor discovery. First, the screening is realized directly in complex proteomes, thus there is no need to express and purify enzymes. Moreover, since the library is screened against several enzymes in parallel, promiscuous agents can be discarded in favour of selective compounds^[97].

Introduction

Another remarkable application of ABPP in chemical biology is represented by the employment of fluorogenic probes for enzyme labelling and localization *in vivo* by microscopy and whole organism imaging. Bogyo's group pioneered this field unravelling the potential of ABPP toward applications in tumour imaging, by exploiting caspase directed ABPs^[98].

Since ABPP plays a key role in chemical biology research, several strategies have emerged for a broader applicability of this technique. Particularly, there is a pressing need of tools to measure the levels and activities of biomolecules directly in cells, tissues, and fluids. In fact, assessment of the functional state of proteins in biological samples requires proteins in their native (functional) state, but some proteins may not tolerate the transfer from the cellular context to a cellular lysate, and only a minority of full probes has been reported to be permeable^[99]. In this scenario, the bio-orthogonal chemistry, or click chemistry, has demonstrated to be able to overcome two of the main limitations of ABPP, that are the interference of bulky tags on enzyme recognition and the ineffective application of traditional ABPP in cellular context.

Bio-orthogonal chemistry is based on the design of warheads decorated with a functional group unable to react with biomolecules, but highly reactive with an orthogonally-functionalized reporter tag (**Figure 8**). The presence of this "latent chemical handle", instead of a bound tag, allows the introduction of the visualization/identification tag in a second step, after the bound-forming event between the enzymes and the warhead^[100]. To be employed in this field, organic reactions need to proceed in aqueous buffer, under mild conditions and rapidly yielding a single desired product. Moreover, both counterparts must be absolutely inert to biological molecules. The Staudinger-Bertozzi reaction is the first example of chemistry applied to bio-orthogonal ligation and was developed by the Bertozzi's group on the basis of the classic Staudinger reaction of azides with triarylphosphines^[101].

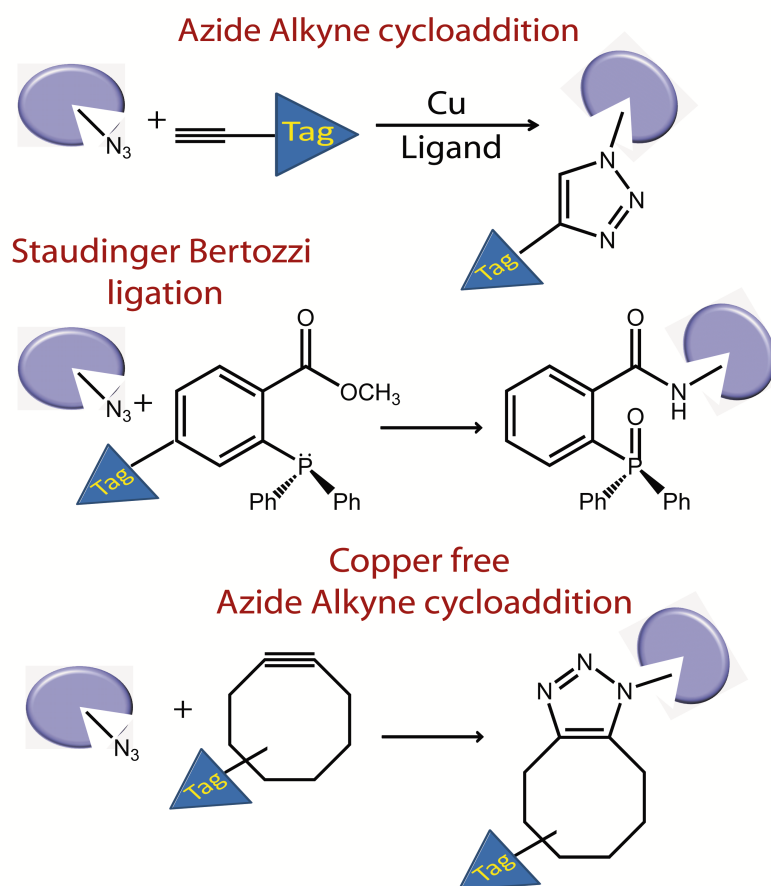
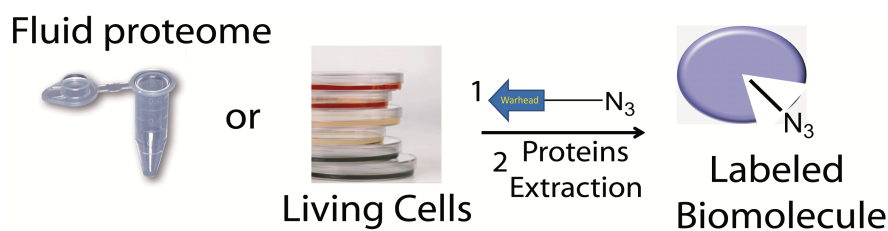


Figure 8. Schematic representation of most common bio-orthogonal reactions in ABPP

The first step of this reaction is the nucleophilic attack of the phosphine at the electrophilic terminal nitrogen of the azide. Through nitrogen loss, an unstable aza-ylide is formed and rapidly hydrolyzed by a water molecule. To improve the kinetics and the bio-orthogonality, Bertozzi's group included an electrophilic trap, a methyl ester, on the triaryl phosphine. The Staudinger-

Introduction

Bertozzi ligation has been used both in living cells and mice, but currently it is no longer widely applied because the reaction is too slow for bio-conjugation purposes^[102].

An extremely fast and effective reaction for bio-conjugation is the copper(I) catalyzed variant of the Huisgen 1,3-dipolar cycloaddition (click reaction). Both the azide and terminal alkyne are compatible with biological samples and give rise to the specific formation of 1,2,3-triazoles in aqueous buffers, without cross-reactions with biomolecules^[103-105]. In recent years, a wide and rapidly growing number of copper-free click reactions have been developed to remove the need of copper. In these settings, the azide-alkyne cycloaddition progresses in a so called “strain prompted” way, thanks to the high reactivity of cyclooctynes^[106].

1.4 Compound centric chemical proteomics

As already mentioned, targets identification of bioactive small molecules is today considered one of the main issues for the clarification of their molecular mechanism of action^[107-109]. Drugs, natural products and toxins explicate their activity through the interaction with biological macromolecules, mostly proteins, forming transient or stable complexes which in turn mediate biological responses^[110]. Both academic and pharmaceutical research spend many efforts to design selective drug candidates that inhibit efficiently one or a few target(s) without cross-react with other cellular enzymes/proteins, minimizing the undesired side effects. The compound selectivity is usually assessed by testing its effects on a panel of purified enzymes, selected as putative additional targets^[111-113]. Nevertheless, these *in vitro* assays often produce partial results because the panel of proteins is obviously limited and do not include unexpected drug targets. Furthermore, the method is tedious,

expensive and the capability of small molecules to target and modulate numerous pathways shouldn't be considered *a priori* as a negative feature, since multi-target drugs may exert an high clinical response^[114]. Therefore, during the past years, a number of alternative strategies have been developed, such as chemical-genetic profiling in yeast, yeast three-hybrid system, transcriptional “signature” analysis, and affinity chromatography on immobilized drugs^[115,116].

Among them, an affinity purification mass spectrometry based technique (AP-MS) has emerged as a valuable and unbiased mean to link bioactive compounds to their cellular targets^[117-120]. This technique, also known as Compound Centric Chemical Proteomics (CCCP), Capture Compound Mass Spectrometry (CCMS) or Affinity Based Chemical Proteomics (ABCP), relies on the capability of a small molecule, anchored to a solid support, to “fish out” from a protein extract its macromolecular targets, then identified by LC-MSMS^[121].

This technique consists of three main steps: (i) chemical immobilization of the small molecule onto a solid support; (ii) affinity enrichment of the compound's cellular partners from a protein mixture; (iii) elution and identification of the captured proteins by means of mass spectrometry coupled to bio-informatics (**Figure 10**).

To be used as a bait, the small molecule has to be immobilized on an inert solid support^[122,123] (eg. Silica or agarose) (**Figure 9**), therefore the presence of a suitable reactive functional group (usually an amine, carboxyl, hydroxyl, or sulfhydryl group) is a fundamental requirement; alternatively, a proper functionalized analogue can be synthesized, as long as the original biological activity is retained^[9].

Usually, the small molecule is not directly immobilized onto the solid support surface, but the matrix is rather modified by a spacer arm that, providing enough space between the beads and the molecule, avoids a potential steric

Introduction

hindrance promoting the interactions between the compound and its macromolecular partners^[124-126] (**Figure 10**).

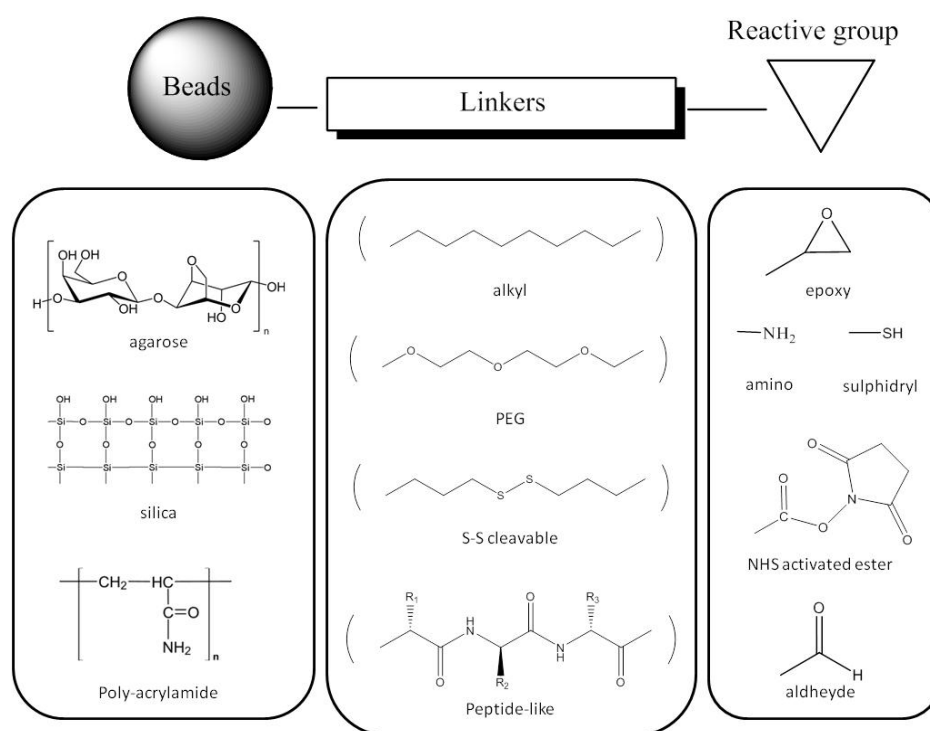


Figure 9. Schematic representation of matrix and linkers.

Linkers used as spacers may have different lengths and hydrophilicities: however, too much long spacers arms (more than 15 atoms) are not preferred because self-interactions can cause their auto-aggregation in aqueous solutions. Moreover, the use of hydrophilic linkers is useful to facilitate the removal of low affinity interactions established between the linker and proteins^[126]. Long-chain alkyl or polyethylene glycol (PEG) spacers respond to the required characteristics and are usually employed. Emerging spacer arms incorporating cleavable sites have been also proposed^[127,128] (**Figure 9**)

to selectively retain the proteins captured by the molecule, eliminating the amount of unspecific binders fished out by the solid supports.

Once the small molecule has been immobilized, the functionalized support can be incubated with the protein mixture. Cells, tissues or serum can be used as source of proteins, as long as the protein extraction and their incubation with the bait are performed in mild conditions to preserve the native state of proteins. After the incubation, the beads are subjected to abundant washings with a saline buffer to reduce the amount of proteins un-specifically adsorbed. Strictly bound proteins are finally eluted by using denaturing buffers, often containing SDS (**Figure 10**).

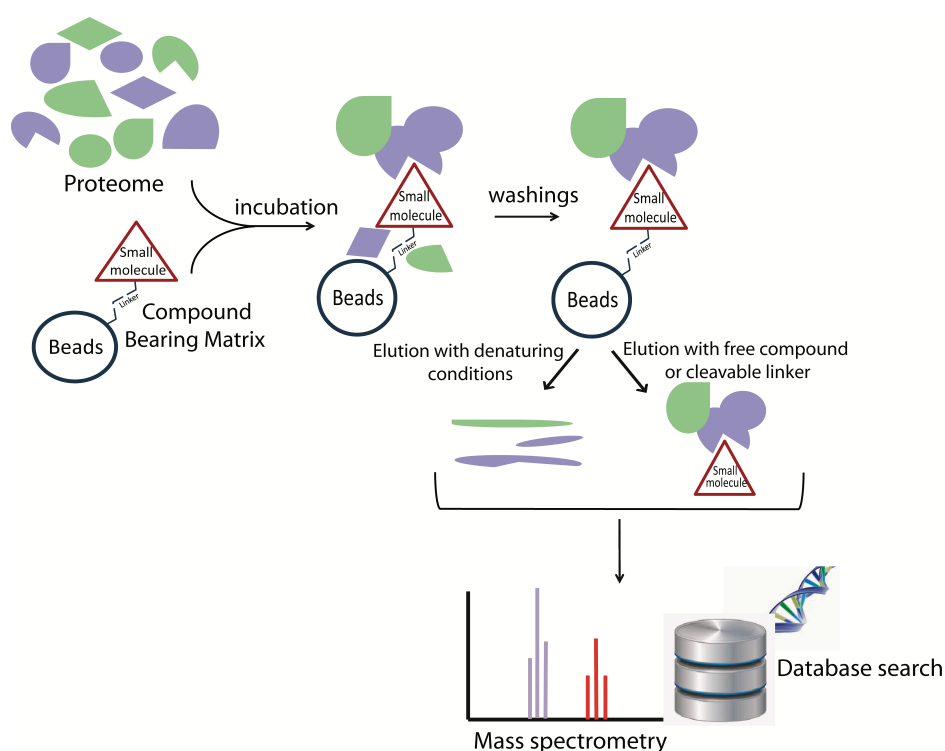


Figure 10. Schematic workflow of CCCP strategy.

Introduction

Proteins eluted from the bait are then separated by means of SDS-PAGE and, after excision from the gel, the bands are subjected to *in situ* digestion and the proteins are identified through nanoLC/MSMS coupled to bio-informatics analysis.

Like any other technique, chemical proteomics has strengths and weaknesses (**Figure 11**). As already mentioned, the main advantage of CCCP is the pseudo-physiologic environment in which the interactions occur. In this setting, the normal abundance of proteins, the presence of natural cofactors and physiological post translational modification are maintained, guaranteeing a more realistic picture of the small molecule interaction profile. Nevertheless, the protein extraction procedure is often unable to capture all the cellular proteins because of their different solubility profile^[9], as in the case of membrane proteins. Moreover, lysis conditions could compromise also the intactness of physiological multi-protein complexes, which are the real cellular functional units^[130]. To address this issue, as extensively described in the previous paragraph, new strategies based on the bio-orthogonal chemistry are emerging to let the interactions between the proteins and bait occur into the cellular environment.

The immobilization of the molecule onto a solid support is also a critical point of the technique. As already mentioned, it could be desirable to verify that the chemical modification does not perturb the biological activity of the compound. Furthermore, when a molecule is immobilized onto a solid matrix, the interactions occur at the interface between the solid and liquid phase; this issue is partially accomplished by the employment of spacers arms to minimize the steric hindrance due to the matrix^[126]. As a valuable alternative to solid supports, linkers containing a biotin portion are also employed. The biotin-linked molecule targets its partners in solution, and later on it is captured by affinity on avidin columns^[131,132].

One of the main drawbacks of these procedures is the residual amount of non-specific proteins that are not completely removed through washings, generating false positives. On this basis, a number of approaches have been introduced to distinguish between specific and un-specific interactors. The simplest method consists in performing a control experiment, incubating the protein mixture with un-derivatized beads; proteins identified in the control experiment are considered as background and discarded^[114]. Although this method has been largely used, false negative can be generated. In fact, some proteins may be true drug-interactor, although they also binds to the solid matrix. Above all, highly abundant proteins may give false negative results due to the high likelihood of their interaction with the solid support^[133]. Quantitative methods have been also introduced to overcome the false negative issue. Samples coming from the drug and control experiments can be tagged and quantified through the already mentioned methods: isotope-coded affinity tag (ICAT)^[134], isobaric tags for relative and absolute quantification (iTRAQ)^[135], dimethyl labelling (see paragraph 1) and stable isotope labelling by amino acids in cell culture (SILAC)^[136]. Proteins enriched from the bait are distinguished from background not merely on their absence in the control experiment, but rather comparing their quantitative (relative) abundance ratio. The main advantage to perform a control experiment with empty beads is its ability to simplify the research of the physiological relevant drug-interactors, “cleaning up” the list of the identified proteins from “sticky” and abundant proteins. However, most of the proteins fished out from the bait are actually true interactors that binds the small molecule with low affinity. Since these kind of low affinity interactions are unlike to be physiological relevant, further experiments are usually required to recognize significant, high affinity interactions.

Introduction

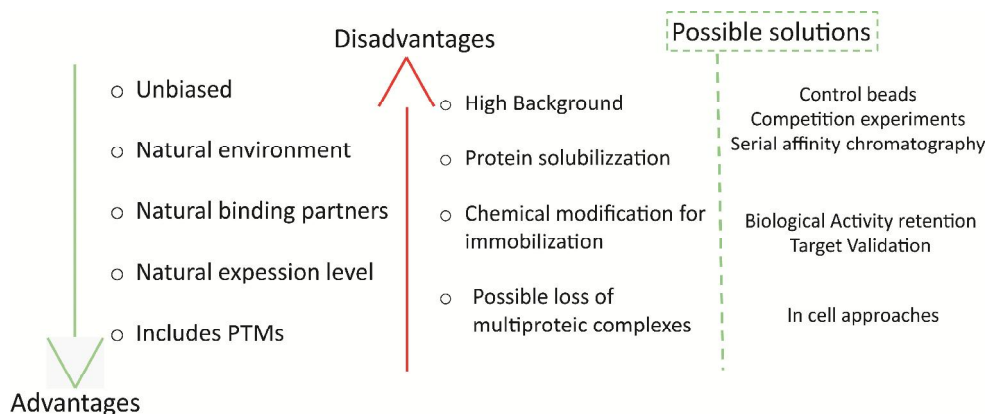


Figure 11. Principal advantages and disadvantages of CCCP technique with most common strategies proposed to overcome shortcomings.

Among the possible approaches, the best should be the employment of control beads bearing a structural analogue of the investigated compound lacking its biological activity. However, this option is not easy to realize, because often the information on the drug biological activity are lacking or, in the case of natural compounds, their synthesis is particularly laborious.

Another procedure to *bona fide* recognize the specific interacting proteins is their competitive elution from the solid support, using the free compound in solution (**Figure 12**)^[125]. In some details, after the affinity chromatography experiment, an aqueous solution of the free ligand is added to the beads, enabling the release of the specific drug-partners. Since the effectiveness of this method can be affected by the slow dissociation kinetics of the specific binding protein(s), in an alternative experimental design, the free ligand is added to the protein mixture before the affinity step. If the affinity enrichment is performed in the presence or absence of the free compound, the following eluted target can be recognized by their different intensity in the gel runs. This approach has some limitations, in particular when compounds have low solubility in aqueous buffer. An alternative procedure, called serial affinity chromatography strategy, has been described^[125]. After the affinity

enrichment, the unbound proteins are not discarded but added to a fresh aliquot of the ligand-bearing resin (**Figure 12**). Non-specific background proteins can be recognized by their ability to equally bind to each matrix sample, whereas specific target(s), almost totally fished out by the first batch, should disappear.

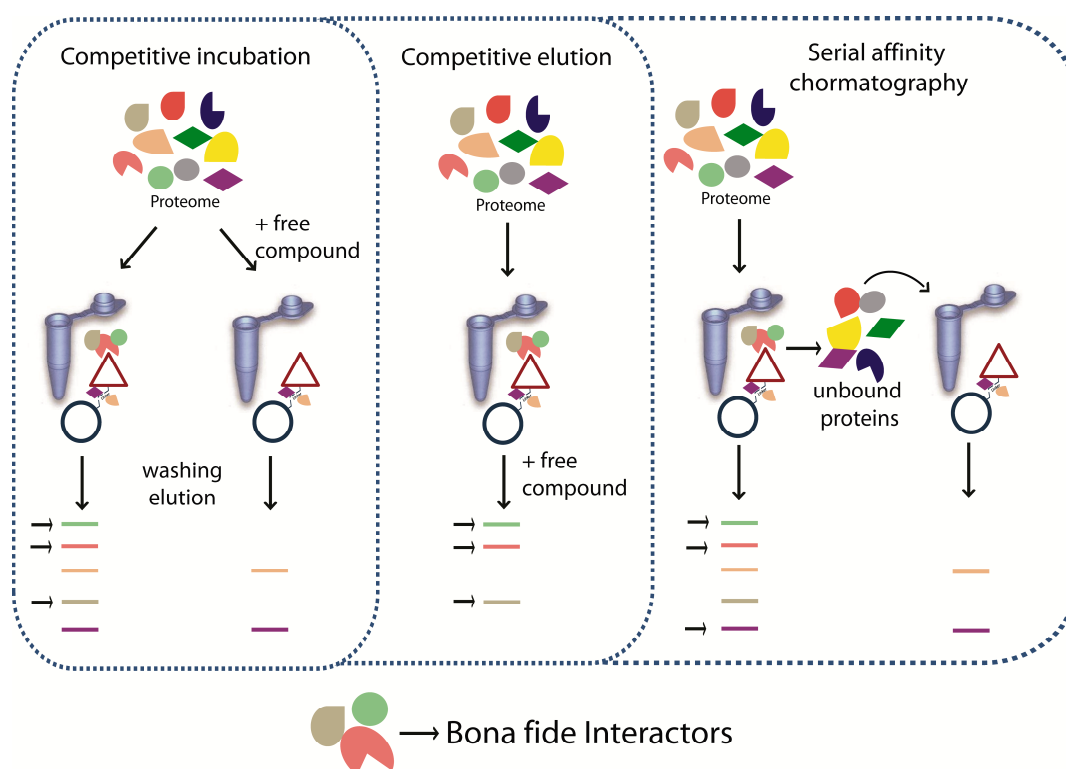


Figure 12. Competitive and Serial Affinity Chromatography

The application of CCCP to the analysis of small molecules interactome has a high potential, mainly due to its unbiased nature. Deconvolution of the raw results by employment of one or more of the above-mentioned filter techniques often drives to a short list of drug-target candidates, that are very likely to be physiologically significant^[117-119]. Without any doubts, further

Introduction

investigations are usually required to validate and to deepen the nature and the relevance of the identified interactions. First of all, techniques as SPR, ITC or Alpha Screen can be used to quantify the affinity of the interaction between the compound and the identified partner(s) (**Figure 13**). When possible, also STD-NMR and co-crystallization can be applied, due to their informative results.

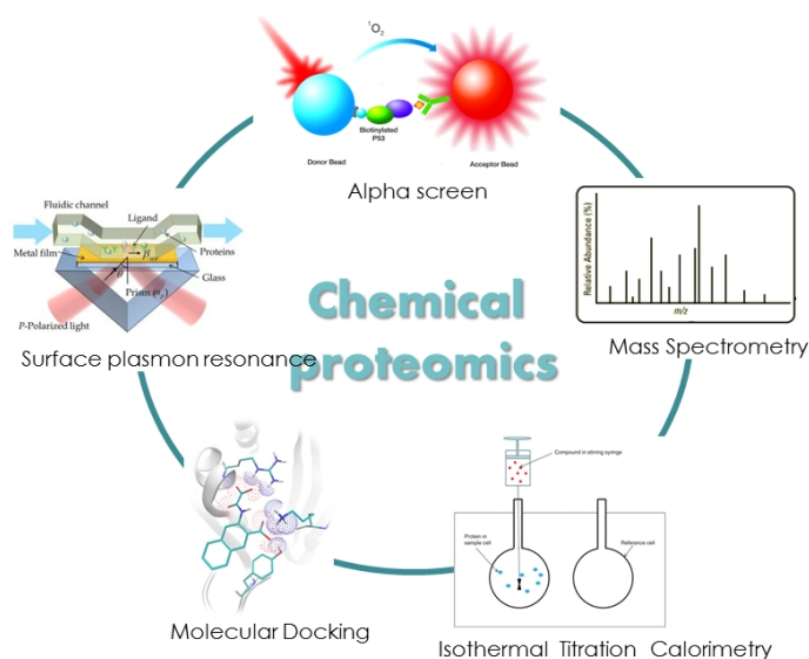


Figure 13. Most common techniques employed to validate and quantify ligand-protein affinity.

Moreover, *in vitro* or *in vivo* biological assays may be employed to investigate the capability of the small molecule to modulate its partner(s) in a purified or biological environment, respectively.

1.5 Aim of the research project

Bioactive small molecules exert their activity through a specific interaction with biological macromolecules. One of key point in the drug discovery and development process is the identification of the interactome of new lead compounds, that is essential to characterize their molecular mechanism of action^[107-109].

The natural environment, particularly marine ecosystem^[137], represent a rich source of secondary metabolites often endowed with intriguing chemical structures and biological activities. A comprehensive account of their interactome can be achieved by means of chemical proteomics approaches, thus enlightening the potentialities of these small molecules as new lead compounds and defining their target and off-target activities.

In this scenario, this research project aimed the analysis of the *in vitro* interactome of some small bioactive molecules extracted from marine sources by means of compound centric chemical proteomic techniques.

Moreover, a chemical proteomic investigation inside a living cell compartment, based on the application of bio-orthogonal chemistry, has been developed and then compared with the classical *in vitro* procedure.

The project has been completed by the study of the interaction profile of the endogenous cyclic nucleotide cCMP, during a training experience at the Utrecht University, under the supervision of Prof. Albert J. Heck.

RESULTS AND DISCUSSION

-CHAPTER 2-

Chemical Proteomics Reveals Heat Shock Protein 60 as the
Main Cellular Target of the Marine Bioactive Sesterterpene
Suvanine

Based on: *ChemBioChem*, 2012, 13, 1953–1958

2.1 Background

Through the process of natural selection natural products have acquired a huge chemical diversity, responsible for their unique biological properties, as they have evolved for optimal interactions with biological macromolecules.

Thus, natural products have proven to be one of the richest source of novel structural classes for biological studies and an essential supply for the discovery of new drugs. Particularly rich is the marine environment and is a wealthy source of plants, animals, and micro-organisms that, because of their adaptation to this unique habitat, produce a wide variety of secondary metabolites^[137]. Some of them are approaching phase II/III clinical trials for the treatment of cancer, algesia, allergy, cognitive and inflammatory diseases^[138,139].

The identification of the cellular interactome of these natural compounds is crucial to define their specific mechanisms of action and to understand their pharmacological effects^[119,122].

Suvanine (SUV) is a tricyclic bioactive sesterterpene, first recovered in the MeOH extract of the sponge *Coscinoderma mathewsi* Lendenfeld (order Dictyoceratida, family Spongiidae), collected at Pohnpei, Micronesia, during a wide screening of marine sponge based on the discovery of thrombin and trypsin inhibitors^[140]. Later, SUV was also found in the ethanolic extract of a different specimen of the same sponge, collected off the coasts of Solomon Islands, showing an interesting anti-inflammatory activity^[141]. Research into new bioactive metabolites from marine sponges of the *Coscinoderma* genus is of interest because these animals contain sulphated terpenoids that often exhibit valuable biological effects. For example, halisulfate 7 is an inhibitor of the catalytic subunits of the mammalian Ser/Thr protein phosphatase calcineurin^[142], while halisulfate 1 is a potent isocitrate lyase inhibitor, and coscinosulfate displays significant inhibitory activity towards CDC25A

Results and Discussion

phosphatase^[142-145]. Preliminary pharmacological studies demonstrated the *in vitro* inhibition by SUV and its derivatives of different secretory phospholipases (sPLA₂), NO and prostaglandin E2 (PGE2) production^[141].

However, the bio-molecular targets and the mechanisms of action responsible for the interesting properties of SUV were not yet defined and represented an interesting task to be solved. To reach this goal, a MS-based affinity chromatography approach has been applied to fish out the biological target(s) of SUV from HeLa cells.

2.2 Generation of Suvanine functional matrix

The first step in a chemical proteomic experiment is the immobilization of the small molecule onto the surface of an appropriate solid support, to allow the recovery and MS-based identification of proteins selected during the affinity chromatography step. The presence of a proper reactive group in the compound structure is hence required.

SUV (**Figure 14**) does not contain a functional group suitable for its immobilization, thus a semi-synthetic transformation was needed. We planned the desulfatation of SUV to obtain its aldehyde derivative that, besides an higher reactivity, retains the anti-inflammatory activity of the natural compound^[141]. The aldehyde containing derivative (SUV-AL) was obtained, as demonstrated by MS analysis and NMR characterization^[121], by incubating the natural compound at 150°C in a mixture of pyridine and dioxane for 2.5h (**Figure 14**).

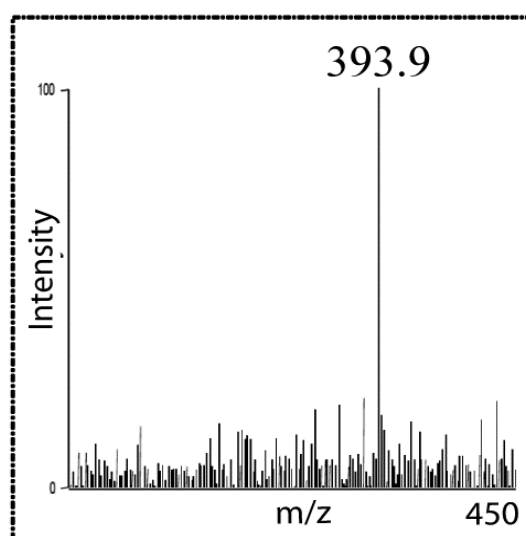
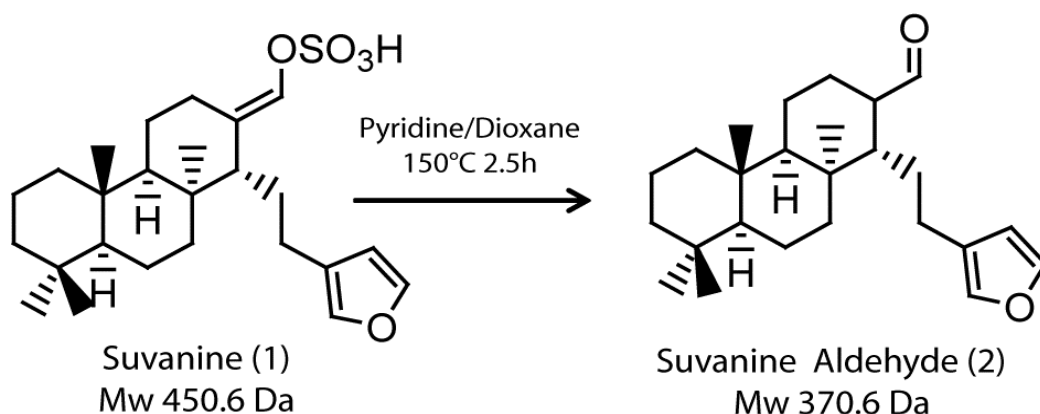


Figure 14. Hydrolytic transformation of Suvanine to its aldehyde derivate and ESI-MS spectrum

As extensively discussed in Chapter 1, the insertion of an appropriate spacer arm between the small molecule and the matrix is particularly advantageous. Thus, on the basis of our previous studies^[117–119], we chose 4,7,10-trioxatridecane-1,13-diamine ($\text{NH}_2(\text{PEG})_3\text{NH}_2$) as linker. Its reactivity with SUV-AL was analysed by a preliminary LC-MS investigation. The reaction was performed in $\text{ACN}/\text{NaHCO}_3$ and, after 2h at r.t., NaBH_4 was added to the

Results and Discussion

mixture to reduce the Schiff base formed by nucleophilic attack of the linker terminal amino group onto the SUV-AL carbonyl aldehyde (**Figure 15**). A main peak at m/z 575.8 Th, consistent with the postulated reaction adduct formation, was actually visible after 30 minutes of reduction (**Figure 16**).

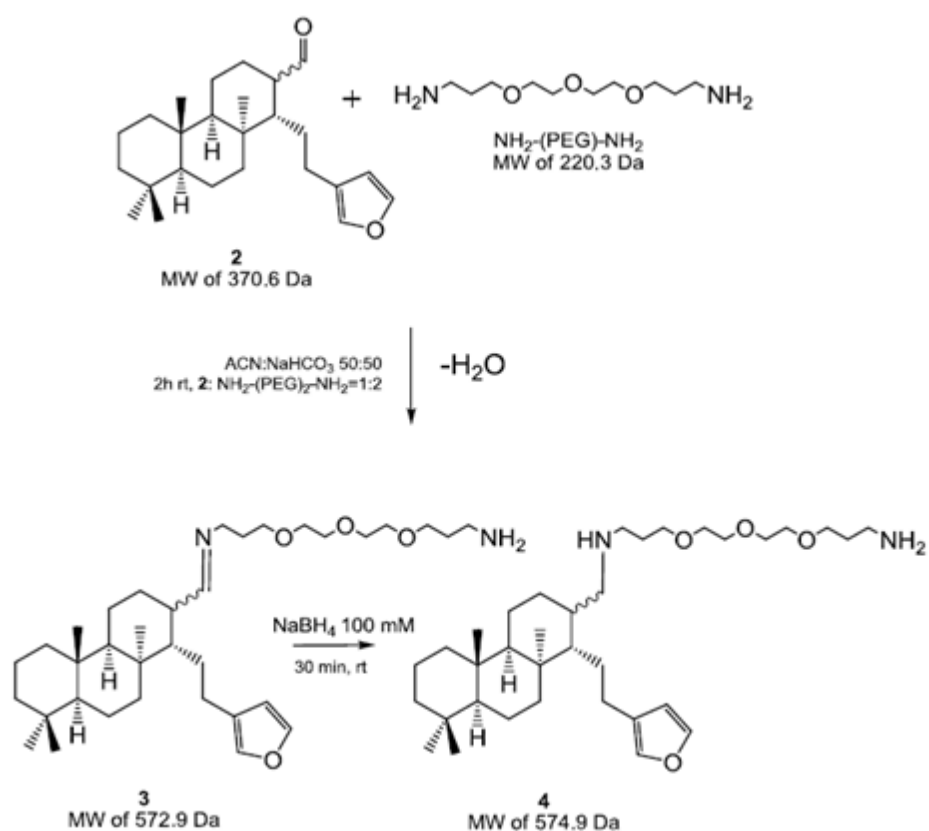


Figure 15. Reaction pathway between SUV-AL and $\text{NH}_2\text{-PEG}_3\text{-NH}_2$ in presence of NaBH_4

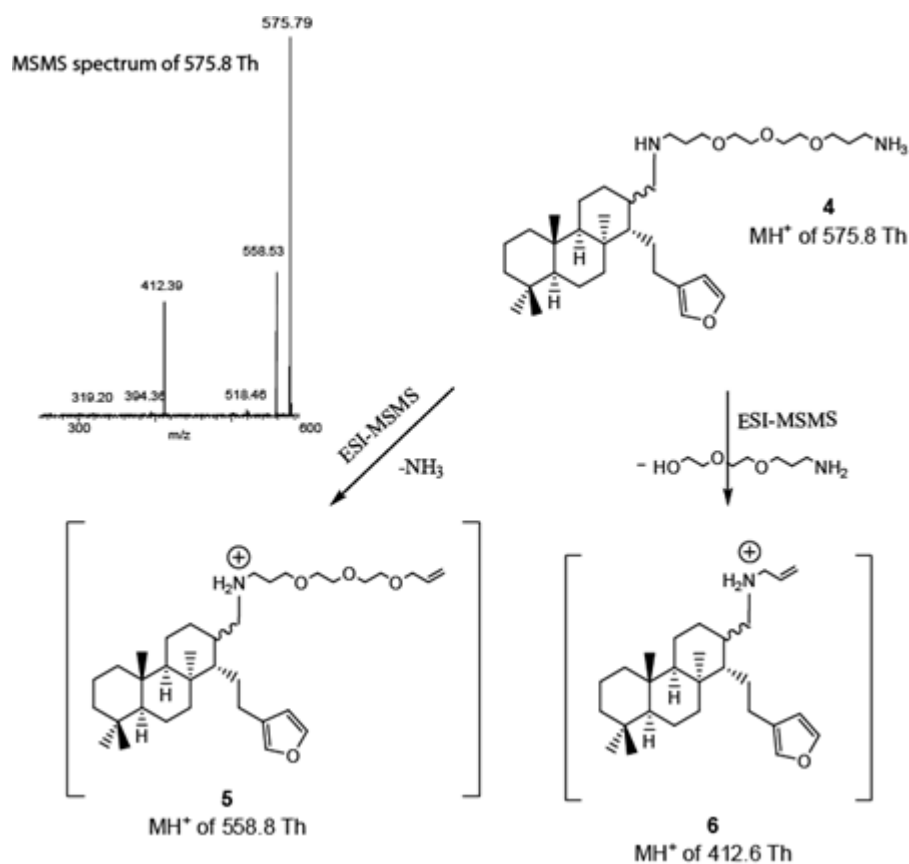


Figure 16. MS spectrum of the ion at 575.8 Th and its fragmentation pathway

Although the synthesized adduct, containing a free amino group, could be directly immobilized onto the carbonyldiimidazole activated beads, in order to optimize the total reaction yield and avoid the formation of a dimeric by-product, observed during the reaction of two SUV-AL molecules with the linker, we preferred to functionalize in a first step the beads with the di-amino linker and then anchor SUV-AL on the solid support (**Figure 17**). To verify the effectiveness of the first reaction, a Kaiser test was carried out, confirming the presence of free amino groups onto the beads surface. Subsequently, SUV-AL was added to the mixture and the reaction monitored by RP-HPLC-UV. Comparing the peaks of SUV-AL before and after 16 h of reaction, a yield of

Results and Discussion

~50% was assessed and a final concentration of 0.01 mmol of SUV-AL per mL resin was estimated. The coupling process was completed by acetylation of the residual unreacted free amino groups.

Finally, as a control matrix (CTR-Matrix) (see Chapter 1 and next paragraph), a batch of linker-bearing resin was subjected to acetylation as reported in **Figure 17**.

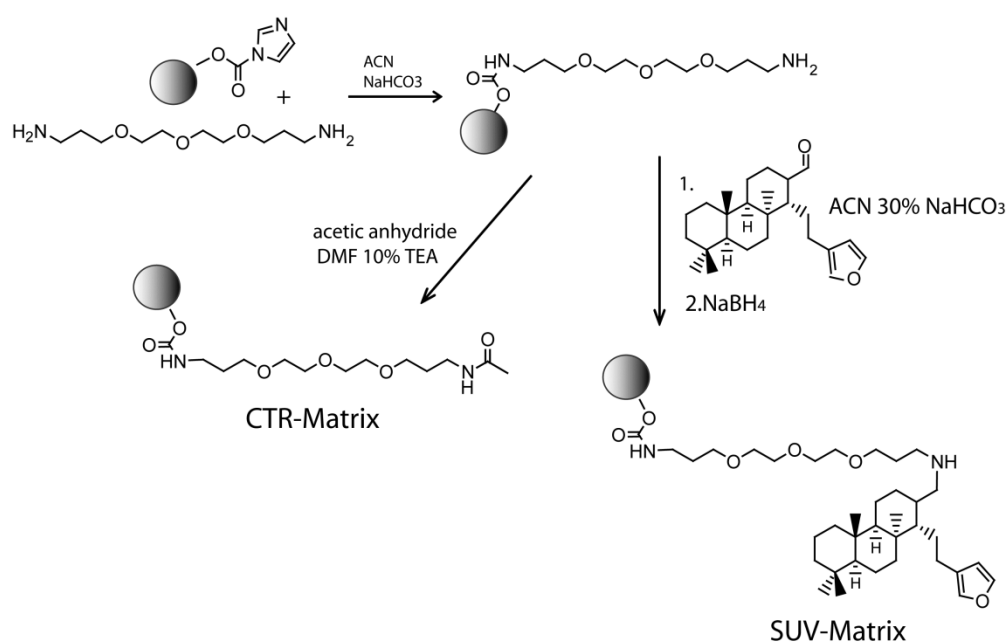


Figure 17. Preparation of SUV functionalized beads and control beads

2.2 Affinity purification and identification of suvanine partners

Samples of SUV-bearing matrix and the control matrix were separately incubated with the crude extracts of HeLa cells, to let the interactions develop between the compound and its potential partners (**Figure 18**). After centrifugation, the solid phase was submitted to several washing steps useful

to reduce non-specific interactions, while the tightly bound proteins were then eluted and resolved by 12% SDS-PAGE (**Figure 18**).

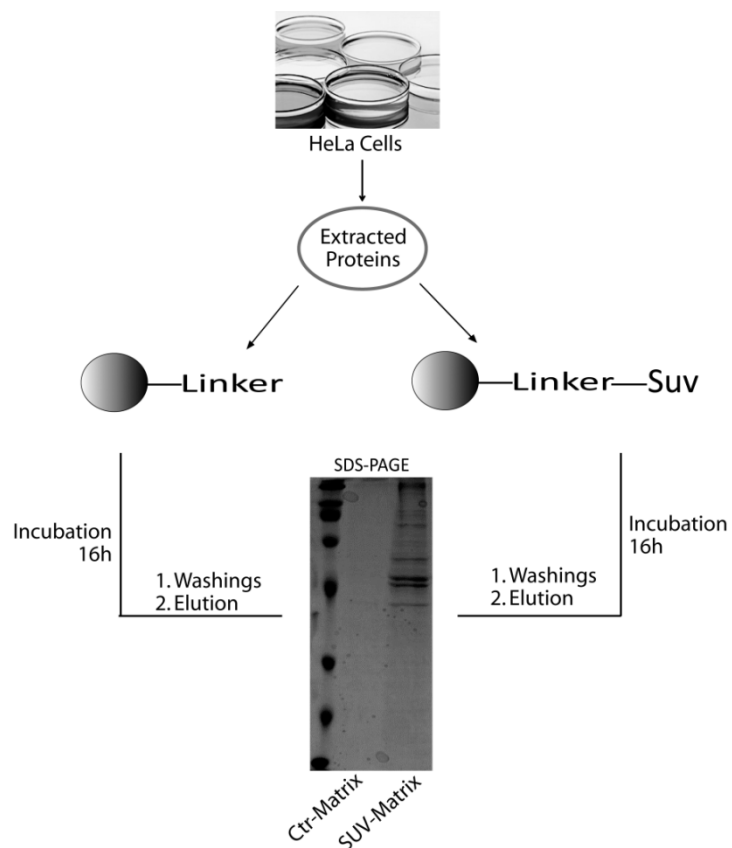


Figure 18. Experimental workflow used to profile SUV interactome.

Both gel lanes were cut into ten pieces and subjected to *in situ* digestion^[146]. The peptide mixtures were then analysed by nano-flow RP-HPLC MS/MS, and protein identification was achieved by submitting the peak lists to Mascot database search. The list of identified proteins was refined by removing the hits found in the control experiments. The results of five independent experiments were combined to generate a smaller list of putative SUV interactors. On the basis of the highest peptide matches (**Table 2**), Heat shock protein 60 (HSP60) was recognized as the prominent SUV biological target.

Results and Discussion

Proteins	Exp1	Exp2	Exp3	Exp4	Exp5
60 kDa HSP, mitochondrial (CH60 human)	25 (21)	50 (39)	50 (35)	24 (23)	24 (23)
importin-5 (IPO5 human)	32 (23)	13 (7)	14 (14)	13 (8)	20 (19)
tubulin b-3 chain (TBB3 human)	16 (15)	24 (22)	13 (11)	13 (8)	12 (11)
tubulin a-4A chain (TBA4A human)	16 (13)	19 (16)	16 (16)	10 (8)	17 (14)

Table 2. List of SUV partners identified in five independent chemical proteomics experiments. The results are reported in terms of number of identified peptides.

Heat shock proteins are molecular chaperones that guide several steps during synthesis, transportation, and degradation of proteins^[147], and are highly conserved and abundant in the cell^[148]. During stress, their synthesis is rapidly up-regulated (in prokaryotic as well as in eukaryotic cells), and changes in intracellular location have been observed, including their expression on the cell surface^[149]. Mammalian HSP60 is also an important auto-antigen during chronic inflammation or atherosclerosis^[150] and exhibits immunoregulatory properties, primarily by inducing pro-inflammatory responses in innate immune cells^[149]. Moreover, HSP60 was found to synergize with IFN- γ in its pro-inflammatory activity modulating gene expression of the cytokines IL-12 and IL-15^[150]. Thus, we moved toward the validation of the direct interaction between HSP60 and SUV, and to assess the potential alteration of the chaperone activity.

2.3 *In vitro* validation of HSP60-suvanine interaction

The ability of SUV and SUV-AL to interact with HSP60 was further explored by exposing samples of the control and suvanine-bearing beads to recombinant

(human) HSP60^[151]. The experimental workflow was very similar to that described above during the fishing of the SUV interactors from the cell extracts. Thus, after 1h of incubation and abundant washings, both CTR-matrix and SUV-matrix were exposed to a high denaturing buffer, and then the eluates were subjected to SDS-PAGE. Comparative analysis of the obtained gel (**Figure 19A**) showed a significant enrichment of HSP60 in the experiment with SUV, compared with the control, thus confirming a direct binding between the small molecule and the protein target.

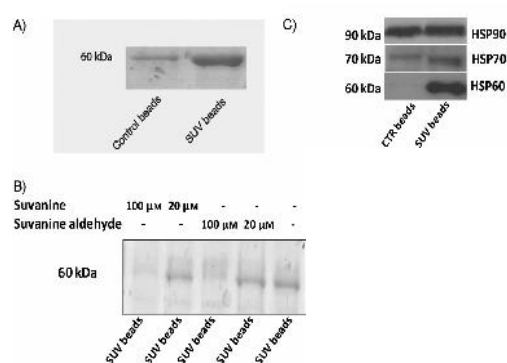


Figure 19. A) SDS-PAGE of HSP60 (~60kDa) on suvanine-modified beads (SUV) and control beads. B) HSP60 binding to suvanine-modified beads is reduced after incubation of HSP60 with SUV and SUV-AL at different concentrations. C) Western blots on eluates from suvanine-modified and control beads (CTR) after incubation with HeLa cell lysate, by using HSP60, HSP70, and HSP90 antibodies.

Then, we tested the binding of both SUV and SUV-AL in their free forms to HSP60, by pre-incubating human recombinant protein with each molecule at different concentrations, and then treating these mixtures with samples of SUV-bearing beads. The resulting gel (**Figure 19B**) showed that both molecules formed stable complexes with HSP60, hampering its capture by the modified beads. The binding specificity of SUV and SUV-AL with HSP60

Results and Discussion

was also assessed against a group of heat shock proteins, such as HSP70 and HSP90. In some details, after exposing the SUV-modified beads to a sample of HeLa cells extract, the eluted proteins were analysed through western blotting using antibodies directed anti-HSP60, HSP70 and HSP90. The blots reported in **Figure 19C** clearly showed a selective enrichment of HSP60 by SUV, while HSP70 and HSP90 were also detected in the control experiment.

Because of the relevance of HSP60 into inflammation and immune responses, our investigation was deepened by using surface plasmon resonance (SPR) for the measurement of the protein affinity to both SUV and SUV-AL. HSP60 was immobilized on a CM-5 sensor chip and both molecules were separately injected at various concentrations onto the chip (0.5–10 μM). The resulting sensogram curves (**Figure 20**) were analysed by curve fitting (1:1 Langmuir algorithm), giving dissociation constants (K_D) of 0.6 (± 0.5) and 1.0 (± 0.8) μM for SUV and SUV-AL, respectively, that suggested the occurring of strong interactions between the counterparts.

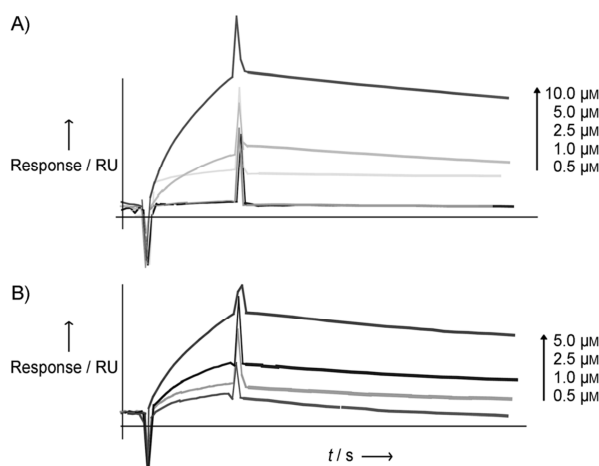


Figure 20. Sensogram curves for the binding of SUV (A) and SUV-AL (B) (0.5–10 μM) with HSP60. Each experiment was performed at least in triplicate.

2.4 HSP60 chaperone activity inhibition by Suvanine

Then, we wanted to assess if the affinity of SUV and SUV-AL with HSP60 could also affect its chaperone activity. Thus, the ability of HSP60 to refold the citrate synthase (CS) to its active state under non-permissive conditions (to minimize spontaneous refolding) was tested *in vitro* in presence and absence of our compounds^[152, 153]. This is a convenient assay, since both thermally and chemically induced CS unfolding and refolding can be easily monitored by a colorimetric test^[152]. Indeed, as schematically reported in **Figure 21** and explained in the experimental section, the completely folded CS is able to catalyse the production of citrate and CoA from Oxalacetate and Acetyl-CoA. Thus, the activity of CS can be spectrophotometrically monitored at 412 nm by adding 5,5'-dithio-bis(2-nitrobenzoic acid) (DTNB) that, reacting with CoA, produces the 2-nitro-5-thiobenzoate anion (TNB), an intense yellow coloured compound.

In our experimental design, CS was chemically unfolded by guanidine and then refolded after addition of the HSP60–HSP10 complex.

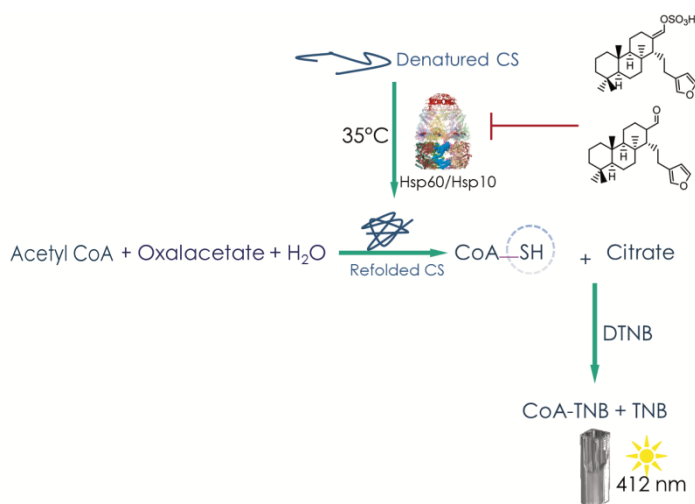


Figure 21. Schematic representation of the colorimetric assay employed to evaluate SUV and SUV-AL capability to inhibit HSP60 activity

Results and Discussion

As shown in **Figure 22**, CS recovers about 80% of its activity after its refolding induced by HSP60–HSP10, whereas in the presence of different amounts of SUV and SUV-AL, the enzyme recovery was decreased as a result of the inhibition of the HSP60–HSP10 chaperone activity.

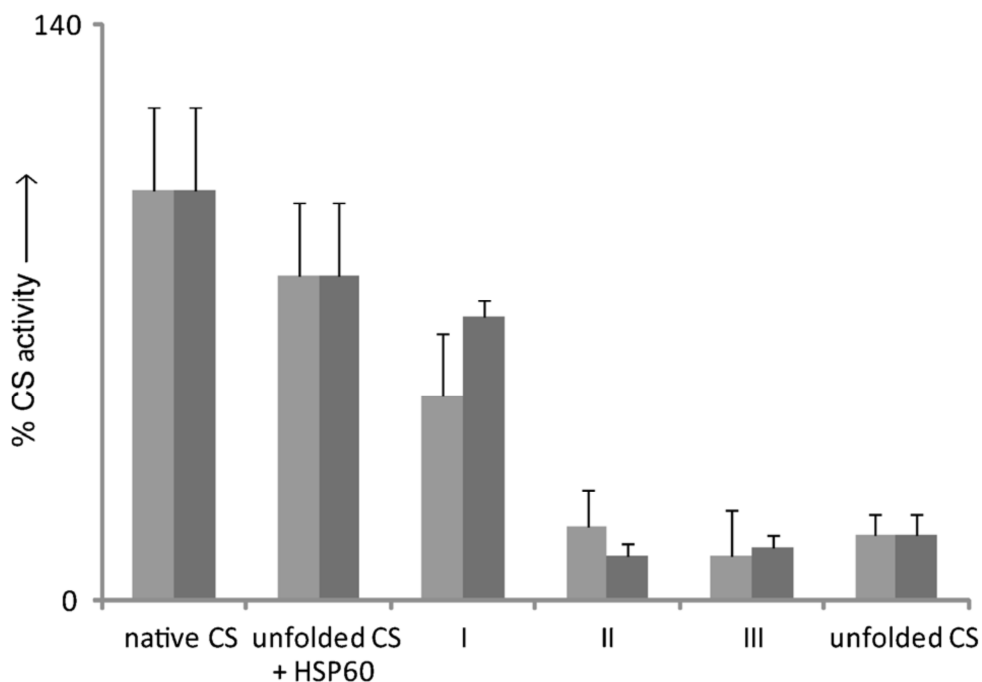


Figure 22. Inhibitory effects of SUV (light gray) and SUV-AL (dark gray) on HSP60 refolding of CS. The data are shown as percentage of CS activity relative to native CS. Activity of CS refolded in the presence of HSP60 pre-incubated with I: 3.2 μ M SUV, 32 μ M SUV-AL; II: 16 μ M SUV, 80 μ M SUV-AL; III: 32 μ M SUV, 160 μ M SUV-AL.

To exclude a direct activity of SUV and SUV-AL on CS, we replicated the same experiment in permissive condition. At room temperature, CS recovered its activity in absence of molecular chaperones, even in presence of both molecules.

It is noteworthy that SUV showed a greater inhibitory effect than its aldehyde congener on the HSP60–HSP10 chaperone activity despite their similar

dissociation constants. This could be attributable to the charged sulphate functionality on SUV, which could enhance HSP60 inhibition. A similar behaviour was also reported in the case of the PLA₂ inhibition^[141].

All the collected data demonstrate that SUV is able to interact with HSP60 inhibiting its chaperone activity. The identification of SUV as a new HSP60 inhibitor could be helpful for future studies on the human HSP60 mechanism of action. Moreover, since this inhibition is strictly connected with the anti-inflammatory properties of SUV, this finding opens the way to the rational design of new potential anti-inflammatory drugs. In fact, despite the importance of this protein in immunoregulatory and inflammatory processes, only few examples of natural compounds, such as mizoribine^[154] and epolactaene^[155], have been reported as HSP60 inhibitors.

-CHAPTER 3-

Heteronemin, a marine sponge terpenoid, targets TDP-43, a key factor in several neurodegenerative disorders.

Based on: *Chem. Commun. (Camb.)*, **2013**, 50, 406–408

3.1 Affinity purification and identification of HET partners

The identification of the entire cellular interactome of a bioactive natural product is crucial to define its specific mechanism of action, giving a rational support to the observed pharmacological effect^[156] and also to identify its off-target activities responsible for multi-pharmacological and/or side effects. Natural compounds are recognized as unique and essential biological probes, mainly due to their peculiar, high functionalized structures. Often, these characteristics are responsible for a multi-target behaviour that should be accurately defined to have a deep comprehension of their pharmacological and toxicological properties.

Heteronemin (HET) (**Figure 23**) is a marine sesterterpene endowed with a significant pharmacological profile, isolated from the sponge *Hyrtios* sp.^[157]. Indeed, HET has been recently discovered as a potent modulator of the TNF α -induced NF- κ B pathway, driven by the inhibition of the proteasome system, and also recognized as an apoptosis inducer^[158]. Due to these interesting properties, HET has been considered a good candidate for the application of a chemical proteomic approach.

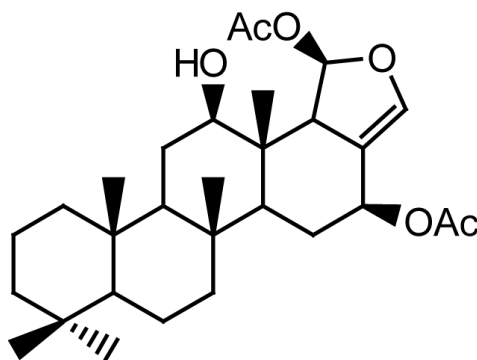


Figure 23. HET structure

Results and Discussion

The natural compound was first immobilized onto an epoxy activated sepharose beads by means of the alcoholic function located on the C ring (**Figure 24**). To assess the reaction yield, integration of RP-HPLC-UV peak areas of the free HET before and after 2.5 h of reaction in ACN/NaHCO₃ was performed (**Figure 24**). Once recovered around 75% of reaction yield, corresponding to 16 μ mol of HET per ml of resin, the coupling process was completed by the inactivation of the free epoxy-groups of the resin with isopropanol.

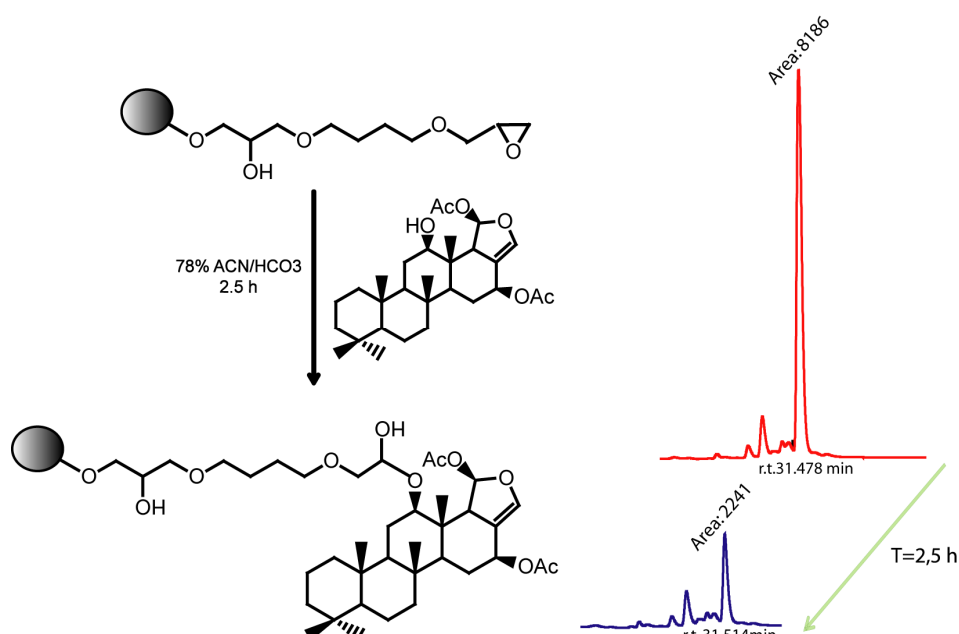


Figure 24. Reaction scheme of HET immobilization on sepharose beads and HPLC profile of free HET before and after coupling reaction.

Then, crude extracts from HeLa cells were incubated with a sample of the HET-bearing matrix to promote the interactions between the compound and its potential protein partners. After removal of the soluble phase, several washing steps were done on the solid phase to reduce non-specific adsorption, while the

tightly bound proteins were eluted with a strong denaturing buffer and then resolved by 12% SDS-PAGE (**Figure 25**). In order to distinguish between specific and residual non-specific interactions, a control experiment was performed with a sample of epoxy-sepharose beads inactivated with isopropanol. On the basis of the comparison between the control and sample gel runs, three bands, at 60, 45 and 20 kDa, were clearly enriched in the HET-related gel lane.

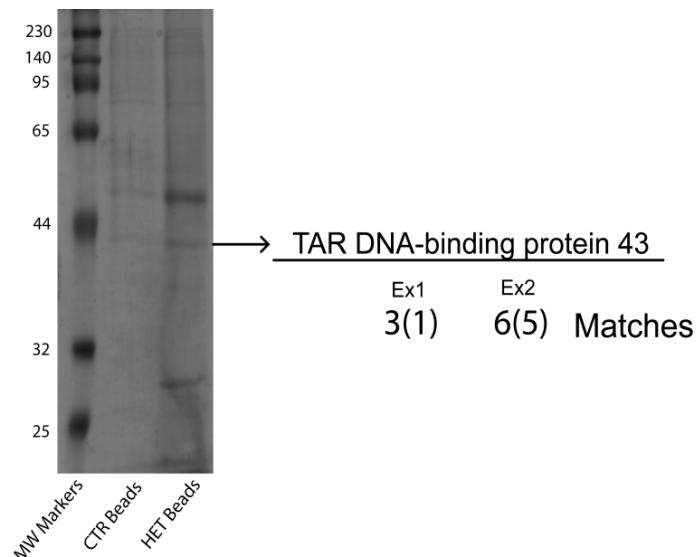


Figure 25. SDS-PAGE of the eluted proteins from HET and control-beads; the arrow corresponds to the band of TDP-43.

After triplication of the experiment on fresh cell lysates, the three bands were cut from each independent experiment, together with the corresponding bands of the control experiment, and subjected to *in situ* digestion^[146]. The peptide mixtures were then analysed by nano-flow RP-LCMS/MS, and protein identification was achieved by submitting the peak lists to Mascot database search. Superimposition of all the results gave the identification of tubulin in the band at 60 kDa, which was also present, even if in lesser amount, in the

Results and Discussion

control lane, TAR-DNA-binding protein 43 (TDP-43) and proteasome subunits α in the bands at 43 and 20 kDa, respectively, which were fully absent in the correspondent control bands. On the basis of these data, the proteasome complex and TDP-43 were recognized as main partners of HET, the first one already reported in literature^[158], while TDP-43 as new potential interactor.

The binding affinity of HET with TDP-43 was then assessed by immunoblotting and surface plasmon resonance (SPR) analyses.

HET-modified beads and control beads were exposed to HeLa cell extracts and eluted proteins were analyzed by western blotting using an anti-TDP43 antibody. In the eluates coming from the HET-bearing matrix, a relevant enrichment of TDP43 was clearly visible (**Figure 26**)

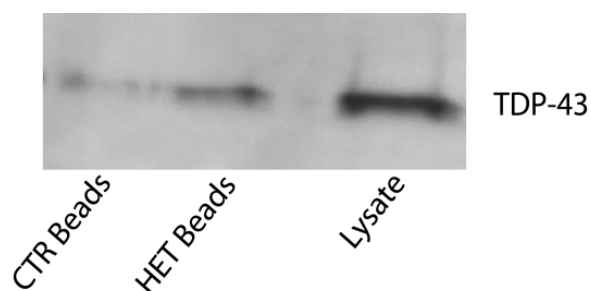


Figure 26. Western blot analysis on proteins eluted from control and HET-beads incubated with HeLa cell lysates.

The interaction affinity between the marine compound and TDP-43 was measured through SPR experiments. The protein was immobilized onto the chip and HET was injected at various concentrations (from 0.01 to 25 μ M). The resulting sensorgrams (**Figure 27**) were analysed by curve fitting (1:1 Langmuir algorithm) giving a dissociation constant (K_D) of 270 ± 120 nM for

the TDP-43-HET complex, thus suggesting a relevant interaction between the counterparts.

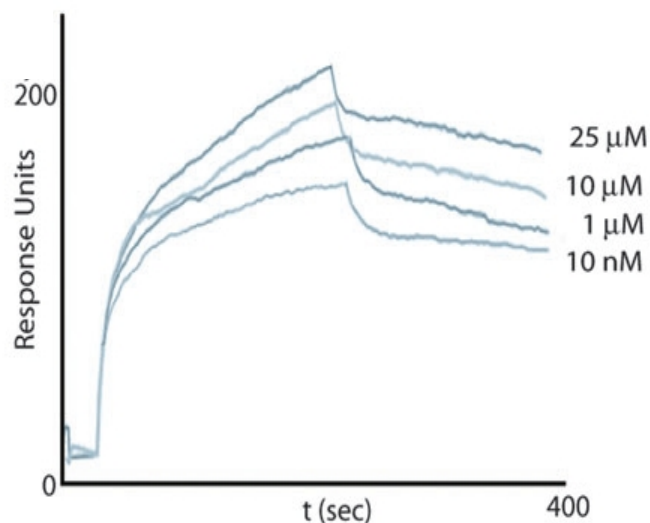


Figure 27. Sensorgrams obtained from the binding of HET (0.01–25 μM) to immobilized TDP-43.

TDP-43 is an abundant and ubiquitous protein, well-conserved among mammals and invertebrates^[159]. Firstly identified as a binding partner of the human immunodeficiency virus TAR DNA element^[160], TDP-43 is known to be involved in transcriptional repression, exon splicing, mRNA generation, cell cycle regulation and apoptosis^[161]. By means of two recognition motifs (RRMs), termed RRM1 and RRM2, TDP-43 binds both mRNA and DNA, thereby regulating mRNA splicing, stability and translation as well as gene transcription^[162].

TDP-43 is also one of the major components of tau-negative and ubiquitin-positive inclusions that characterize amyotrophic lateral sclerosis (ALS) and front-temporal lobar degeneration (FTLD) linked to TDP-43 pathologies

Results and Discussion

(FTLD-TDP)^[163]. The disease-related TDP-43 protein is characterized by hyper-phosphorylation, cleavage, ubiquitination, mislocalization and aggregation into insoluble aggregates^[164-166]. Moreover, although TDP-43 regulates mRNA levels under normal physiological conditions, some evidence indicates that TDP-43 is a stress-responsive RNA-associated factor. Exposure to a variety of stressors, which promote oxidative stress, and to heat shock leads to accumulation of insoluble TDP-43 aggregates similar to those observed under pathological conditions^[167,168]. More recently, several studies have demonstrated that exposure to stress causes TDP-43 re-localization into stress granules (SGs), cytoplasmic foci that represent both sites of translational stalled RNAs and active sites of RNA regulation and sorting^[169,170]. Although the descriptive nature of SG localization reveals a physical incorporation of TDP-43 within SGs, whether TDP-43 has an active role or a causal role within SGs remains uncertain.

On the basis of the relevance of TDP-43 in several neurodegenerative disorders, our study has been extended to the evaluation of the HET effects on TDP-43 biological activity, whose results will be discussed below.

3.2 HET enhanced TDP-43 aggregation *in vitro*

In several neurodegenerative disorders, TDP-43 becomes increasingly insoluble showing an aberrant pattern of phosphorylation and ubiquitination^[171]. Therefore, we focused our attention on the modulation of the TDP-43 aggregation state induced by HET through immunoblot analysis. TDP43 has a strong tendency to form high molecular weight aggregates both *in vitro* and in cell^[171]. Indeed, the recombinant TDP43 easily aggregates upon gentle mixing at room temperature^[172]. Therefore, as suggested by Cohen and co-workers^[172], TDP-43 was stored at high concentrations in a detergent-

containing buffer (25 μ M in 33% glycerol, 80 mM Tris-HCl, 0.1% SDS 1 mM DTT) in order to keep TDP-43 in a non-aggregated state, and then immediately diluted (1:500) and added to HET (50 folds molar excess) or DMSO as control. Samples were then centrifuged and both pellets and supernatants were carefully separated and diluted with a mix of urea and thiourea before loading on a 10% SDS-PAGE. As shown in **Figure 28**, the treatment of TDP-43 with HET resulted in an increased amount of high molecular weight bands corresponding to TDP-43 supra-molecular adducts insoluble in urea buffer.

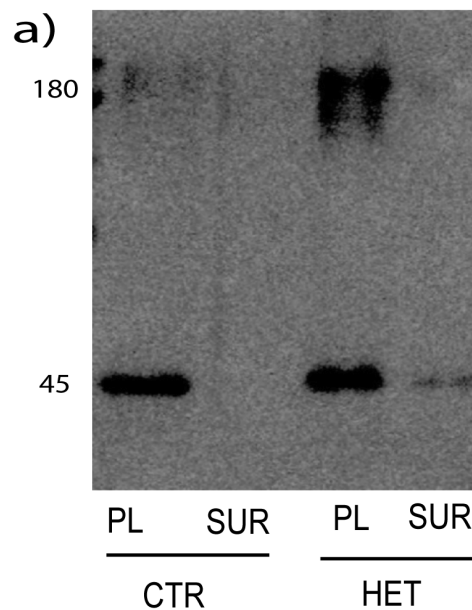


Figure 28. Western blotting analysis of the pellet and supernatant fractions of recombinant TDP43 treated or not with HET 2.5 μ M.

3.3 HET inhibits bt-TAR-32 DNA binding to TDP-43

Several reports have indicated that the solubility of TDP-43 is largely influenced by its binding to the cognate single-strand DNA (ssDNA) or RNA

Results and Discussion

(ssRNA), suggesting an intimate relationship between TDP-43 aggregation process and the factors that alter its DNA or RNA binding affinity^[173]. Since the single strand (ss)-DNA bt-TAR-32 is well known to specifically targets TDP-43^[174], we moved to measure the HET effect on this binding by Amplified Luminescent Proximity Homogeneous Assay Screen (alpha-screen)^[175]. The application of this versatile technology, a bead-based proximity assay, allowed us to measure the potential inhibition of the oligonucleotide binding to TDP-43 by HET. Briefly, samples of GST-fused TDP-43 and biotinylated ssDNA were bound on photosensitive acceptor and donor beads, respectively, and their affinity was measured by recording the intensity of the chemiluminescent signal produced during the interaction event, in presence and absence of HET (**Figure 29**).

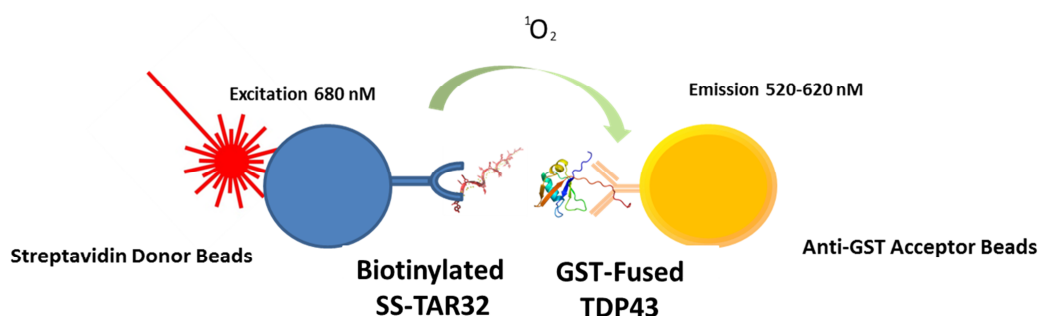


Figure 29. Schematic representation of Alpha screen experiment.

As reported in **Figure 30**, HET produces a concentration dependent reduction of the signal relative to TDP-43 interaction with ssDNA, with a measured IC_{50} of 10.1 ± 0.5 nM. This evidence connects the mere interaction between TDP-43 and HET to a specific biological effect of the marine metabolite on the protein function, that is a relevant inhibition of the TDP-43 binding to its DNA target strand. Since the TDP-43 RNA-recognition domains RRM1 and RRM2, strictly involved in the DNA or RNA binding, are located in the middle

domain of the protein, on the basis of our results a possible interaction of HET with this region can be postulated.

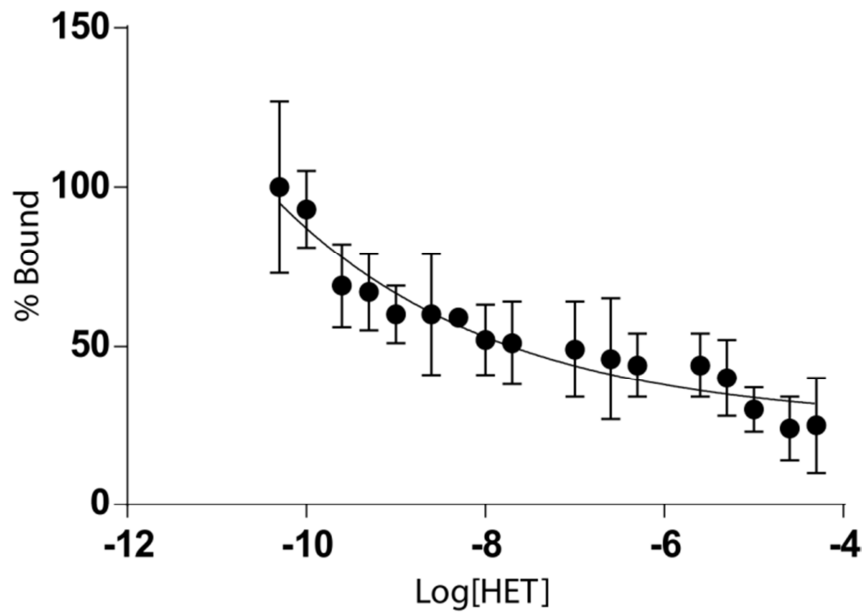


Figure 30. Inhibition of bt-TAR-32 binding to TDP-43 by HET by alpha-screen. Data are reported as percentage of bt-TAR-32 bound vs log [Het]. The curve was convoluted using GraphPad Prism. Each point represents three determinations from three experiments.

3.4 HET increases cytoplasmic TDP43 content and its localization in stress granules.

To deeply investigate the effect of HET on TDP-43 in the whole cell compartment, HeLa cells were incubated with the marine metabolite and/or heat-stressed, and then analyzed by immunofluorescence. These experiments were planned to measure the potential involvement of HET in the TDP-43

Results and Discussion

cellular localization in HeLa models. Additionally, since the heat stress treatment has been reported to drive TDP-43 into stress granules^[176,177], we were also interested in measuring the effect of our marine drug on this pathway. An immunofluorescence assay was used to observe the TDP-43 cellular localization. HeLa cells were incubated with HET at 10 μ M for 2h and then with different primary antibodies, one against TDP-43 and another against a stress granules marker called HuR (human antigen R). The labelling was visualized with fluorescently conjugated secondary antibodies.

As expected, in the vehicle (less than 1% DMSO) treated cell sample the TDP-43 expression is restricted to the nucleus and no stress granules were present in the cytosol (**Figure 31a**). After a heat-shock treatment of 1h at 43°C, many SGs were formed in the cell cytosol, together with a low quantity of TDP-43 coming from the nucleus (**Figure 31b**). Upon treatment with HET 10 μ M for 2h, a clear cytoplasmic accumulation of TDP-43 was observed with no evidence of stress granules development (**Figure 31c**). When HeLa cells were first incubated with HET for 2h and then heat shocked for 1h a clear increase of HuR positive and TDP-43 positive SGs were observed (**Figure 31d**). In order to quantify the differences between the sample treated or not with HET and heat-shocked at 43°C, we compared the counts of HuR positive granules (SGs) and the TDP-43 positive SGs. While in the HET treated cell sample very few SGs were detected, a relevant number of HuR-positive SGs was found in the heat-shocked cells. Moreover, when the cells were pre-treated with HET before heat shock, the increase of the total SGs and of TDP43 positive SGs per cell was higher than the control untreated cells (**Figure 32**), thus indicating that HET promotes TDP-43 aggregation also in a living cell system. All experiments were repeated in presence of MG132, a known proteasome inhibitor, which induced the formation of SGs and TDP-43 positive SGs only in a very low extent in respect to HET (**Figure 32**).

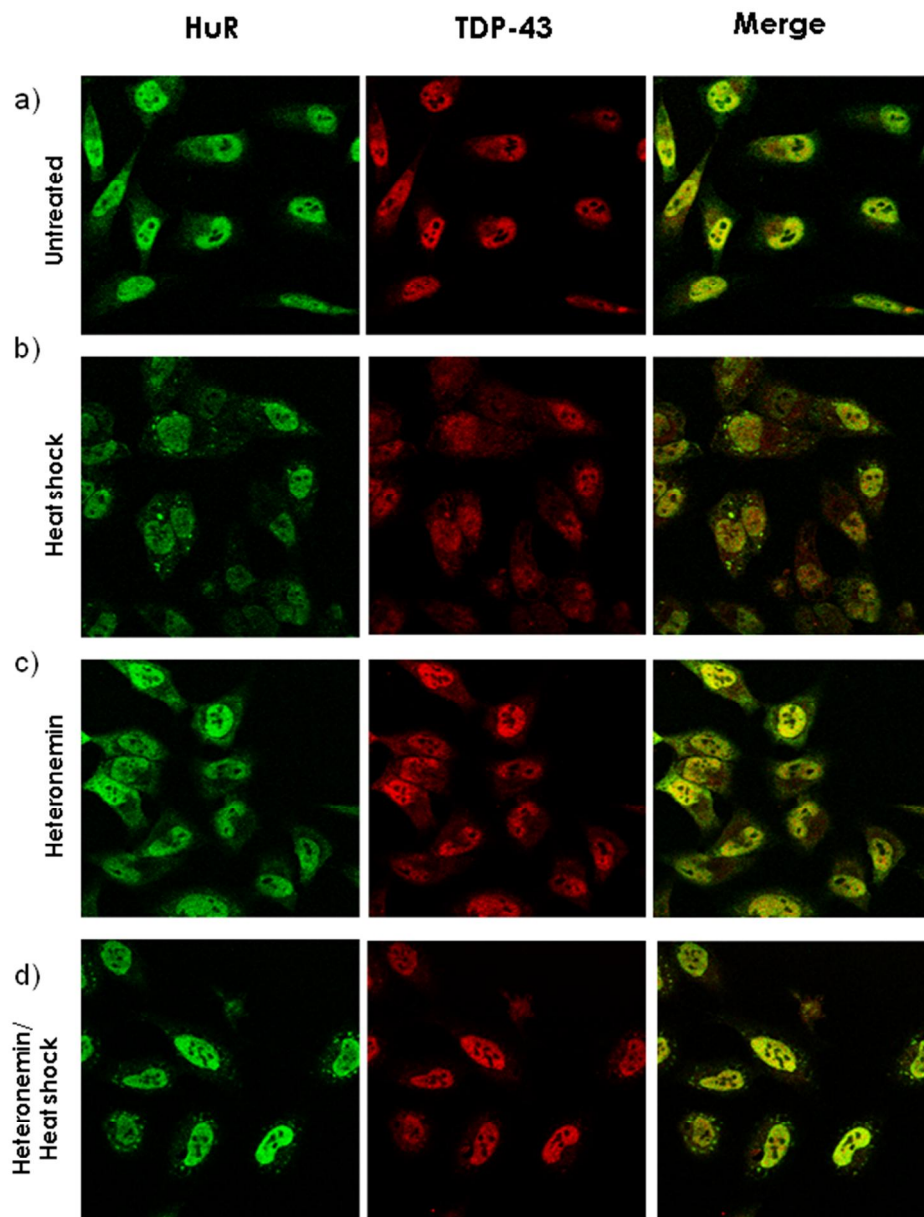


Figure 31 HeLa cells cultured on cover slips were left untreated (a) or pre-treated with 10 μ M HET (c), then 43 °C heat shocked (b,d) and subsequently immuno-labeled for TDP-43 and the SG marker HuR. TDP-43 localization to SGs is indicated by the merged images showing the overlap between red and green signals

Results and Discussion

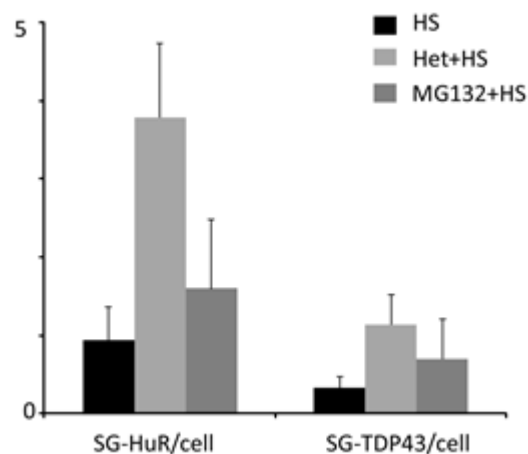


Figure 32. TDP-43 and HuR-positive SGs were counted in HS, HET+HS and MG132 treated cells. A minimum of 200 cells were counted across multiple fields of view (and multiple coverslips) for each treatment. The total number of HuR or TDP-43 positive SGs was divided by the total number of cells to provide a mean measure of SGs per cell. Data were expressed as fold induction of HuR positive mean SGs in HS cells set to 1.

Since it is reported that HET inhibits TNF α -induced NF- κ B activation through proteasome inhibition in chronic myelogenous leukemia cells^[158] and a clear involvement of the proteasome inhibition in the cytoplasmic accumulation of TDP-43 in some neuronal cells is also reported^[178], we performed a following experiment to exclude the possibility of a proteasome inhibition by HET in HeLa cells. In details, proteasome activity was measured upon HET administration to HeLa cells by detecting the proteasome-mediated proteolysis of a fluorogenic peptide substrate, specific for the chymotrypsin catalytic subunit^[114]. Since the chymotrypsin-like activity of the HeLa proteasome was not impaired by the treatment with HET for 2 h at 10 μ M (**Figure 33**), the previously measured biological effect of HET on TDP-43 cellular localization can be evidently attributed to the direct interaction between the counterparts. MG 132, a known proteasome inhibitor, was used as positive control.

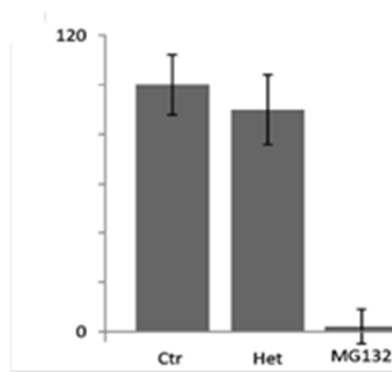


Figure 33. Analysis of proteasomal chimotrypsin-like activity. Inhibition in HeLa cells by HET and MG132.

Finally, to confirm the immunofluorescence data by independent experiments, immunoblot analysis was carried out separately on the supernatants and pellets portions upon HET and vehicle treatment of HeLa cell lysates. As clearly reported in **Figure 34**, HET confirmed its ability to induce an accumulation of insoluble TDP-43 species found in pellets whereas MG132, used as control, did not affect the TDP-43 solubility profile.

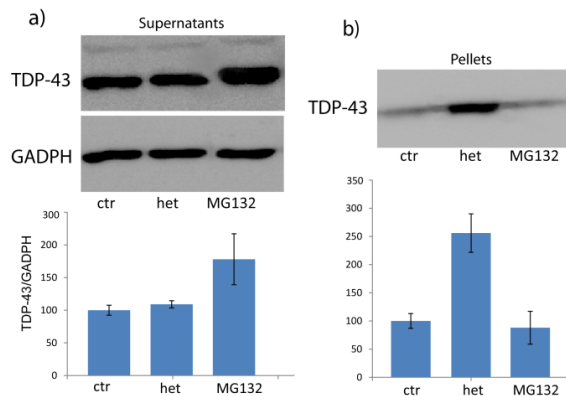


Figure 34. Western blotting analysis of TDP43 found in supernatant (soluble proteins, a) and pellet (b) fractions of HeLa cell lysates treated or not with HET 10 μ M and MG132 50 μ M.

Histograms were the results of image quantification analysis of three independent experiments.

Results and Discussion

Huang and coworkers^[173] recently reported that TDP43 aggregation is mostly retarded or even prohibited in the presence of its cognate DNA/RNA, and that the loss of the binding ability to DNA/RNA causes TDP-43 to form large aggregates. Thus, since our TDP43/bt-TAR-32 binding analysis revealed the role of HET in lowering the TDP43 affinity to its target DNA, and the following experiments demonstrated the HET-induced cytoplasmic translocation and aggregation of TDP43, a mechanistic insight could be depicted, in which the marine compound targets TDP-43 lowering its affinity towards nucleic acids, that in turn induces a translocation of the protein to the cytoplasm and a consequent tendency to form insoluble aggregates in the form of stress granules. This stress granules are known to contribute to the pathogenesis of several disorders, including fragile-X syndrome, spinal muscular atrophy, and ischemia reperfusion injury, caused by altered RNA-binding proteins^[164-167].

Our findings provide the evidence that HET is involved in the binding, solubility alteration, subcellular localization and formation of small nuclear inclusions of TDP-43 protein. These data suggest a role for this marine compound as a novel stressor and promoter of TDP-43 localization to HuR positive stress granules, and consequently as a relevant chemical tool in TDP-43-based cellular investigations.

-CHAPTER 4-

In cell chemical proteomics by copper-catalyzed Huisgen 1,3 dipolar
cycloaddition

Based on: “In cell Scalaradial Interactome Profiling Using a Bio-Orthogonal
Clickable Probe” *Submitted*

4.1 Background

Mass-spectrometry-based chemical proteomics has been revealed as a powerful technique to define the interactome of bioactive compounds opening the way to the design of new therapeutic or biotechnological tools^[114,115]. As extensively discussed in the introduction (see chapter 1), classical methodologies based on the *in vitro* employment of small-molecules anchored on solid supports, are characterized by some limitations, mostly due to cellular lysis. In fact, this process exploits sonication or detergents that can alter the multi-protein complexes or even lead to a change in the protein conformation, in turn compromising the interaction with the small molecule probe^[180]. Moreover, *in vitro* protocols require the immobilization of the small molecule onto a solid surface, which could orient the molecule into a forced conformation altering the recognition of some potential interactors^[9]. For these reasons, new approaches based on the bio-orthogonal chemistry have been proposed to recover the targeted proteins of a small molecule in living systems. As a matter of fact, bio-orthogonal reactions have demonstrated to be highly reliable, selective and bio-compatible, finding a large employment in ABPP procedures and applications in the fields of bio-organic chemistry, drug discovery, proteomics and DNA research^[181]. Substantially, three organic reactions, belonging to the class of the so-called click-chemistry approaches, have proven to match the bio-orthogonality criteria, that are kinetics, selectivity and compatibility with non-organic solvents: the copper-catalysed azide-alkyne cycloaddition, the Staudinger-Bertozzi ligation, and the copper free cycloaddition (see chapter 1). The former one, a variant of the Huisgen's 1,3-dipolar cycloaddition, is to date the most investigated click-chemistry reaction, and relies on the ability of an azide and a terminal alkyne to yield a stable triazole ring in presence of Cu(I) as a catalyst^[182,183].

Results and Discussion

Aiming the optimization and tuning of an in cell protocol to “fish out” the macromolecular partner(s) of a small molecule, we first applied the *in vitro* pull down method to identify the targets of Scalaradial (SLD), and then we used these results as a reference point for the development of the new in cell approach.

SLD is a sesterterpenoidic molecule with a scalarane-skeleton, isolated by Cimino and co-workers^[184,185] from the sponge *Cacospongia mollior*, endowed with a relevant anti-inflammatory profile both in *in vitro* and *in vivo* models [186-190].

The experimental workflow for the *in vitro* approach is almost similar to that previously described for Suvanine (chapter 2) and Heteronemin (chapter 3) (**Figure 35A**), save that we employed a spacer arm containing a cleavable site. This kind of linkers are useful to perform the targets elution step in non-denaturing conditions, allowing also the minimization of the background proteins (**Figure 37**). Briefly, SLD was (i) functionalized with a di-amine linker containing a disulphide bond and immobilized onto a solid support; (ii) then, the SLD-bearing matrix was used in the affinity chromatographic step, and (iii) after several washings, the tightly bound proteins were recovered by breaking the disulphide bond with a reducing agent and then identified with nanoLC-MSMS. In the last step (iv) western blot analysis and surface plasmon resonance were employed to validate the obtained results.

The in cell protocol starts with the decoration of the small molecule with an appropriate functional group for the bio-orthogonal reaction, such as an azide or a terminal alkyne. Then, the living cell sample is treated with the tagged molecule to allow its translocation inside the cells and develop the interactions in a native environment. After a mild lysis the cell content is treated with the appropriate mixture of reagents to promote the linking of the drug, carrying its selected protein partners, onto a solid matrix (**Figure 35B**). On this basis, we chemically modified SLD with an azide-bearing spacer arm and then

optimized the conditions of the copper catalyzed Huisgen cycloaddition reaction in solution, before the application in a living cell context.

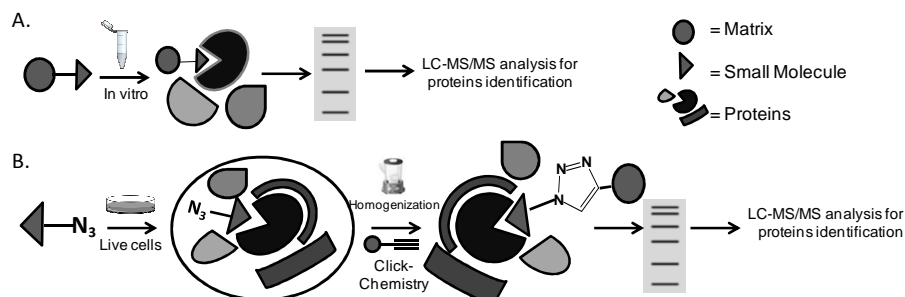


Figure 35. Workflow of *in vitro* (A) and cell-based (B) chemical proteomics of small molecules followed by nano-ESI-LCMSMS targets identifications.

4.2 *In vitro* SLD Proteome Profiling

The *in vitro* affinity purification experiments were carried out immobilizing SLD on carbonyl-di-imidazole (CDI) agarose beads through the insertion of an opportune spacer arm, between the matrix and the molecule, to minimize steric hindrance during the affinity chromatography phase.

The immobilization was achieved in two steps: (i) SLD was first linked to the 2-(2-amino-ethyl-disulfanyl)-ethyl-amine linker (TIOS), exploiting the reactivity of the SLD di-aldehyde moiety with the terminal amino group of the spacer arm (**Figure 36**), and (ii) then the obtained adduct was linked to the CDI solid support. The reaction between SLD and TIOS was monitored by RP-HPLC-MSMS and produced, in 1h, a covalent SLD-TIOS adduct (**Figure 36A**). The reaction mechanism was postulated on the basis of our previously published data^[189,190] and of MS and MSMS analysis. In particular, a Schiff base intermediate, formed after reaction between the TIOS amino group and one of the aldehyde moieties on the SLD D ring, evolved in a pyrrole adduct

Results and Discussion

by elimination of a water molecule. This last product was then purified by mean of RP-HPLC-UV and put in reaction with the CDI-agarose matrix. The immobilization, mediated by a condensation reaction between the primary amine of SLD-TIOS and the carboxyl group onto the matrix surface, was monitored by RP-HPLC-UV after injection of small aliquots of the reaction suspension and integration of the SLD-TIOS peak areas at $t=0$ and after 16 h of reaction (**Figure 36B**).

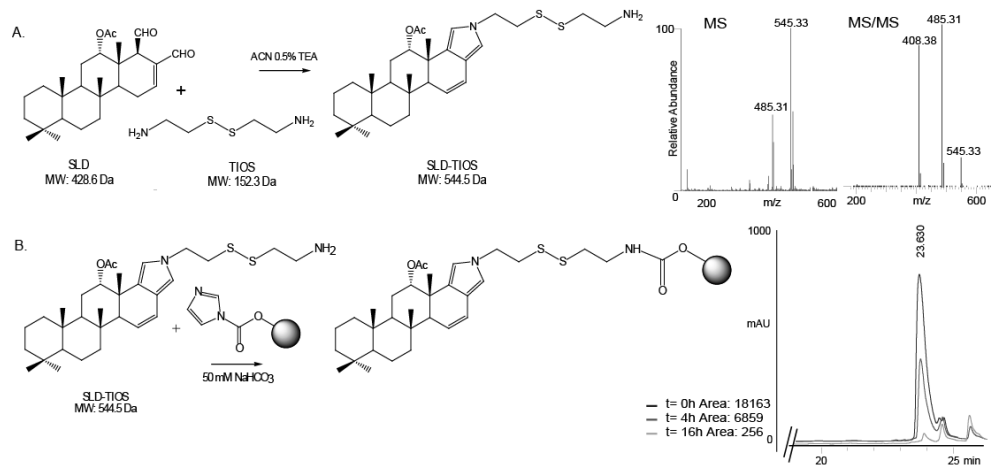


Figure 36. A) SLD-TIOS formation reaction scheme and MS and MS/MS spectra. MS spectrum, shows the MH^+ of SLD-TIOS at m/z of 545.3 and its spontaneous fragment at m/z of 485.3, produced by in-source loss of acetic acid. The MSMS spectrum shows also a peak at m/z of 408.3 corresponding to the induced loss of 2-aminoethanethiol. B) SLD-TIOS immobilization on CDI agarose solid matrix. HPLC-UV trace at 220 nm of reaction supernatant after 0, 4, 16 h of reaction.

Then, the SLD-bearing matrix was used as a bait in the affinity chromatography experiments with crude HeLa cells extracts. After keeping the suspension under rotary shaking for 1h at 4°C, the unbound proteins were discarded and the low affinity bound proteins removed after several washings with a saline buffer. The tightly bound proteins were recovered after cleavage of the disulphide bond of the linker with DTT, a typical expedient allowing the

reduction of the unspecific proteins content (**Figure 37**). Furthermore, to definitively exclude background proteins, a control experiment was performed incubating a matrix-linker adduct sample with the same cellular lysate. Proteins eluted from both resins (SLD and CTR matrixes) were then resolved by 12% SDS-PAGE (**Figure 37**).

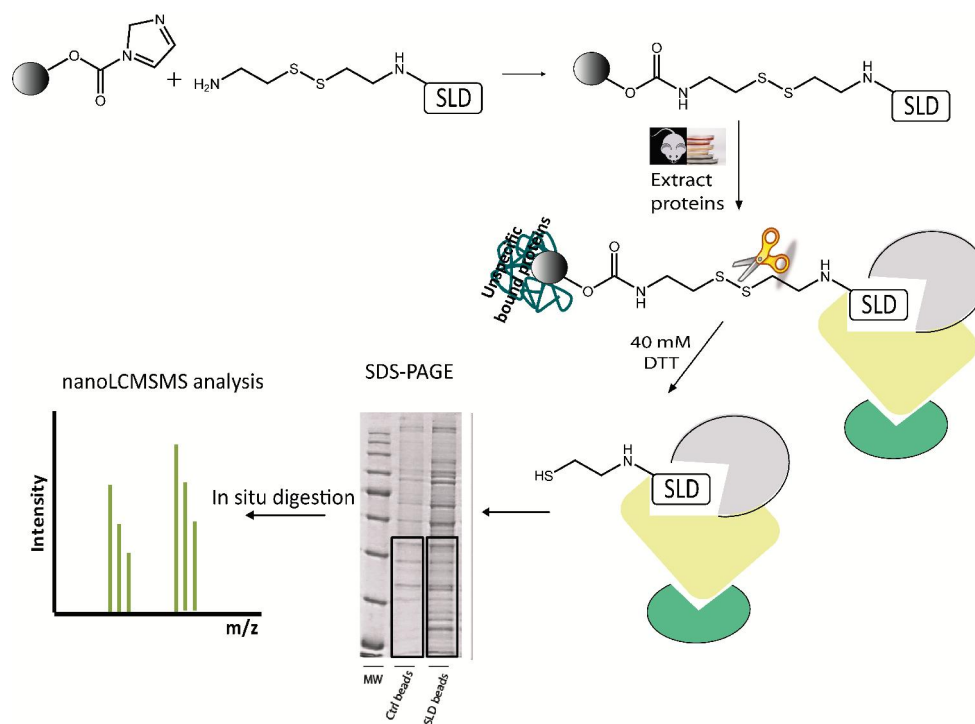


Figure 37. Representation of the experimental workflow for *in vitro* SLD pull down. Proteins selected by SLD and control matrix were released by cleaving the disulphide bridge contained in the spacer arm and separated by SDS-PAGE. Visible enriched bands were *in situ* digested and analysed through LC-MSMS.

The gel lane portions framed within the black boxes (**Figure 37**) were divided in a few pieces and subjected to an *in situ* digestion protocol. The peptide mixtures were finally analysed through nano-flow RP-HPLC-MSMS and the proteins identified by submitting the peak lists to the Mascot database.

The list of the SLD interacting proteins was refined by removing the hits

Results and Discussion

shared with the control experiments and superimposing the results of three independent experiments. This refinement led to the identification of several members of the 14-3-3 and peroxiredoxin families (**Figure 38**).

n.	SwissProt	Proteins	Matches
1	ANXA2_HUMAN	Annexin A2	24
2	PRDX1_HUMAN	Peroxiredoxin-1	22
3	EF1A1_HUMAN	Elongation factor 1-alpha 1	19
4	1433E_HUMAN	14-3-3 protein epsilon	18
5	1433B_HUMAN	14-3-3 protein beta/alpha	16
6	1433T_HUMAN	14-3-3 protein theta	14
7	1433Z_HUMAN	14-3-3 protein zeta/delta	12
8	1433G_HUMAN	14-3-3 protein gamma	11
9	1433F_HUMAN	14-3-3 protein eta	11
10	PRDX2_HUMAN	Peroxiredoxin-2	10
11	CYBP_HUMAN	Calcyclin-binding protein	9
12	ECH1_HUMAN	Delta(3,5)-Delta(2,4)-dienoyl-CoA isomerase, mitochondrial	9
13	PRDX6_HUMAN	Peroxiredoxin-6	8
14	PRDX4_HUMAN	Peroxiredoxin-4	8
15	GBLP_HUMAN	Guanine nucleotide-binding protein subunit beta-2-like 1	7
16	MARE1_HUMAN	Microtubule-associated protein RP/EB family member 1	7
17	ANXA5_HUMAN	Annexin A5	6
18	RS3_HUMAN	40S ribosomal protein S3	5
19	MDHM_HUMAN	Malate dehydrogenase, mitochondrial	4
20	EF1B_HUMAN	Elongation factor 1-beta	4
21	CPNS1_HUMAN	Calpain small subunit 1	4
22	RS8_HUMAN	40S ribosomal protein S8	3
23	CN166_HUMAN	UPF0568 protein C14orf166	3
24	PSA5_HUMAN	Proteasome subunit alpha type-5	3
25	ANXA1_HUMAN	Annexin A1	3
26	PSMG1_HUMAN	Proteasome assembly chaperone 1	3
27	ECHM_HUMAN	Enoyl-CoA hydratase, mitochondrial	2
28	EF1D_HUMAN	Elongation factor 1-delta	2
29	LYP1_HUMAN	Acyl-protein thioesterase 1	2
30	PSME1_HUMAN	Proteasome activator complex subunit 1	2
31	PSME3_HUMAN	Proteasome activator complex subunit 3	2
32	HSPB1_HUMAN	Heat shock protein beta-1	2
33	CLIC1_HUMAN	Chloride intracellular channel protein 1	2
34	PSA4_HUMAN	Proteasome subunit alpha type-4	2
35	EI2BA_HUMAN	Translation initiation factor eIF-2B subunit alpha	2
36	PDC10_HUMAN	Programmed cell death protein 10	1
37	GDIB_HUMAN	Rab GDP dissociation inhibitor beta	1

Figure 38. List of SLD interacting proteins obtained after removing hits shared with control and superimposing results from experiments. Number of peptides matched in best MASCOT identification is reported

Due to the high identification scores, we chose 14-3-3 ϵ and PRX1, whose interaction was validated by western blotting and surface plasmon resonance, as reference probes for the optimization of the in cell protocol. Briefly, the

proteins eluted from the control and SLD resin beads were blotted using antibodies anti-14-3-3 ϵ and anti-PRX1. The enrichment of the two proteins in the SLD lanes compared to the control was evident (**Figure 39**), confirming the mass-spectrometric results.

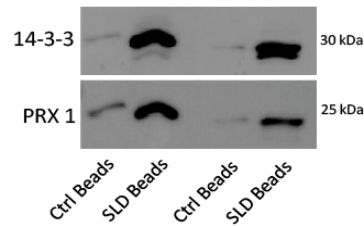


Figure 39. Western blot analysis using 14-3-3 ϵ and PRX1 as probes on proteins eluted in two independent experiments from control and SLD-beads after incubation with HeLa cell lysates.

The interactions of SLD with 14-3-3 ϵ and PRX1 were further confirmed by SPR, allowing also the calculation of the respective dissociation constants. The SPR assay was performed by immobilizing both proteins onto a CM5 sensor chip and injecting solutions containing increasing amounts of SLD. The resulting dissociation constants of 2.24 ± 2.07 and 0.99 ± 0.18 μ M for PRX1 and 14-3-3 ϵ , respectively, suggested a relevant interaction between the counterparts (**Figure 40**).

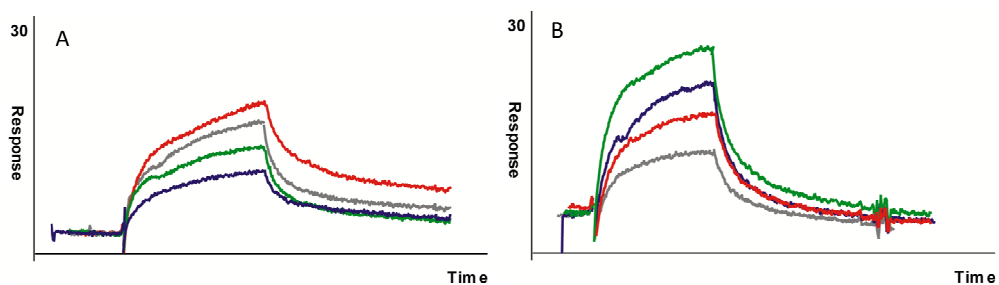


Figure 40. Sensorgrams obtained from the binding of SLD (0.01–25 μ M) to immobilized PRX1 (A) and 14-3-3 ϵ (B).

4.3 In cell Scalaradial proteome profiling

4.3.1 Design and synthesis of SLD-AZ:

The in cell fishing for partners experiment started with the functionalization of SLD with an azide containing linker (**Figure 35B**). Even if, from a theoretical point of view, both functional groups (alkyne/azide) are feasible, our choice was due to the reported potential reactivity of alkynes in the cellular environment^[191]. In particular, the 11-azido-3,6,9-trioxaundecan-1-amine (TRX-AZ, **Figure 41**) linker was chosen for its stability and solubility in aqueous buffer, and for its permeability toward the cellular membranes^[192]. The reaction was carried out under stirring for 1h at 25°C in ACN 0.5% triethylamine using a 10-fold molar excess of the TRX-AZ linker. The product formation was monitored by RP-HPLC-UV, MS and MSMS analyses (**Figure 41**).

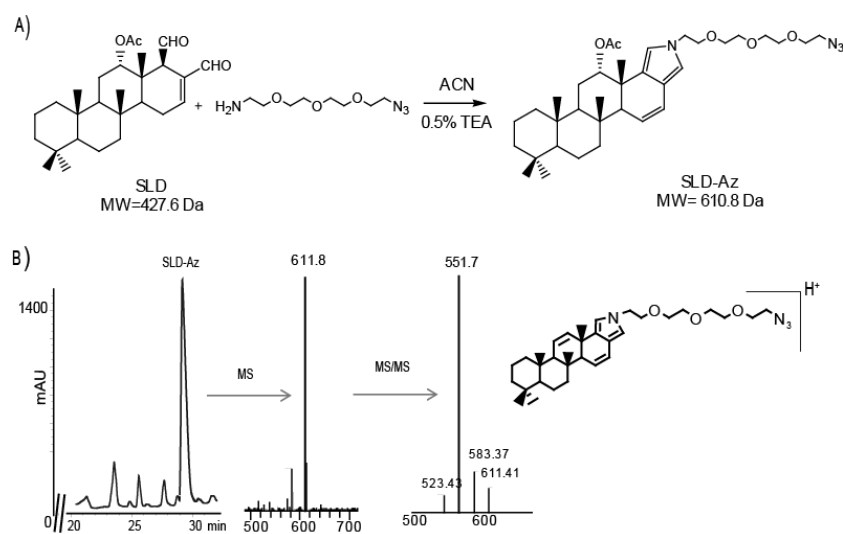


Figure 41. Panel A reports SLD-TRX-AZ interaction pathway. Panel B shows its HPLC-UV trace, MS and MS/MS spectra. In the MS spectrum, the base peak at m/z of 611.8 corresponds to MH^+ of SLD-AZ adduct whereas its fragment at m/z of 551.7, visible in MSMS spectrum, is due to the loss of acetic acid.

A species at 610.8 Da was monitored and recognized as the final product, confirming the same reaction mechanism proposed for SLD-TIOS. The reaction was finally scaled-up and the SLD-AZ probe purified by RP-HPLC and lyophilized.

4.3.2 Click Chemistry Optimization

Since a variety of conditions for a Cu(I) catalysed azide-alkyne cyclization are reported, we performed the reaction in different experimental settings to find out the best conditions for our experiment.

Indeed, the cycloaddition catalytic cycle relies on Cu(I) (**Figure 42**), a very unstable species.

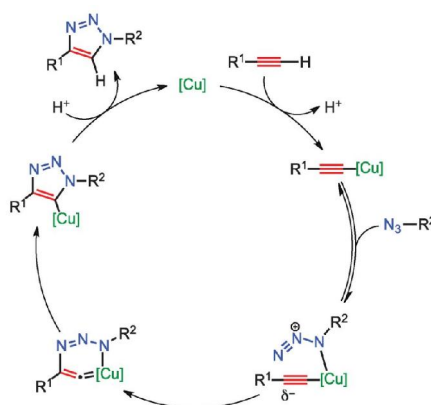


Figure 42. Copper catalyzed cycle of azide-alkyne cycloaddition

The improvement of the reaction yield is obtained employing Cu(II)SO₄ in presence of a reducing agent, able to generate Cu(I) *in situ*, together with a stabilizing agent. We chose Na-Ascorbate as reducing agent and Tris-[(1-benzyl-1H-1,2,3-triazol-4-yl)methyl]amine (TBTA) as stabilizer. The reaction conditions were optimized exploring the reactivity of SLD-AZ with the selected acetylene counterpart, 4-pentyn-1-amine (PINA linker, **Figure 43A**),

Results and Discussion

working in a bio-mimetic context, even if in absence of the proteins. Therefore, SLD-AZ was treated with PINA in a saline buffer (PBS at pH 7.4) containing a small amount of DMSO (less than 10 %), to increase the reagents solubility. The reaction was monitored by RP-HPLC-UV and MS analyses. The best result, in terms of reaction yield and kinetics, was obtained using 100 μM CuSO_4 , 5 mM Na-Ascorbate and 100 μM TBTA under nitrogen, as proven by the monitoring, after 30 minutes of reaction, of a triazole adduct at a retention time of 23 min (m/z 694.45 Th, **Figure 43 B**).

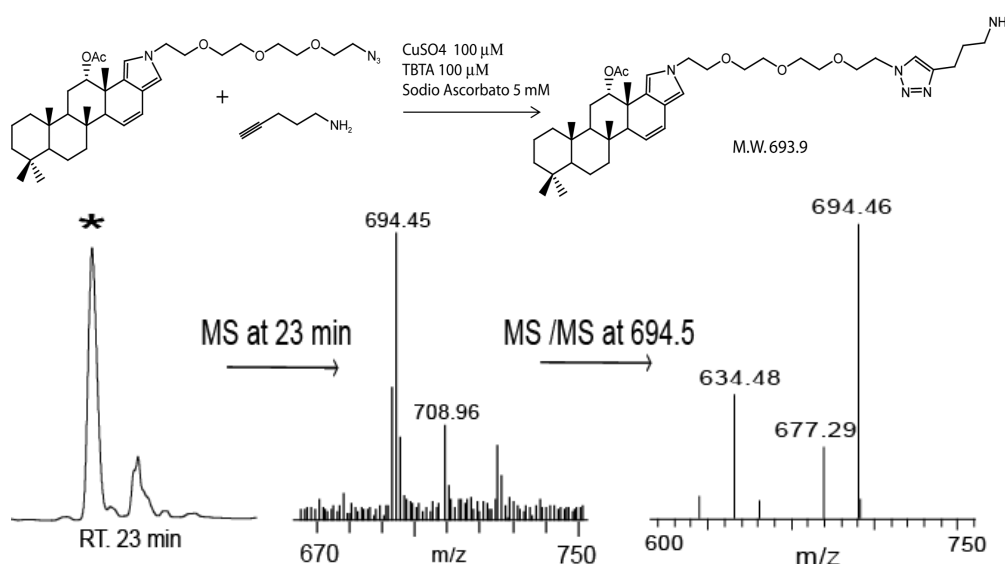


Figure 43. Panel A reports SLD-AZ interaction pathway with the linker PINA. Panel B shows HPLC-UV trace, MS and MS/MS spectra of the product. In the MS spectrum, the base peak is at m/z of 694.5 corresponding to MH^+ of SLD-AZ adduct with PINA linker, its fragments at m/z of 677.3 and 634.5, visible in MSMS spectrum, are the loss of ammonia and acetic acid, respectively.

Once established the ability of SLD-AZ and PINA to give rise to the expected product in solution, we moved to analyse their reactivity in a cell lysate by an *in situ* click chemistry-based pull down assay (**Figure 44**). Therefore, SLD-

AZ adduct (1 and 10 nmol) was incubated with HeLa cell lysates for 1 h at 4°C, and then mixed with 50 μ L of CDI-Agarose matrix bearing PINA linker, in presence of 100 μ M CuSO₄, 5 mM Na-Ascorbate and 100 μ M TBTA under nitrogen. As control, the experiment was carried out in the same conditions using TRX-AZ as a probe. The solid phase was extensively washed in PBS buffer and SLD partners were eluted, separated by 12% SDS-PAGE and revealed through immunoblotting using anti-14-3-3 ϵ and anti-PRX1 antibodies (**Figure 44**).

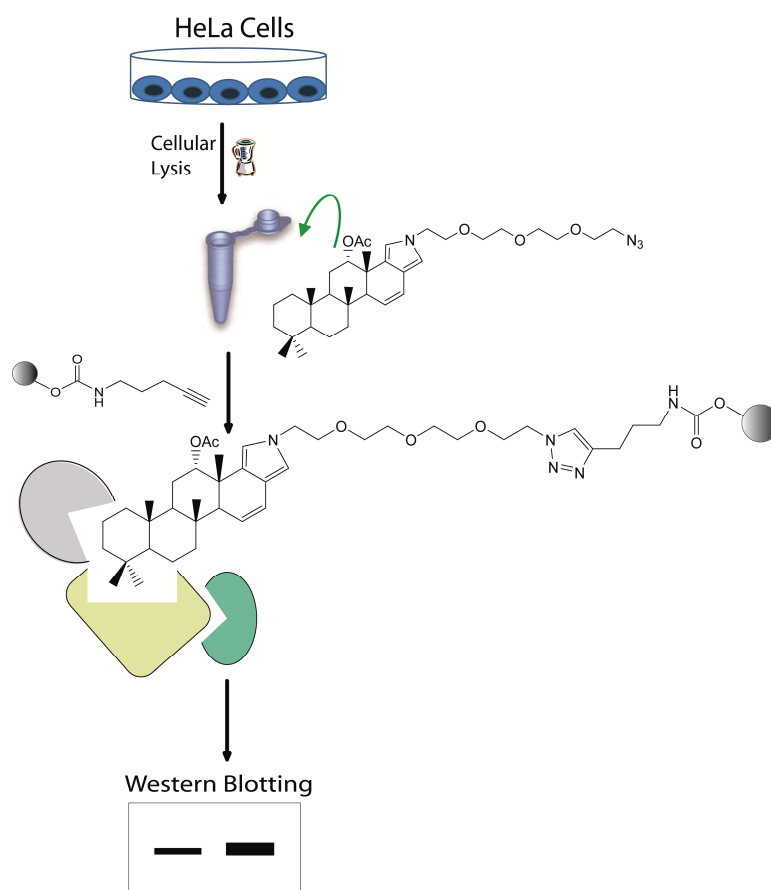


Figure 44. Schematic workflow of an *in situ* click chemistry-based pull down assay used to optimize Huisgen cycloaddition in presence of protein extract.

Results and Discussion

As reported in **Figure 45**, 10 nmol of SLD-AZ selectively fished out 14-3-3 ϵ and PRX1, as demonstrated by the presence of a slight band only in the SLD-AZ lane. To improve the reaction yield, the experiment was replicated using 10 nmol of SLD-AZ and modifying the click-chemistry reaction conditions (250 μ M CuSO₄, 2.5 mM Na-Ascorbate and 500 μ M TBTA, under nitrogen). As reported in **Figure 45B**, the new experimental conditions prompted a further enrichment of the selected proteins.

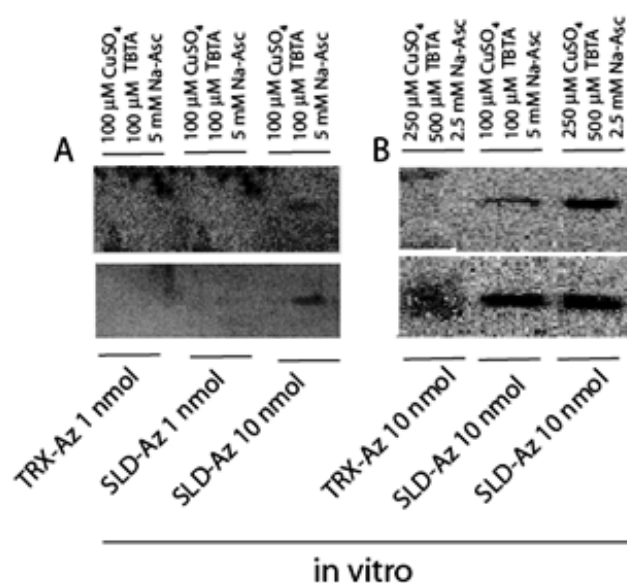


Figure 45. Western blot analysis on proteins eluted from control and SLD-beads incubated with HeLa cell lysates (*in vitro*) using 14-3-3 ϵ and PRX1 as probes. Panel A and B are relative to SLD-based pull down using different quantity of metabolite and different click chemistry conditions as reported.

4.3.3 Large-Scale Pull-Down/LC-MS/MS analysis

The *in cell* pull down experiments were preceded by the measure of the effects of SLD-AZ on HeLa cell proliferation, applying the MTT assay and

comparing the results with that of SLD. As shown in **Figure 46**, both molecules showed the same profile, and did not affect the cell viability at the tested doses.

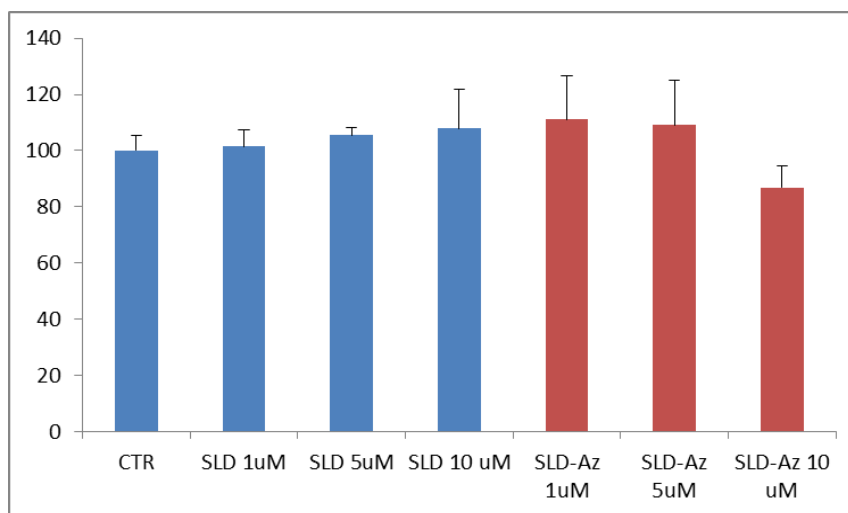


Figure 46. MTT analysis shows that both SLD and SLD-AZ does not affect HeLa cell proliferation at tested doses.

HeLa cells were then treated with 1 μ M SLD-AZ and 1 μ M TRX-AZ, as control for 6 hours, to allow the drug internalization and the cellular target(s) selection. Cells were then washed with PBS to remove the un-internalized drug residue, and lysed by mean of dounce homogenization with a gentle lysis buffer. Both lysates were then separately treated with 250 μ M CuSO₄, 2.5 mM Na-Ascorbate, 500 μ M TBTA and 10 μ L of PINA-bearing matrix under nitrogen for 45 minutes at room temperature, to promote the modified Huisgen 1,3-cycloaddition. Moreover, a parallel reaction without Na-Ascorbate was carried out to provide an additional negative control. Proteins fished out from the three resin samples were then separated by SDS-PAGE and subjected either to immunoblotting or coomassie staining.

Results and Discussion

As reported in **Figure 47**, immunoblotting showed that both PRX-1 and 14-3-3 ϵ were clearly enriched by SLD-AZ, confirming the effectiveness of the in cell approach in the finding of a small molecule interactors.

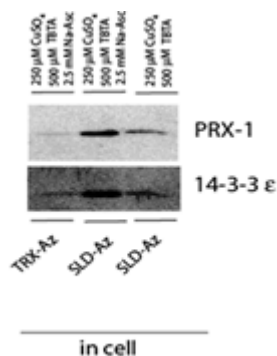


Figure 47. 14-3-3 ϵ and PRX 1 enrichment operated by SLD-AZ in live HeLa cells fished out by CDI-Agarose beads modified with PINA linker.

To further investigate the potential of the new methodology in the target discovery, we analyzed the entire sub-proteome selected by our probe.

To this end, the coomassie stained gel (both SLD-AZ and controls gel lanes) (**Figure 48**) was subjected to *in situ* protein digestion, the peptide mixtures were analysed through nano-flow LC-MSMS and the proteins identified by database search using the Mascot server.

The resulting SLD-AZ interacting target(s) list was refined by removing the hits shared with the control experiments, thus obtaining a list of approximately 90 proteins. The identified proteins were clustered through the STRING software (<http://string-db.org/>) to give the network of the functional complexes binding SLD *in vivo*. However, as also reported by Cravatt and co-workers^[180], we experienced that this methodology suffers of a high background, probably due to high amounts of low-affinity abundant proteins. Nevertheless, looking at the STRING output (**Figure 48**), a key correlation appears between PRDX1, located at the centre of a large protein network, and

both the 14-3-3 isoforms and the proteasome machinery, the latter a target also detected in the *in vitro* pull down, even if as a minor interactor.

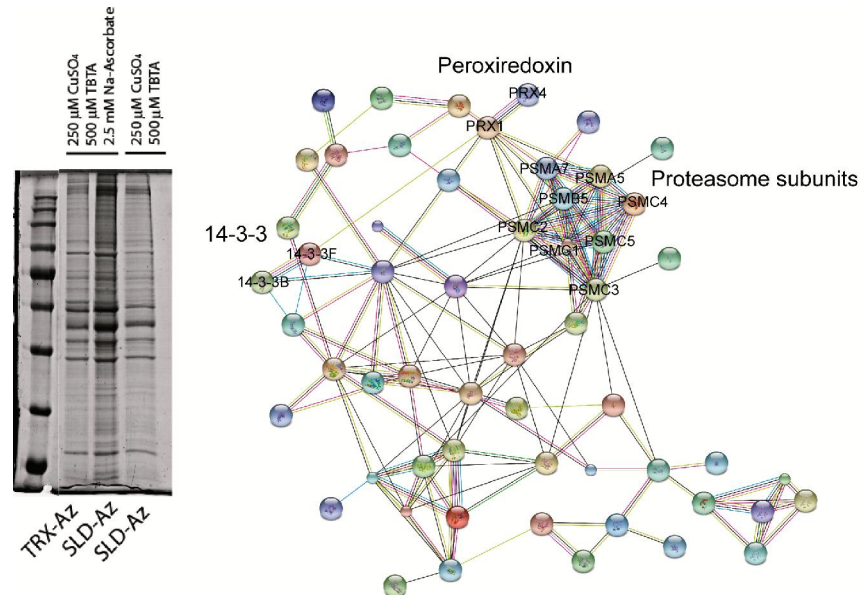


Figure 48. 12% SDS-PAGE of proteins eluted from in cell fishing for partners of SLD and control pull-down. Interactions network obtained clustering proteins identified as SLD targets in HeLa living cells

This last evidence was confirmed by western blotting. The proteins eluted from SLD-AZ and control experiments were blotted with monoclonal antibodies against the α -7 subunit, a component of 20S proteasome, and Psmc3, a proteasome regulator. As reported in **figure 49**, the blotting showed a substantial enrichment of both proteins only in the samples containing SLD-AZ and the whole catalytic mixture.

Results and Discussion

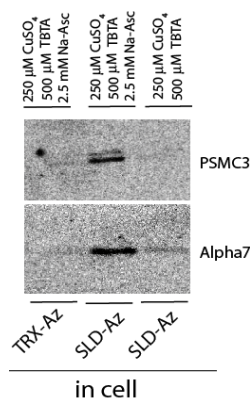


Figure 49. Proteins eluted from control and SLD-beads after *in cell* pull down were transferred onto nitrocellulose membrane and probed with antibodies anti-proteasome alpha 7 subunit and anti-PSMC3

Reported results indicate that we have successfully optimized an in cell pull down LC-MS/MS methodology based on the click-chemistry copper-catalysed variant of the Huisgen 1,3-dipolar cycloaddition for the interactome profiling of the anti-inflammatory marine metabolite scalaradial. The concurrent definition of its *in vitro* profiling helped as reference point for the validation of the in cell procedure. We obtained a list of cellular potential targets and, among them, PRXs, 14-3-3 isoforms and proteasome were selected as relevant SLD partners on the basis of their involvement in the inflammatory process. These targets, then validated by SPR and western blotting analyses, are functionally connected to the PI3K and NF- κ B pathways already known to be modulated by SLD^[186-190].

4.4 In-Cell Oleocanthal Proteome Profiling

The effectiveness of the click chemistry-based in cell proteome profiling technique was assessed applying the above-mentioned approach to another compound, Oleocanthal (OLC). This olive-oil phenolic component is known

to interfere with different pathways of relevant human diseases, such as inflammation^[193] and Alzheimer's disease^[194-198]. OLC had been already studied through the classical in vitro AP-MS approach, demonstrating its highly specific binding with the molecular chaperone HSP90. More in details, HSP90 was identified as OLC main target in two cell lines (HeLa and U937), and several independent assays showed the OLC ability to covalently bind HSP90 and inhibit its chaperone activity, with a significant reduction of Akt and Cdk4 levels. Moreover, OLC was also able to modulate the HSP90 supramolecular arrangement, stimulating the formation of high molecular weight structures^[133].

The azide-OLC derivative was synthesized (**Figure 50**) and incubated with a sample of HeLa cells.

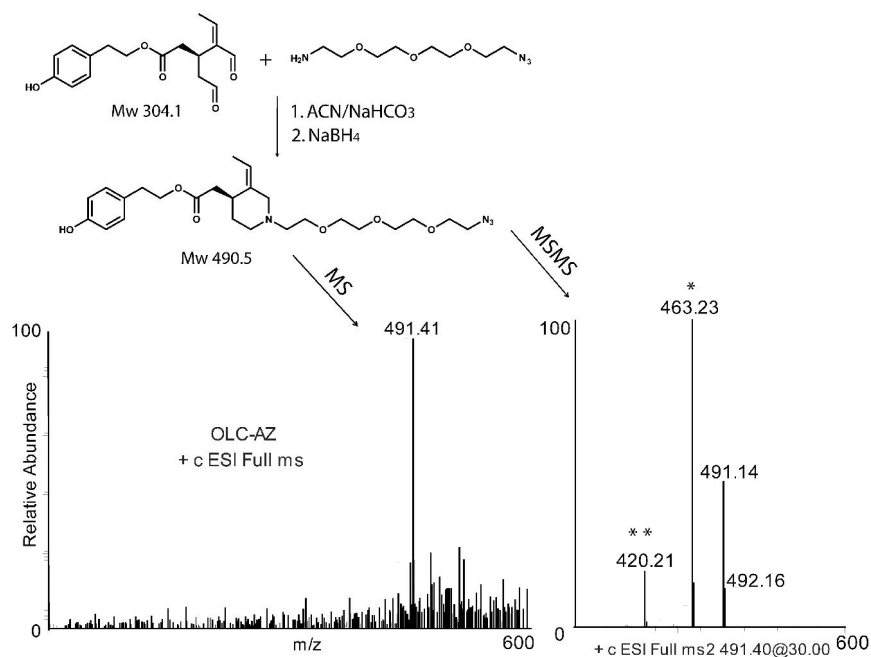


Figure 50. OLC coupling reaction with TRX-AZ and mass spectrometric analysis of obtained product. MS spectrum shows the MH^+ ion of the piperidinic OLC-TRX adduct and MSMS spectrum shows the diagnostic loss of ethylene and ethyl azide.

Results and Discussion

The reaction of OLC with TRX-AZ was performed in ACN/NaHCO₃ for 30 minutes at r.t. using a ten-fold molar excess of the azide linker. The Schiff base intermediate, produced by the condensation of the terminal amino group on TRX-AZ and one of the OLC aldehyde carbonyls, was reduced with NaBH₄, giving rise to a stable piperidine adduct, purified by HPLC-UV and characterized by LC-MSMS (**Figure 50**).

HeLa cells were then treated with 100 μM OLC-AZ or TRX-AZ and, after three hours of incubation, supernatants were discarded and cells were harvested with PBS and gently lysed by homogenation.

The modified Huisgen's cycloaddition reaction was carried out for 45 minutes in presence of 100 μM CuSO₄, 5 mM Na-Ascorbate and 100 μM TBTA. The OLC interactors were finally eluted and analysed by western blotting using an anti-HSP90 antibody. The resulting chemiluminescence signal intensities, reported in **figure 51**, revealed the ability of the OLC-AZ probe to recruit its main cellular interactor.

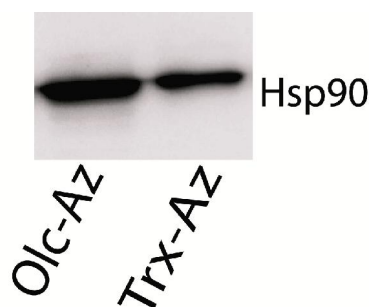


Figure 51. Western blotting on proteins enriched in cell by OLC and TRX-AZ using an anti Hsp90 antibody.

The gathered results confirm that the Huisgen's cycloaddition *in vivo* chemical proteomics approach is an effective tool to allow the molecular recognition

step to take place in living cells leading to the isolation of a large set of sub-proteomes. This feature could represent an interesting strength point of the technique, allowing a more comprehensive analysis of the interactomic profile of a small molecule. On the other hand, this could hamper an easier selection of the more likely physiological relevant potential partners.

-CHAPTER 5-

New insights in the cCMP interaction profile by chemical proteomics.

5.1 Background

The purine cyclic nucleotides 3',5'-cyclic adenosine monophosphate (cAMP) and 3',5'-cyclic guanosine monophosphate (cGMP) play a pivotal role in the cellular context, acting as second messengers and mediating the cellular effects of a wide range of hormones and neurotransmitters^[199,200]. Beside the natural existence of 3'-5'-cyclic cytidine monophosphate (cCMP) has been controversially debated^[201-207], recent evidences have confirmed that many cell types contain cCMP at micromolar concentrations^[208]. Moreover, several experiments have been performed to evaluate the ability of cCMP to cross-activate the cAMP and cGMP dependent protein kinases. Particularly, cCMP was found to relax aortic smooth muscle and inhibit platelet aggregation by activating cGMP dependent protein kinases^[209], and its functional interaction with HCN channels was also examined^[210]. Furthermore, Rab23 was identified as the first protein selectively phosphorylated in response to cCMP^[211]. Nevertheless, a specific cCMP receptor has not yet been identified and the only attempt to analyse the cCMP interactome led to the exclusive identification of PKA as main molecular target^[212].

Chemical proteomics has been demonstrated to be a powerful tool for the isolation of PKA and PKG related sub-proteomes. Moreover, the employment of cAMP- and cGMP-bearing matrices drove to the discovery of new AKAPS, unravelling many aspects of the cyclic nucleotides related cellular response^[213-215].

Therefore, an affinity chromatography approach was chosen to disclose potential new macromolecular target(s) of cCMP.

5.1 Fishing out cCMP interactors

Although the occurrence of cCMP has been proved in multiple cell lines, the physiological relevance of this cyclic nucleotide has not been clarified yet. Aiming at the analysis of the comprehensive interactome of this potential second messenger, we developed a chemical proteomics approach using cCMP as a bait. An analogue of cCMP endowed with a six carbons spacer arm, N4-(6-Aminohexyl)cytidine-3',5'-cyclic monophosphate (4-AH-cCMP), was immobilized onto agarose beads and used as a bait to fish out its biological targets (**Figure 52**). 4-AH-cCMP was put in reaction with NHS-activated beads and the reaction yield was evaluated by means of RP-HPLC-UV. Comparing the peak areas of 4-AH-cCMP at the beginning and after 16h of reaction, a 30% yield was assessed, and the final concentration of cCMP was estimated to be 3 $\mu\text{mol/ml}$ resin.

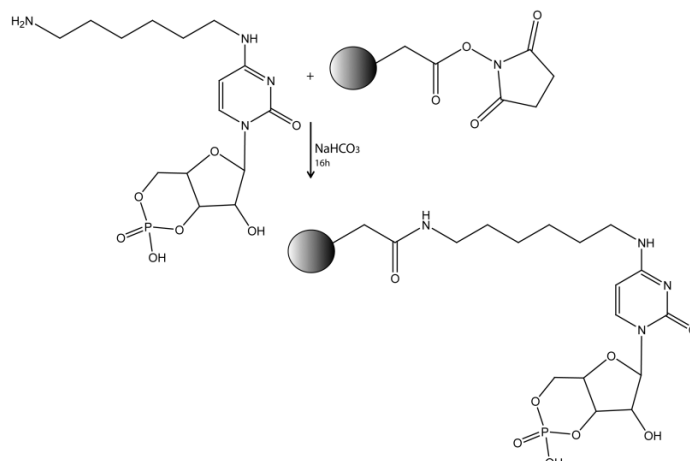


Figure 52. Reaction scheme of cCMP immobilization onto NHS activated agarose beads.

The residual free reactive groups on the beads surface were quenched applying a solution of a primary amine (2-Amino-2-hydroxymethyl-propane-1,3-diol). Moreover, control beads were also prepared treating an NHS-activated agarose sample directly with the amine solution.

Control beads and cCMP-beads were then incubated with a HEK293 cellular lysate, keeping the suspension under gentle shaking for 1 hour at 4°C. Subsequently, the unbound proteins were discarded and both matrixes were subjected to several washing with a saline buffer containing a small quantity of surfactant to minimize the background amount. The tightly bound proteins were finally eluted by means of a denaturing buffer and subjected to 1D-gel electrophoresis. The coomassie-stained protein bands were cut out, digested, and analysed by nanoLC tandem mass spectrometry. Only proteins highly enriched by cCMP, compared with control, were taken into account. cAMP and cGMP macromolecular effectors, such as PKA and PKG, were found along with other secondary interactors of these proteins (AKAPS) (**Figure 53**).

Proteins	Score	Peptides	PSMs
cAMP-dependent protein kinase type I-alpha regulatory subunit	3628	32	120
cAMP-dependent protein kinase type I-beta regulatory subunit	889	16	42
cAMP-dependent protein kinase type II-alpha regulatory subunit	3253	28	93
cAMP-dependent protein kinase type II-beta regulatory subunit	1636	16	42
cGMP-dependent protein kinase 1	1376	20	51
A-kinase anchor protein 1, mitochondrial	393	7	11
A-kinase anchor protein 11	2420	41	87
A-kinase anchor protein 13	87	3	3
A-kinase anchor protein 2	64	2	2
A-kinase anchor protein 5	110	3	3
A-kinase anchor protein 7 isoform gamma	54	1	1
A-kinase anchor protein 8	102	4	4
A-kinase anchor protein 8-like	122	4	4
A-kinase anchor protein 9	1090	31	40

Figure 53. Table of cCMP interactors belonging to purine cyclic nucleotides dependent pathway.

Results and Discussion

The chemical structure of the cyclic portion of cCMP resembles the structure of the most common cyclic nucleotide cAMP and cGMP, and this could account for the enrichment of all the isoforms of PKA and PKG regulatory subunits. These findings are in agreement with previous studies reporting the ability of cCMP to activate PKG in platelet aggregation and in smooth muscle relaxation^[209].

In order to obtain a more focused list of cCMP specific interactors, a competition experiment was also developed pre-incubating different batches of cellular lysate with cyclic and not cyclic nucleotides, such as adenosine diphosphate (ADP), guanosine diphosphate (GDP), cAMP and cGMP (**Figure 54**).

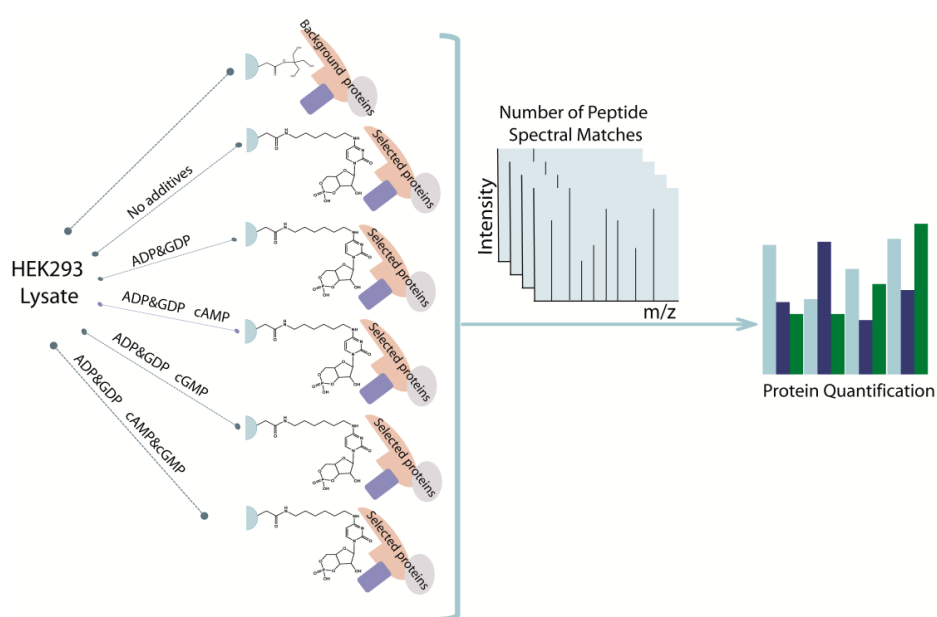


Figure 54. Schematic representation of competition assay coupled to PSMs quantization for cCMP interactome definition.

This is a common procedure, reported in literature, useful to eliminate interactors shared between cyclic and acyclic nucleotides^[214,215]. More in details, the competition experiments were performed adding to the cellular

lysate ADP and GDP; (ii) ADP, GDP and cAMP (iii) ADP, GDP and cGMP (iv) ADP, GDP, cAMP, cGMP (as reported in experimental section), and comparing the proteins enriched from the bait in the absence and in presence of the other nucleotides. In parallel, a control experiment was carried out to subtract background proteins.

The electrophoretic profiles, reported in **Figure 55**, show the ability of ADP and GDP to compete for the interaction of PKA and PKG regulatory subunits with the anchored cCMP. These findings suggest a cCMP weak affinity for these proteins.

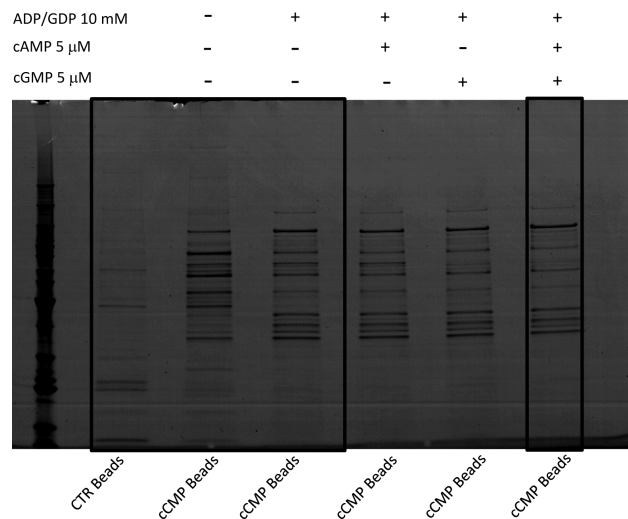


Figure 55. Coomassie stained SDS-PAGE obtained from competition experiments illustrating as new protein bands became evident in presence of non-cyclic nucleotides and persist also in presence of cAMP and cGMP.

Notably, in presence of ADP and GDP in the incubation mixture, new bands were observable after the coomassie staining, that were also visible when cAMP and cGMP were added to the mixture, indicating the presence of specific cCMP interactors.

Results and Discussion

The gel lanes portions framed with black boxes (**Figure 55**) were cut in small pieces, *in situ* digested and analysed by nanoLC-MSMS, giving the protein identification. A semi-quantitative estimation of the abundance of each protein in all the experimental conditions was also assessed comparing their number of PSMs (Peptide spectral matches), to weigh the specificity of the interaction. Only proteins whose binding to cCMP-matrix was not competed by the presence of other nucleotides were considered as potential specific interactors. Moreover proteins identified with less than five PSMs were discarded, in order to obtain highly confident results. Interestingly, several proteins belonging to the heterogeneous nuclear ribonucleoproteins class were considerably enriched, in presence of both ADP and GDP in the incubation mixture (**Figure 56**).

Proteins	Ratio	
	ADP/GDP	vs Nothing
Heterogeneous nuclear ribonucleoprotein U-like protein 2		12.20
39S ribosomal protein L16, mitochondrial		7.00
ELAV-like protein 1		6.00
Importin subunit alpha-2		6.00
Heterogeneous nuclear ribonucleoprotein A3		4.63
Heterogeneous nuclear ribonucleoprotein D-like		4.00
Heterogeneous nuclear ribonucleoprotein U		3.65
Heterogeneous nuclear ribonucleoprotein A/B		2.73
RNA-binding motif, single-stranded-interacting protein 1		2.50
Protein FAM98A		2.17
Heterogeneous nuclear ribonucleoproteins A2/B1		2.15
Interleukin enhancer-binding factor 3		2.00
40S ribosomal protein S3		18.00
Kelch repeat and BTB domain-containing protein 3		7.00
Histone H2B type 1-K		6.00
Guanine nucleotide-binding protein subunit beta-2-like 1		5.00
40S ribosomal protein S18		5.00
RNA-binding motif protein, X chromosome		5.00
40S ribosomal protein S2		3.50
Nucleolin		3.00
40S ribosomal protein SA		3.00
Histone H2A type 1-H		2.33
40S ribosomal protein S4, X isoform		2.33

Figure 56. Table shows proteins whose ability to bind cCMP-bearing matrix is increased in presence of ADP and GDP and the ratio between counted PSMs

The ability of non-cyclic nucleotides to prevent the binding of PKA and PKG to cCMP indicate a low affinity interaction. On the other hand, the occurrence of the heterogeneous nuclear ribonucleoproteins only in presence of ADP and GDP in the protein mixture suggests that these proteins should be considered as secondary cCMP partners. However, the biological role of this interaction could be of interest, although the apparent low affinity between the counterparts, since several cellular pathways are modulated through weak interactions^[9]. Indeed, the binding of cCMP to heterogeneous nuclear ribonucleoproteins may be functionally relevant in the cellular environment, opening the way to new studies on unexplored roles for cytidine derived cyclic nucleotide.

-CHAPTER 6-

Conclusions

Conclusions

Several bioactive small molecules explicate their activity through protein modulation. One of the main issues in the field of pharmaceutical science is the discovery of new compounds endowed with intriguing pharmacological profiles and virtually free of side effects. Indeed, although medicinal chemistry spends many efforts in designing highly specific compounds, a lot of them share a multi-target interaction profile^[9].

The natural environment represents one of the main source of new therapeutic agents^[137]. In particular, marine drugs are endowed with intriguing chemical structures, often responsible for their relevant biological activities. The translation of a biological effect in a therapeutically useful drug requires a comprehensive knowledge of its biological profile. Chemical proteomic approaches offer the peculiar chance to investigate the entire interactome of a small molecules in a single experiment and in an unbiased fashion^[9]. Due to the high feasibility demonstrated by affinity chromatography coupled to mass-spectrometry in identifying physiologically relevant drug-targets^[117-119], an AP-MS approach has been optimized to fish out the specific targets of some secondary metabolites from marine sources, Suvanine, Heteronemin and Scalaradial.

Suvanine (SUV) is a tricyclic bioactive sesterterpene endowed with an anti-inflammatory activity, isolated from different specimens of *Coscinoderma* sponges^[141]. *Coscinoderma* genus is a rich source of sulfated terpenoids, often exhibiting valuable biological effects. SUV and its derivatives were found to inhibit *in vitro* different secretory phospholipases (sPLA₂) and to reduce NO and prostaglandin E2 (PGE2) production^[141].

By means of an MS-based affinity chromatography approach, HSP60 has been identified as the main biological target of SUV in HeLa cells. The specificity of the interaction between SUV and HSP60 was assessed by western blot analysis and was also validated by surface plasmon resonance and pull down

Conclusions

assays using the recombinant protein. A low micro-molar dissociation constant ($0.6\pm 0.5\ \mu\text{M}$) of the SUV-HSP60 complex was measured by SPR, suggesting a strong interaction. This interaction might give evidence of the suvanine anti-inflammatory potential, because of the involvement of this molecular chaperon in the inflammatory response. On this basis, the ability of SUV in inhibiting HSP60 activity was demonstrated by an *in vitro* assay. Since the mammalian HSP60 plays an important role during chronic inflammation and atherosclerosis^[150], SUV could be considered a candidate lead compound for the rational design of novel HSP60 inhibitors^[121].

The above procedure was also applied to the marine sesterterpene Heteronemin (HET). HET was isolated from the sponge *Hyrtios erecta*^[157] and was found to inhibit proteasome machinery in K562 cells^[158]. The interaction with the proteasome subunit was confirmed also in our chemical proteomics experiment. Surprisingly, along with the proteasome we recovered TDP43 that was recognized, on the basis of the experimental data, as the main cellular partner of HET in HeLa cells. These results were confirmed by western blot and surface plasmon resonance experiments, that gave a dissociation constant of $270\pm 200\ \text{nM}$. TDP43 is considered an “hot target” in pharmaceutical research, due to its involvement in several neurodegenerative diseases. Actually, TDP43 has an high tendency to aggregate^[163] generating inclusions that are often found in neurodegenerative disorders^[164]. On this basis, we have investigated the HET modulation of TDP43 aggregation both *in vitro* and *in vivo*. TDP43 gave rise to the formation of high molecular aggregates and was revealed to translocate from nucleus to cytoplasm upon HET treatment, and to localize in stress granules upon heat shock co-treatment . Using alpha screen technology, HET was also shown to decrease TDP43 affinity toward its cognate DNA, the oligonucleotide TAR32, with an IC_{50} of $10\ \text{nM}$ (± 0.5)^[216]. By using a similar approach, the interactome of Scalaradial, a sesterterpenoidic molecule with a scalarane-skeleton, isolated^[184,185] from the

sponge *Cacospongia mollior*, was disclosed. SLD was found to bind proteins belonging to the 14-3-3 and peroxiredoxin classes. The interaction with Peroxiredoxin 1 (PRX1) and 14-3-3 ϵ was further confirmed by SPR, showing a high affinity towards both proteins.

A new approach based on bio-orthogonal chemistry has also been optimized to investigate the interaction profile of small molecules directly in a living systems. By using copper-catalyzed azide-alkyne cycloaddition, scalaradial, conveniently decorated, was anchored to a solid support and its macromolecular partners were then characterized. Thus, the previously found interactions of SLD with 14-3-3 and PRX1 were confirmed in living HeLa cells, and the bio-orthogonal reaction was proved as valuable mean for in cell *fishing for partners* approach. Analysis of the whole SLD proteome gave a set of new protein complexes. This feature could represent a key factor of this technique, allowing a more comprehensive analysis of the interactome profile of a small molecule, even if, on the other hand, could hamper the selection of the relevant physiological partner(s). Moreover, we experienced that this methodology suffers of a higher background signal, probably due to a higher amount of low affinity interactions with abundant proteins.

The above methodology was also applied to Oleocanthal, as further confirmation on the effectiveness of this approach. OLC ability to bind and modulate HSP90 activity was confirmed^[190].

In a last study, chemical proteomics was applied to the investigation of cyclic nucleotides-related cellular response, in particular using cCMP (3'-5'-cyclic cytidine monophosphate) as a bait. The cCMP interactome was deeply investigated by means of competition experiments, and a list of macromolecular partners was obtained, containing, along with the well known PKA and PKG, also new interactors belonging to the heterogeneous nuclear ribonucleoproteins family.

EXPERIMENTAL SECTION

-CHAPTER 7-

In vitro and in cell chemical proteomics on marine
compounds target discovery : Experimental procedures

7.1 Suvanine target discovery

7.1.1 Synthetic procedure to obtain suvanine-aldehyde

A solution of SUV (15 mg, 0.033 mmol) in pyridine (0.5 mL) and dioxane (0.5 mL) was heated at 150°C for 2.5 h in a reaction vial. After the solution was cooled, the mixture was evaporated to dryness, and then purified by HPLC on a m-Bondapak C18 column (30cm x 3.9 mm; Waters) with MeOH/H₂O (80:20) to give aldehyde as a mixture of two diastereoisomers (9.2 mg, 80%).

7.1.2 Generation of the suvanine functional matrix

CDI activated beads (Pierce, Rockford, IL) (0.2 mL) were treated with 4 μmol 4,7,10-trioxa-1,13-tridecanediamine (Sigma-Aldrich) (NH₂(PEG)₃NH₂) dissolved in NaHCO₃ (50 mM) with CH₃CN (30%) at pH 8.5 and incubated for 16 h at room temperature with continuous shaking. Then, to verify the presence of free amine groups on the modified matrix surface, beads were washed with ethanol and subjected to a Kaiser test^[217]. The obtained amine beads were then treated with SUV-AL (1.5 mg) dissolved in CH₃CN (400 μL), NaHCO₃ (30%, 50 mM) at pH 8.0. The reaction mixture was kept for 16 h at room temperature under continuous shaking and the amount of immobilized 2 was estimated by integrating the peaks of the free SUV-AL species after HPLC injections of supernatants at t=0, 2, and 16 h, in an 1100 Series chromatographer (Agilent).

HPLC runs were carried out on a C₄ column (250 x 2.0 mm; Phenomenex, Torrance, CA) at a flow rate of 200 mLmin⁻¹. The gradient (solution A: TFA (0.1%); solution B: TFA (0.07 %), H₂O (5%), CH₃CN (95 %)) was 10–95% B

Experimental Section

over 45 min. The same experimental conditions were applied for the preparation of the control matrix. Briefly, activated CDI-Agarose support (200 μL) was mixed with acetylated $\text{NH}_2(\text{PEG})_3\text{NH}_2$ (4 μmol) dissolved in NaHCO_3 (50 mM) containing CH_3CN (30%) at pH 8.5. The matrices were stored at 4°C in acetone.

7.1.3 Affinity purification and identification of Suvanine partners

HeLa cells were grown in Dulbecco's modified Eagle medium (DMEM) supplemented with fetal bovine serum (10% (v/v)), penicillin (100 U mL^{-1}), streptomycin (100 mg mL^{-1}), glutamine (4 mM), HEPES (10 mM), and sodium pyruvate (10 mM) at 37°C in a 5% CO_2 atmosphere (all reagents from Sigma–Aldrich). The cells were collected by centrifugation (10000 rpm, 3 min) and washed three times with phosphate saline buffer (PBS; sodium phosphate (50 mM), NaCl (150 mM), pH 7.5). The obtained pellet was dissolved in 1 mL ice-cooled PBS containing Igepal (0.1%) and glycerol (5%) and supplemented with protease inhibitor cocktail. The obtained solution was sonicated for 2 min in a Vibra-Cell (amplitude 30%; Sonics, Newton, CT) and clarified by centrifugation (10000 rpm, 10 min, 4°C).

The supernatant was collected, and the protein concentration was tested with a Bradford assay^[218] and adjusted to 1 mg mL^{-1} .

SUV-bound beads suspension (50 μL) and the same amount of the control matrix were separately incubated with HeLa total protein preparation (1 mg) under continuous shaking (16 h, 4°C). The beads were precipitated by centrifugation (1200 rpm, 3 min, 4°C) and washed six times with PBS (pH 7.4). The bound proteins were eluted by boiling the beads in SDS-PAGE sample buffer (Tris·HCl 60 mM, pH 6.8 with 2% SDS, 0.001 % Bromophenol Blue, 10% glycerol, 2% 2-mercaptoethanol). The eluted proteins were

separated on 12% SDS-PAGE, and stained with G-250 Coomassie stain (Bio-Rad, Hercules, CA).

7.1.4 Suvanine interactome identification

Each SDS-PAGE gel lane from control and suvanine-based experiments was cut in ten pieces. Each piece was washed with ultrapure water and CH₃CN and subjected to in situ protein digestion as described by Shevchenko^[146]. Briefly, each slice was reduced with 1,4-dithiothreitol (DTT, 10 mM) and alkylated with iodoacetamide (50 mM), then washed and rehydrated in trypsin solution (12 ngmL⁻¹) on ice for 1 h. After the addition of ammonium bicarbonate (30 μL, 10 mM, pH 7.5), protein digestion was allowed to proceed overnight at 37°C. Supernatants were collected and peptides were further extracted from gel slices using 100% CH₃CN. Finally, second supernatants were collected and combined with first ones. Peptide samples were dried and dissolved in formic acid (FA, 10%) before MS analysis. Peptide mixtures (5 μL) were injected into a nano-ACQUITY UPLC system (Waters) and separated on a 1.7 mm BEH C18 column (Waters) at a flow rate of 400 nLmin⁻¹. Peptide elution was achieved with a linear gradient (solution A: H₂O (95 %), CH₃CN (5 %), FA (0.1%); solution B: CH₃CN (95 %), H₂O (5 %), FA (0.1 %)); 15–50% B over 55 min). MS and MS/MS data were acquired with a Q-TOF Premier mass spectrometer (Waters). The five most intense doubly and triply charged ions were chosen by MassLynx software (Waters) and fragmented. The resulting MS data were processed by ProteinLynx (Waters) software to generate peak lists for protein identifications. Database searches were carried out on the Mascot server (<http://www.matrixscience.-com/>). The SwissProt database (release 2012_03, 21 March 2012, 535248 sequence entries, 189901164 amino acids abstracted from 208076 references) was employed (settings: two missed

Experimental Section

cleavages; carbamidomethyl (C) as fixed modification and oxidation (M) and phosphorylation (ST) as variable modifications; peptide tolerance 80 ppm; MS/MS tolerance 0.8 Da).

7.1.5 In vitro validation of HSP60–suanine interaction

Human recombinant HSP60 (Enzo Life Science, Framingham, NY) at the concentration of 0.18 mM was incubated with immobilized suanine-beads (20 μ L) in PBS buffer for 1 h at 4°C followed by gentle mixing. Several PBS washing steps were performed, and the bound protein was eluted by addition of SDS sample buffer to the beads. As negative control, the same amount of HSP60 was incubated with control beads. Similar pull-down experiments were performed by pre-incubating HSP60 with and without SUV or SUV-AL (20 and 100 μ M) in PBS buffer for 1 h at 4°C followed by gentle mixing, and the mixtures were added to suanine-modified beads (20 μ L). Several washing steps were performed with PBS and the bound protein was eluted by addition of SDS sample buffer to the beads. All samples were analyzed by SDS-PAGE (12%), and proteins were stained with Coomassie stain. Then, suanine-modified beads suspension (50 μ L) and the same amount of the control matrix were treated as above (see affinity purification step) and the eluates were analysed by Western blotting. Briefly, each sample was resolved on a 12% SDS-PAGE gel, and transferred onto a nitrocellulose membrane. The membrane was incubated for 1h in a blocking solution containing Tris (25 mM, pH 8), NaCl (125 mM), Tween-20 (0.05 %), and nonfat dried milk powder (5%), then incubated overnight at 4°C with primary monoclonal antibodies raised against HSP60 (BD Biosciences), HSP70 (Enzo Life Science) and HSP90 (BD bioscience), at dilutions of 1:2000, 1:1000, and 1:1000, respectively. Finally the membranes were incubated for 1 h with

mouse peroxidase-conjugated secondary antibody (1:5000; Thermo Scientific). HSPs were detected by using the Amersham enhanced chemiluminescence (ECL) detection system (GE Healthcare).

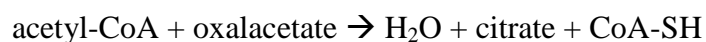
7.1.6 HSP60–suvanine binding affinity by surface plasmon resonance

HSP60 was immobilized onto a CM5 sensor chip by using standard amine coupling procedures. Phosphate buffered saline (10 mM Na₂HPO₄, NaCl 150 mM, pH 7.4) was used as running buffer. The carboxymethyl dextran surface was activated with a 5 min injection of a 1:1 ratio of EDC and NHS (100 mM at 5 μLmin^{-1}). HSP60 was diluted to 30 ngmL⁻¹ in sodium acetate (10 mM, pH 4.5) and injected onto the activated chip surface (flow rate 5 μLmin^{-1}). Protein concentration was adjusted to obtain an optimal response (~15 000 RU). Remaining active groups were blocked with a 7 min injection of ethanolamine·HCl (1.0 M, pH 8.5) at 5 μLmin^{-1} . For these biosensor experiments, SUV and SUV-AL (0.5–5 μM) were diluted in PBS containing 2% DMSO. Each concentration was tested at least three times. As they dissociated to baseline within a reasonable time, no regeneration was required among injections. The interaction experiments were carried out at a flow rate of 10 μLmin^{-1} over a 3 min injection time. The dissociation time was set at 600s. Rate constants for association (k_a), dissociation (k_d) and the dissociation constant (K_D) were obtained by globally fitting data from all the injection of different concentrations of each compound by using BIAevaluation software (GE Healthcare) with a simple 1:1 Langmuir binding model.

7.1.7 Suvanine inhibition of HSP60 chaperone activity

Active citrate synthase (CS) catalyses the following reaction:

Experimental Section



As 5,5'-di-thio-bis-2-nitrobenzoic acid (DTNB) was added in the mixture, CoA-SH undergoes the following reaction:



CoA-S-S-TNB formation can be easily measured at 412 nm. CS (Sigma-Aldrich) was incubated at 15 μM in buffer (Tris·HCl (100 mM, pH 8), guanidine·HCl (6M), DTT (20 mM)) for 2h at room temperature. This solution was then diluted (1:100) in renaturing buffer (Tris·HCl (50 mM, pH 7.5), MgCl_2 (10 mM), KCl (10 mM)) at 35°C in the presence or absence of (human) HSP60/HSP10 complex and at different concentrations of SUV and SUV-AL. For this, CS was incubated with HSP60 (3 μM), HSP10 (2 μM), and ATP (2 μM) with or without SUV and SUV-AL (3–150 μM) as follows: SUV and SUV-AL were first incubated with HSP60 (30 min, 4°C), then HSP10 was added and incubated (30 min, 4 °C), and finally CS refolding was started by addition the obtained complex and ATP at 35°C. Several incubations were performed to test for possible direct effects of SUV or SUV-AL on CS renaturation by allowing CS refolding at 25°C in absence of HSP60/HSP10 with and without SUV and SUV-AL (32 and 160 μM) under the same conditions. Colorimetric measurements were performed after 3h of incubation at 35°C with stirring. Each solution (20 μL) was diluted in Tris·HCl (1 mL, 50 mM, pH 8) with EDTA (2 mM), oxalacetic acid (0.1 mM), DTNB (0.1 mM), and acetyl-CoA (0.15 mM), and absorbance was measured at 412 nm

7.2 HET target discovery

7.2.1 Generation of the HET functional matrix

Epoxy-activated Sepharose™ 6B matrix was swollen with water (200 µL/mg) for 60 min and extensively washed with water.

HET (2 mg, 4,1 µmol) was diluted in 450 µL of 78% MeCN/ 22% NaHCO₃ at pH 8.0 and added to 200 µL of matrix at room temperature for 2.5 hours with continuous shaking. A control matrix was obtained in the same experimental conditions without the marine metabolite. The amount of immobilized HET was estimated by integrating the peaks of the free HET after HPLC injections of supernatants at t=0 and 2.5 h in a 1100 Series Chromatographer (Agilent). HPLC runs were carried out on a C18 column (Jupiter Proteo C18 5µ 250 x 2.00 mm, Phenomenex, Torrance, CA) at a flow rate of 0.200 mLmin⁻¹. Elution was achieved by means of a linear gradient of B from 10 to 95% over 25 min (solution A: H₂O and TFA (0.1%); solution B: MeCN and TFA (0.1%)).

Both resins were washed 3 times with 1 mL of phosphate saline buffer and then incubated with a mixture of water/isopropanol (1:2) for 4 h at room temperature to inactivate the free epoxy-groups. Then, matrices were washed extensively with PBS to remove traces of isopropanol and stored at 4°C in PBS 30% ethanol.

7.2.2 Affinity purification and identification of HET partners

HeLa cells were grown in Dulbecco's modified Eagle medium (DMEM) supplemented with 10% (v/v) fetal bovine serum, 100 U/ml penicillin, 100 mg/ml streptomycin, at 37°C in a 5% CO₂ atmosphere (all reagents were from

Experimental Section

Sigma–Aldrich). Cells were collected by centrifugation (10000 rpm, 5 min), washed three times with PBS and re-suspended in 1X ice cooled PBS containing Igepal (0.1%), supplemented with a protease inhibitor cocktail. The obtained suspensions were sonicated for 2 min with Vibracell (Sonics) setting an amplitude of 30% and cellular debris were removed by centrifugation at 10000g for 10 min at 4 °C. Protein concentration was determined using Bradford assay and adjusted to 1 mg/ml. HET-bound bead suspension (50 µL) and the same amount of the control unbound matrix were separately incubated with 1 mg of HeLa extract under continuous shaking (16 h, 4°C). The beads were collected by centrifugation (1200, 1 min, 4°C) and washed six times with PBS (pH 7.4). The bound proteins were eluted by boiling the beads in SDS-PAGE sample buffer (60 mM Tris/HCl pH 6.8, 2% SDS, 0.001% bromophenol blue, 10% glycerol, 2% 2-mercaptoethanol). The eluted proteins were separated on 10% SDS-PAGE, and stained with Coomassie G-250 (Bio-Rad, Hercules, CA).

7.2.3 HET partners identification

Three bands from SDS-PAGE gel lane relative to the HET-based and control experiments were cut and digested. The experiment has been repeated three times using an opportune control matrix bearing the linker without any metabolite. Each piece was washed with ultrapure water and CH₃CN and subjected to *in situ* protein digestion as described by Shevchenko^[146]. Briefly, each slice was reduced with 10 mM 1,4-dithiothreitol (DTT) and alkylated with 54 mM iodoacetamide, then washed and rehydrated in trypsin solution (12 ng/mL) on ice for 1 h. After the addition of ammonium bicarbonate (30 µL, 50 mM, pH 7.5), proteins digestion was allowed to proceed overnight at 37°C. The supernatant was collected and peptides were extracted from the

slice using 100% CH₃CN and both supernatants were combined. The peptide samples were dried and dissolved in formic acid (FA, 10%) before MS analysis. The peptide mixture (5 µL) was injected into a nano-ACQUITY UPLC system (Waters). Peptides were separated on a 1.7 mm BEH C18 column (Waters) at a flow rate of 400 nL/min. Peptide elution was achieved with a linear gradient (solution A: 95 % H₂O, 5 % MeCN, 0.1% FA; solution B: 95 % MeCN, 5 % H₂O, 0.1 % FA); 15–50% B over 55 min). MS and MS/MS data were acquired with a Q-TOF Premier mass spectrometer (Waters). The five most intense doubly and triply charged peptide ions were chosen by MassLynx software (Waters) and fragmented. The resulting MS data were processed by ProteinLynx (Waters) software to generate peak lists for protein identifications. Database searches were carried out on the Mascot server (<http://www.matrixscience.com/>). The SwissProt database (release 2012_03, 21 March 2012, 535248 sequence entries, 189901164 amino acids abstracted from 208076 references) was employed (settings: two missed cleavages; carbamidomethyl (C) as fixed modification and oxidation (M) and phosphorylation (ST) as variable modifications; peptide tolerance 80 ppm; MS/MS tolerance 0.8 Da).

7.2.3 *In vitro* validation of TDP43–HET interaction

HET-modified beads suspension (50 µL) and the same amount of the unmodified matrix were treated as described above and the eluates were analyzed by Western blotting. Briefly, each sample was resolved on a 10% SDS-PAGE gel, and transferred onto a nitrocellulose membrane. The membrane was incubated for 1 h in a blocking solution containing 25 mM Tris pH 8, 125 mM NaCl, 0.1% Tween-20, 5% non-fat dried milk, then incubated overnight at 4°C with primary monoclonal antibody raised against TDP43

Experimental Section

(Sigma-Aldrich) at 1:8000 dilution. Membranes were then incubated for 1 h with rabbit peroxidase-conjugated secondary antibody (1:5000; Thermo Scientific). TDP43 was detected using an enhanced chemiluminescent substrate (ECL) and LAS 4000 (GE Healthcare, Waukesha, WI, USA) digital imaging system.

7.2.4 TDP43–HET binding affinity by surface plasmon resonance

TDP43 was immobilized onto a CM5 sensor chip by using standard amine coupling procedures using PBS as running buffer. The carboxymethyl dextran surface was activated with a 5 min injection of a 1:1 ratio of EDC and NHS (100 mM at 5 $\mu\text{L}/\text{min}$). TDP43 was diluted to 30 ng/ μL in potassium acetate (10 mM, pH 4.5) and injected onto the activated chip surface (flow rate 5 $\mu\text{L}/\text{min}$) until reaching $\sim 16\,000$ RU. Remaining active groups were blocked with a 7 min injection of ethanolamine·HCl (1.0 M, pH 8.5) at 5 $\mu\text{L}/\text{min}$. For these biosensor experiments, HET (0.01–25 μM) was diluted in PBS containing 1% DMSO. Each concentration was tested at least three times. The interaction experiments were carried out at a flow rate of 10 $\mu\text{L}/\text{min}$ over a 3 min injection time. The dissociation time was set at 600 s. Rate constants for association (k_a), dissociation (k_d) and the dissociation constant (K_D) were obtained by globally fitting data from all the injection of different concentrations of each compound by using BIAevaluation software (GE Healthcare) with a simple 1:1 Langmuir binding model. The same experiment was carried out immobilizing the following proteins that didn't bind HET: Heat Shock Protein 90 and bovine serum Albumin.

7.2.5 In vitro effect of HET on TDP43 aggregation

TDP-43 stock solution (25 μ M in 33% glycerol, 80 mM Tris-HCl, 0.1% SDS 1 mM DTT) was diluted in 1:500 in PBS containing 2 mM DTT and 5% glycerol at a final concentration of 50 nM and incubated with a 50 molar fold of HET. Since the small molecule was withdrawn from 50X stock solutions in DMSO, a control experiment was performed adding an equal amount of DMSO to protein solution. Samples were then subjected to agitation (1200 rpm) for 15 minutes and centrifuged for 30 min at 16000 g; pellets and supernatants were carefully separated and a solution of 8 M urea and 2 M thiourea was added to each sample to reach a final concentration of 2.6 M Urea and 0.67 M thiourea. Following 10 min of incubation on ice, 10 μ L of each sample was diluted with 5 μ L of loading buffer and ran on a 10% SDS-PAGE. Western blotting analysis was then performed as reported above.

7.2.6 Alpha-screen assays to monitor TDP43 binding to bt-TAR32-DNA

TDP-43 with a glutathione S-transferase (GST) tag on the C-terminus was purchased from Abnova. Single-stranded DNA oligonucleotide (TAR32) biotinylated (bt) at the 5' end, was synthesized by LifeTechnologies . The TAR-32 sequence is 5'-CTG CTT TTT GCC TGT ACT GGG TCT CTG TGG TT-3' and corresponds to the first 32 nucleotides of the sequence identified by Ou *et al.* to bind to TDP-43^[160]. AlphaScreen GST detection kit was purchased from PerkinElmer. Different concentrations of bt-TAR-32 and GST-TDP43 were tested to optimize measurements. Finally, assay mixtures contained TDP-43 at final concentration of 0.1 nM, bt-TAR-32 5 nM, 10 μ g/mL of AlphaScreen streptavidin donor beads and anti-GST acceptor beads diluted in assay buffer (25 mM Tris [pH 7.4], 0.1% chaps). More in details,

Experimental Section

TDP-43 (0.2 nM) was pre-incubated with 20 µg/mL anti-GST acceptor beads in assay buffer for 30 min at room temperature and then added to assays containing 10 nM bt-TAR-32 also pre-incubated with 20 µg/mL streptavidin donor beads for 30 min at room temperature. Later on, acceptor and donor beads were combined in 384-well plates. After 3 h of incubation in the dark at room temperature, to ensure the binding reaction was at equilibrium, the AlphaScreen signal was measured on a EnSpire Alpha plate reader (PerkinElmer, Waltham, MA, USA).

To test the effect on TDP43-TAR32 binding, HET (0.05 nM-50 µM) was pre-incubated with TDP-43 (0.2 nM) pre-bound to AlphaScreen anti-GST acceptor beads for 30 min at room temperature. DMSO concentration was less than 1% in each sample. Assays were initiated by the addition of bt-TAR-32 at 10 nM pre-bound to AlphaScreen streptavidin donor beads. After incubation in the dark at room temperature for 3 h, the AlphaScreen signal was measured. IC50 values were determined from nonlinear regression fits of the data in GraphPad Prism.

7.2.7 Proteasome assay

100-mm plates of HeLa cells were separately treated with HET 10 µM and MG132 50 µM for 3 h whereas cells exposed to vehicle were utilized as control. Then, cells were abundantly washed, scraped off and harvested by centrifugation. The cell pellets were incubated with lysis buffer (PBS 1X, 0.1% Igepal) for 5 min on ice and sonicated for two pulses of 10 s, at 30% output power, using a *Vibracell* sonicator. Lysates were then centrifuged for 10 min at 10000g and 4°C to remove cellular debris, and the protein concentration was determined according to Bradford using BSA as standard. 10 µg of each sample were diluted in 100 µl assay buffer (25 mM HEPES pH

7.4, 0.5 mM EDTA, 1 mM ATP) and fluorogenic peptides Suc-LLVY-amc (10 μ M) was used to measure the chymotrypsin-like activities of the 20S proteasome. The release of 7-amino-4-methylcoumarin (amc) was monitored for 2 hours by emission at 460 nm (excitation 380 nm) using a multi-well plate Perkin Elmer LS55 Fluorescence Spectrometer. The experiments were performed in triplicate.

7.2.7 HET influence on TDP43 cellular localization

For immunofluorescence analysis, 4×10^4 cells/well were seeded on cover slips in 24-well plastic plates. After 24h, cells were treated with 10 μ M HET (2h, 37 $^{\circ}$ C) or 50 μ M MG132 (3h, 37 $^{\circ}$ C) followed or not by heat shock treatment (1h, 43 $^{\circ}$ C). At the end of the treatments, cells were fixed in 4% paraformaldehyde (PFA) in PBS and subsequently permeabilized with 0.5% Triton X-100 for 15 min. Cover slips were blocked with 1% bovine serum albumin (BSA) and 10% normal goat serum in PBS for 1 h and incubated with antibodies against TDP-43 (1:2000; Sigma T1705) and HuR (1:200; Santa Cruz sc-5261), diluted in blocking buffer for 2 h at room temperature. Labelling was visualized with the fluorescently conjugated secondary antibodies DyLight 594 anti-rabbit and DyLight 488 anti-mouse (Jackson). All secondary antibodies were diluted 1:2000 in PBS. Images were collected on a Zeiss LSM 510 confocal microscope using LSM software. Images shown are representative of multiple fields and triplicate cover slips per experiment. TDP-43 and HuR-positive SGs were counted in cultures where indicated. A minimum of 200 cells was counted across multiple fields of view (and multiple coverslips) for each treatment. The number of TDP-43 and HuR-positive SGs were counted in each cell. The total number of SGs was divided by the total number of cells to

Experimental Section

provide a measure of mean SGs per cell. SGs were not observed in untreated cells.

7.2.8 HET influence on TDP43 cellular aggregation

HeLa cells were separately treated with 10 μ M HET, 50 μ M MG132 or vehicle (less than 1% DMSO) as control and incubated for 3 hours at 37°C in a 5% CO₂ atmosphere. Subsequently, cells were harvested and lysed by sonication as described above. Resulting lysates were centrifuged for 10 min at 10000g and 4°C to separate lysis buffer-soluble and insoluble fractions. Supernatants were collected and the protein concentration was determined according to Bradford using BSA as standard. The lysis buffer-insoluble fractions were re-suspended in a denaturing buffer (Tris 30mM, Urea 8M, thiourea 2 M and chaps 4%) and solubilisation was favoured over night under continuous shaking. Urea-soluble samples (5 μ L) and lysis buffer-soluble extracts (10 μ g) were resolved on a 10% SDS-PAGE gel and subjected to western blotting analysis using anti-TDP-43 antibody as reported above. The experiments were conducted in triplicate and GADPH antibody was used for normalization.

7.3 In vitro and in cell Scalaradial interactome profiling

7.3.1 In-Vitro Proteome Profiling

SLD (1.5 mg, 3.5 μ mol) has been incubated with tenfold molar excess of 2-(2-amino-ethyl-disulfanyl)-ethyl-amine (TIOS) in ACN 0.5 % TEA. The reaction mixture was kept at room temperature for 30 minutes and product formation was monitored by using Agilent 1100 series chromatograph equipped with

Phenomenex Jupiter C18 5 μ 150 x 2.00 mm column at the flow rate of 0.200 ml/min. The elution was achieved by means of a linear gradient from 5% to 95% of B in 20 minutes (A: H₂O, 0,1% TFA; B: 95% ACN, 5% H₂O, 0,07% TFA) and monitored with an UV detector at the wavelength of 220 nm.

The product formation was monitored (r.t. 25,5 min) by acquiring mass spectra on LCQ-DECA (Thermo Finnigan) equipped with an ESI source.

The adduct, 2.7 μ mol, was purified by means of the abovementioned chromatographic conditions, lyophilized and put in reaction with CDI-Agarose in 800 μ l of ACN/NaHCO₃. Immobilization yield was assessed by injecting small aliquots of the reaction mixture in HPLC and evaluating the reduction of SLD-TIOS peak areas. After 16h, the immobilization yield resulted to be 98 % and the matrix preparation was completed by adding to the solid support 400 μ l of 50 mM TRIS (Tris(2-aminoethyl)amine, pH=9) and maintaining the reaction under stirring for three hours. A control matrix was prepared in parallel by adding 2.1 μ mol of TIOS, solubilized NaHCO₃ 50 mM, to 300 μ l of CDI-Agarose. Linker immobilization was established analysing a small aliquot of beads with Kaiser test. Briefly, after extensive washings with ethanol, 20 μ l of ninidrin (6% in ethanol), 20 μ l di fenol (80% in ethanol), and 20 μ l of KCN were added to the matrix and the development of violet colour, indicating the presence of primary amines onto the beads surface, was detect after 5 min at 50°C. To the control matrix was added a solution containing acetic anhydride in DMF 5% TEA to acetylate free amines and a Kaiser test has been performed to verify the absence of free amines on modified resins.

HeLa cells were grown and collected as already described (see chapter 7.1.4) and resuspended in ice-cooled PBS containing Igepal (0.1%) and a protease inhibitor cocktail. Cell lysis was achieved by dounce homogenation and cellular debris were removed by centrifugation at 10000g for 10 min at 4 °C. Protein concentration was determined using Bradford assay and adjusted to 1 mg/ml. SLD-bound bead suspension (50 μ L) and the same amount of the

Experimental Section

control-matrix were separately incubated with 1 mg of HeLa total protein extract under continuous shaking (1h, 4°C). Beads were collected after centrifugation (1200 rpm, 3min, 4°C) and washed three times with PBS (pH 7.4). The bound proteins were detached from the beads by breaking the disulphide bond contained into the TIOS linker with DTT 40 mM. The suspension was maintained at 37°C for 15 minutes to favourite disulphide bridge cleavage. SDS-PAGE loading buffer (60 mM Tris/HCl pH 6.8, 2% SDS, 0.001% bromophenol blue, 10% glycerol, 2% 2-mercaptoethanol) was added to each sample and, after 5min at 95°C, denatured eluates were separated on 10% SDS-PAGE, and stained with Coomassie G-250 (Bio-Rad, Hercules, CA). SDS-PAGE gel lanes were cut and digested. The experiment has been repeated twice using an opportune control matrix bearing the linker without any metabolite. Each piece was washed with ultrapure water and CH₃CN and subjected to in situ protein digestion as described by Shevchenko as already described (see chapter 7.1.4). Peptide samples re-suspended in formic acid (FA, 10%) and analysed with an ACQUITY UPLC system (Waters) coupled to a LTQ-Orbitrap XL (ThermoScientific).

Peptides were separated on a 1.7 mm BEH C18 column (Waters) at a flow rate of 400 nL/min. Peptide elution was achieved with a linear gradient (solution A: 95 % H₂O ,5 % CH₃CN, 0.1% FA; solution B: 95 % CH₃CN, 5 % H₂O, 0.1 % FA); 15–50% B over 55 min). MS and MS/MS data were acquired on high-performance liquid chromatography mass spectrometry system. The ten most intense doubly and triply charged peptide ions were chosen for fragmentation. Mascot generic files (mgf) for database search were generated by the software MassMatrix MS data file conversion. Database searches were carried out on the Mascot server (<http://www.matrixscience.com/>). The SwissProt database (release 2013_02, 6 February 2013, contains 539,165 sequence entries comprising 191,456,931 amino acids abstracted from 216,632 references) was employed. Searches were performed allowing two missed

cleavages; carbamidomethyl (C) as fixed modification and oxidation (M) and phosphorylation (ST) as variable modifications; peptide tolerance 25 ppm; MS/MS tolerance 0.8 Da.

7.3.2 Validation experiments

After exposing SLD-bearing matrix and control matrix to the cellular lysate, eluted proteins were separated on 12% SDS-page and transferred to a nitrocellulose membrane.

The membrane was incubated for 1 h in a blocking solution containing 25 mM Tris pH 8, 125mM NaCl, 0.05% Tween-20, 5% non-fat dried milk prior of exposition to primary antibodies raised against 14-3-3 ϵ (1:500) and PRX1 (1:500; Novus Biologicals). The recognition of specific epitopes was favourite overnight, at 4°C. Then, membrane was incubated for 1 h with an anti-rabbit peroxidase-conjugated secondary antibody (1:5000) (Sigma-Aldrich). 14-3-3- ϵ and PRX1 were detected by a chemo-luminescence detection system.

14-3-3 ϵ and PRX1 were immobilized onto two different flow cells of a CM5 sensor chip using standard amine coupling procedures. Phosphate-buffered saline, which consisted of 10 mM Na₂HPO₄ and 150 mM NaCl, pH 7.4, was used as running buffer. The carboxymethyl dextran surface was activated as already described and both proteins were diluted to a final concentration of 30 ng/ μ l in 10 mM sodium acetate, pH 4.5 and injected separately onto the two flow cells. After protein injections a Δ RU of 9000 for PRX1 and a Δ RU of 14000 was recordered. The activated carboxymethyl dextran surface was finally blocked with a 7-min injection of 1.0 M ethanolamine-HCl, pH 8.5, at 5 μ l/min.

SLD solutions (0.01-10 μ M), were prepared in running buffer containing 1% of DMSO and injected at least three times. Since the dissociation back to

Experimental Section

baseline was achieved within a reasonable time frame, no regeneration has been required. The interaction experiments were carried out at a flow rate of 10 $\mu\text{l}/\text{min}$, employing a 3 min injection time. The dissociation time was set at 600 seconds. Rate constants for associations (k_a) dissociations (k_d) and the dissociation constants (K_D) were obtained by globally fitting data from injections of all concentrations, using the BIAevaluation software, using the simple 1:1 Langmuir binding model.

7.3.3 Design and Synthesis of SLD-AZ

SLD (1.5 mM) was coupled with 11-azido-3,6,9-trioxaundecan-1-amine (TRX-AZ, 15 mM) in ACN at 0.5% TEA for 1h at 25°C under stirring. Product formation has been monitored by RP-HPLC-UV at 220 nm using Agilent 1100 binary pump and Phenomenex column (Jupiter C18 150X2 mm 5 μ) at 0.2 mL/min. Gradient was from 5% to 95% buffer B (A= 100% H₂O and 0.1% TFA and B= 95% ACN, 5% H₂O and 0.1% TFA) in 25 min. Mass spectra were acquired on LCQ-DECA ThermoFinnigan equipped with an ESI source.

7.3.4 Click Chemistry Optimization

SLD-AZ (1.25 mM) has been incubated for 1h with the linker 4-pentyn-1-amine (PINA linker 2.50 mM) in 200 μL of PBS at pH 7.4 and less than 10% DMSO. Later on, with 100 μM CuSO₄, 5 mM Na-L-(+)-Ascorbate and 100 μM Tris-[(1-benzil-1,2,3-triazol-4-yl)metal]amine (TBTA) under nitrogen and stirring. Product formation has been monitored by RP-HPLC-UV and MS analysis as reported above.

7.3.5 *In-Situ* Proteome Profiling

To obtain an azide-coated matrix, 500 μ L of CDI resin has been mixed with 5 μ mol of PINA linker in PBS buffer at pH of 7.4 for 3h at r.t.

SLD-AZ (1 and 10 nmol) was incubated with HeLa cell lysate (obtained as described above) for 1 h at 4°C and then mixed with 50 μ L of CDI-Agarose PINA-bearing matrix in presence of CuSO₄, Na-L-(+)-Ascorbate and TBTA under nitrogen. As control, the experiment has been carried out in the same conditions using the TRX-Az as bait. After several washes in PBS buffer to remove the unbound proteins, SLD partners were eluted, separated by 12% SDS-PAGE and transferred onto a nitrocellulose membrane and probed as described above with antibodies directed against 14-3-3- ϵ and PRX1.

7.3.5 Cell Viability Assay

Cell viability was assessed by 3-(4,5-dimethylthiazol-2-yl)-2,5-diphenyltetrazolium bromide (MTT) assay^[219]. After SLD and SLD-AZ treatment in a concentration range from 1 μ M to 10 μ M, the mitochondrial-dependent reduction of 3-(4,5- dimethylthiazol-2-yl)-2,5-diphenyltetrazolium bromide (MTT) to formazan was used to assess the effect of the two molecules.

7.3.6 In cell fishing for partners

Live HeLa cells were grown as described above, treated with 1 μ M of SLD-AZ and 1 μ M of TRX-AZ for 6 hours and then washed with fresh media to remove the excess of drug which did not pass through cell membranes. Cell

Experimental Section

were then lysed by dounce homogenation in a mixture containing PBS 0.1% Igepal and proteases inhibitors. 1 mg of lysates were then treated with 250 μ M CuSO₄, 2.5 mM Na-L-(+)-Ascorbate and 500 μ M TBTA under nitrogen to promote Huisgen 1,3 cycloaddition on 10 μ L of PINA derived CDI-Agarose beads for 45 minutes at 4°C. The same reaction was carried out both on the same sample without 2.5 mM Na-L-(+)-Ascorbate and on TRX-AZ treated cell lysates as negative controls. Pull-down samples were then separated by SDS-PAGE followed both by immune-blotting analysis as described above or Comassie staining. SDS-PAGE gel lanes were cut, digested and analysed as reported. Western blotting analysis on proteasome were carried out using primary monoclonal antibodies raised against α -7 proteasome subunit (1:500) and Psmc3 (1: 500) (Santa Cruz Biotechnology). Then, membrane was incubated for 1 h with an anti-mouse peroxidase-conjugated secondary antibody (1:5000). A chemo-luminescence detection system has been used.

7.3.7 In cell fishing for partners using Oleocanthal as bait

Oleocanthal (1 mg, 3.3 μ mol) was put in reaction with 33 μ mol of TRX-AZ in ACN/NaHCO₃. After 30 minutes at room temperature, a solution containing 100 mM NaBH₄ was added to the reaction mixture to allow imine reduction for 30 minutes at room temperature. Product formation (OLC-AZ) was monitored by injecting the reaction mixture in HPLC (Agilent 1100 series equipped with Jupiter Proteo C18 250x2.00 5 μ M) and by eluting the adduct by means of a linear gradient of B from 10% to 95% in 25 minutes (solution A: TFA (0.1%); solution B: TFA (0.07 %), H₂O (5%), CH₃CN (95 %)). MS analysis was performed using LCQ-Deca equipped with an ESI source.

HeLa cells were grown as described, and treated with OLC-AZ or TRX-AZ at the concentration of 100 μ M. After 3 h, supernatants were discarded and cells

were harvested and extensively washed prior cellular lysis performed as described.

The coupling reaction of OLC-AZ and TRX-AZ to PINA-bearing matrix was performed by employing 100 μ M CuSO₄, 100 μ M TBTA, 5mM Na-Ascorbate, maintaining the suspensions under agitation for 45 minutes.

After abundant washings in PBS, strictly bound proteins were eluted with SDS-PAGE loading buffer, separated by 10% SDS-PAGE and transferred onto nitrocellulose membrane.

HSP90 was detected by incubating the membrane with the specific primary antibody (BD-Biosciences), overnight at 4°C and with an anti-mouse peroxidase-conjugated secondary antibody (1:5000; Thermo Scientific). Signals were detected using an enhanced chemiluminescent substrate (ECL) and LAS 4000 digital imaging system.

-CHAPTER 8-

New insights in cCMP interaction profile by chemical proteomics: Experimental procedures

Materials

N4-(6-Aminoethyl)cytidine- 3', 5'- cyclic monophosphate, (4-AH-cCMP) was purchased from BIOLOG (Bremen, Germany). CDI-activated resin and NHS-activated agarose were obtained from Pierce. Protease inhibitor cocktail, complete mini, was from Roche Diagnostic. All the other chemicals (analysis grade) were purchased from commercial sources. For all experiments high purity water, obtained from a Milli-Q system (Millipore, Bedford, MA), was used.

8.1 Pull down experiments using cCMP as bait

500 μ l of NHS-activated agarose were treated with a 5 mM solution of 4-AH-cCMP in 1 ml of NaHCO_3 (50mM) at pH=8.5 under continuous shaking. The amount of immobilized 4-AH-cCMP was estimated by integrating the peaks of the free species after HPLC injections of supernatants at t=0 h, t=2 h and t=24 h. HPLC runs were carried out using LC 10AD VP, with a ZOBRAE Eclipse Plus C18 column (2.1x50mm, 1.8-micron) and a solution of 95% H_2O 5% acetonitrile (ACN) 0.1% formic acid (FA) was used as eluent at a flow rate of 0.150 mlmin^{-1} . After 24 hours the unbound cCMP was removed and a 500 mM Tris solution was added to the beads to quench unreacted functional groups onto beads surface. A control matrix was obtained incubating 500 μ l of NHS-Activated Agarose with Tris buffer.

HEK293 cells were collected centrifuging at 10000 rpm for 5 min and washed three times with phosphate-saline buffer (PBS, 50 mM sodium phosphate, 150 mM NaCl). The obtained pellets were dissolved in ice-cool PBS containing 0.1% Tween-20, supplemented with a protease inhibitor (1 complete min/15 mL, Roche) and lysed by dounce homogenation. Cellular debris were removed

Experimental Section

by centrifugation in an eppendorf table top centrifuge at 14000 rpm for 10 min at 4° C. Supernatants were carefully collected and pellets re-suspended in lysis buffer (500 µL) to increase the yield of the lysis procedure. The second supernatant, obtained by centrifugation (14000 rpm, 10 min, 4°C), was added to the first one and the protein concentration was determined using a Bradford assay. Prior to addition of the beads, the lysate was diluted to a final concentration of 1 mg/mL using lysis buffer. Depending on the yield of total protein from the extraction procedure, in each pull-down, 10 µL of beads mixture was used per mg of protein. The obtained lysate-beads suspension was incubated for 1 h at 4°C by rotary shaking. Several washings with lysis buffer were carried out and proteins strictly bound to the resins were eluted by boiling them with an SDS sample loading buffer (Biorad)

8.2 cCMP interactome profiling by competition experiments

Cellular extracts were obtained lysing HEK293 as described above, diluted to a final concentration of 1 mg/mL in lysis buffer. Two aliquots, each containing 4 mg of proteins, were withdrawn and incubated separately with control matrix and cCMP-bearing matrix. To the remaining protein solution, ADP and GDP were added to a final concentration of 10 mM and the obtained mixture was further subdivided in 4 equal batches, each containing 4 mg of proteins. Aliquots were separately treated for 30 min at 4°C with (i) 5 µM cAMP, (ii) 5 µM cGDP, (iii) cAMP and cGMP at the same concentrations. All batches were then incubated with 40 µL of cCMP-bearing matrix for 90 minutes at 4°C under continuous shaking. Later on, the unbound proteins were discarded and, after abundant washings with lysis buffer, the tightly bound proteins were eluted with SDS-sample loading buffer and separated by SDS-PAGE (Criterion XT Bis-Tris Precast Gels, BioRad). Resulting gel was stained with a

coomassie solution (GelCode Blue Stain Reagent - Pierce). For protein identification, coomassie stained gel was cut in small pieces and digested as previously reported. Briefly, each slice was reduced with 1,4-dithiothreitol (DTT, 10 mM) and alkylated with iodoacetamide (54 mM), then washed and rehydrated in trypsin solution (12 ngml⁻¹) on ice for 1h. After the addition of ammonium bicarbonate (30 μ L, 50 mM, pH 7.5), protein digestion was allowed to proceed overnight at 37°C. The supernatants were collected and peptides were extracted from the slice by using 100% CH₃CN, dried in vacuo and resuspended in 10% FA.

The peptide samples were analysed on an LTQ-Orbitrap XL instrument (Thermo, San Jose, CA) connected to an Agilent 1200 HPLC system. All columns were packed in house. The trap column was made using Aqua C18 material (Phenomenex, Torrance, CA). Reprosil-pur C18 3 μ m (Dr. Maisch, Ammerbuch-Entringen, Germany) was used for the 35 cm analytical column with 50 μ m inner diameter. Solvent A consisted of 0.1M acetic acid in Milli-Q water, and solvent B consisted of 0.1M acetic acid in 80% acetonitrile. The flow rate of 5 μ Lmin⁻¹ was passively split and reduced to an effective flow rate of 100 nLmin⁻¹.

The gradients were as follows: 60 min LC method, 10 min solvent A; 10-40% solvent B within 30 min; 100% solvent B for 2 min; 15 min solvent A.

Nanospray was achieved using a distally coated fused silica emitter (New Objective, Cambridge, MA) (outer diameter, 360 μ m; inner diameter, 20 μ m; tip inner diameter, 10 μ m) biased to 1.7 kV. The LTQ-Orbitrap mass spectrometer was operated in data-dependent mode, automatically switching between MS and MS/MS. Full-scan MS spectra (300–1500m/z) were acquired with a resolution of 60,000 at 400 m/z and accumulation to a target value of 500,000. The five most intense peaks above a threshold of 500 were selected for collision-induced dissociation in the linear ion trap at a normalized collision energy of 35%.

Experimental Section

Charge state screening was enabled, and precursors with unknown charge state or a charge state of 1 were excluded. The obtained data were processed with proteome discoverer 1.3 (Thermo, Bremen, Germany) using Mascot (version 2.4.1 Matrix Science, London, UK) for database searching. The SwissProt human database was searched, allowing 2 missed cleavages, carbamidomethyl as fixed modification on cysteines, as well as oxidation (M) and phosphorylation (ST) as variable modifications. The peptide tolerance was set to 25 ppm and the MS/MS tolerance to 0.8 Da. Semi-quantitative analysis was performed by comparing PSMs. Only proteins identified with more than five PSMs were taken into account.

Bibliography

- [1] Anderson N.L., Anderson N.G., *Electrophoresis*, (1998), **19**,1853-61.
- [2] Blackstock W.P., Weir M.P., *Trends Biotechnol.*, (1999), **17**, 121-7.
- [3] Altelaar A.F., Munoz J., Heck A.J., (2013). *Nat. Rev. Genet.*, **14**, 35-48
- [4] Aebersold R., Mann M., *Nature*, (2003), **422**, 198-207.
- [5] Makarov A., *Anal. Chem.*, (2000), **72**, 1156-62
- [6] Makarov A., Denisov E., Kholomeev A., Balschun W., Lange O., Strupat K., Horning S., *Anal. Chem.*, (2006), **78**, 2113-20
- [7] Cox J., Mann M., *Annu. Rev. Biochem.*, (2011), **80**, 273-299.
- [8] Cox J., Mann M., *Cell*, (2007), **130**, 395-398.
- [9] Rix U., Superti-Furga G., *Nat. Chem. Biol.*, (2009), **5**, 616-24
- [10] Han X., Jin M., Breuker K., McLafferty F.W., *Science*, (2006), **314**, 109-12
- [11] Tran J.C., Zamdborg L., Ahlf D.R., Lee J.E., Catherman A.D., Durbin K.R., Tipton J.D., Vellaichamy A., Kellie J.F., Li M., Wu C., Sweet S.M., Early B.P., Siuti N., LeDuc R.D., Compton P.D., Thomas P.M., Kelleher N.L., *Nature*, (2011), **480**, 254-8
- [12] Yates J.R., Ruse C.I., Nakorchevsky A., *Annu. Rev. Biomed. Eng* (2009), **11**, 49-79.
- [13] Klose J., *Humangenetik*, (1975), **26**, 231-43
- [14] O'Farrell P.H., *J. Biol. Chem.*, (1975), **250**, 4007-21
- [15] Abdallah C., Dumas-Gaudot E., Renaut J., Sergeant K., *Int. J. Plant Genomics*, (2012), **2012**, Article ID 494572
- [16] Lopez J.L., *J. Chromatogr. B Analyt. Technol. Biomed. Life Sci.*, (2007), **849**, 190-202

Bibliography

- [17] Laemmli U.K., *Nature*, (1970), 227, 680-685
- [18] Shevchenko A., Wilm M., Vorm O., Mann M., *Anal. Chem.*, (1996), **68**, 850-8
- [19] Wilm M., Mann M., *Anal. Chem.*, (1996), **68**, 1-8
- [20] Washburn M.P., Wolters D., Yates J. R., *Nat. Biotechnol.*, (2001), **19**, 242-7
- [21] Vollmer M., Horth P., Nagele E., *Anal. Chem.*, (2004), **76**, 5180-5
- [22] Issaq H.J., Chan K.C., Janini G.M., Conrads T.P., Veenstra T.D., *J. Chromatogr. B Anal. Technol. Biomed. Life Sci.*, (2005), **817**, 35-47.
- [23] Wang H., Hanash S., *J. Chromatogr. B Anal. Technol. Biomed. Life Sci.*, (2003), **787**, 11-8
- [24] Dormeyer W., Mohammed S., van Breukelen B., Krijgsveld J., Heck A.J., *J. Proteome Res.*, (2007), **6**, 4634-45
- [25] Taouatas N., Altelaar A.F., Drugan M.M., Helbig A.O., Mohammed S., Heck A.J., *Mol. Cell. Proteomics*, (2009), **8**, 190-200
- [26] Dai J., Wang L.S., Wu Y.B., Sheng Q.H., Wu J.R., Shieh C.H., Zeng R., *J. Proteome Res.*, (2009), **8**, 133-41
- [27] Alpert A.J., *J. Chromatogr.*, (1990), **499**, 177-96.
- [28] Boersema P.J., Dvecha N., Heck A.J., Mohammed S., *J. Proteome Res.*, (2007), **6**, 937-46
- [29] Cargile B.J., Talley D.L., Stephenson J.L. Jr., *Electrophoresis*, (2004), **25**, 936-45
- [30] Hubner N.C., Ren S., Mann M., *Proteomics*, (2008), **8**, 4862-72
- [31] Henzel W.J., Watanabe C., Stults J.T., *J. Am. Soc. Mass Spectrom.*, (2003), **14**, 931-42
- [32] Olsen J.V., Mann M., *Proc. Natl. Acad. Sci. U.S.A* , (2004), **101**, 13417-22

- [33] Hunt D.F., Yates J.R., Shabanowitz J., Winston S., Hauer C.R., *Proc. Natl. Acad. Sci. U.S.A.*, (1986), **83**, 6233-7
- [34] Syka J.E., Coon J.J., Schroeder M.J., Shabanowitz J., Hunt D.F., *Proc. Natl. Acad. Sci. U.S.A.*, (2004), **101**, 9528-33
- [35] Zubarev R.A., *Curr. Opin. Biotechnol.*, (2004), **15**, 12–6
- [36] Lau K.W., Hart S.R., Lynch J.A., Wong S.C., Hubbard S.J., Gaskell S.J., *Rapid Commun. Mass Spectrom.*, (2009), **23**, 1508–14
- [37] Syka J.E., Coon J.J., Schroeder M.J., Shabanowitz J., Hunt D.F., *Proc. Natl. Acad. Sci. U.S.A.*, (2004), **101**, 9528–33.
- [38] Zubarev R.A., *Curr. Opin. Biotechnol.* (2004), **15**, 12–6
- [39] Zhang Y., Ficarro S.B., Li S., Marto J.A., *J. Am. Soc. Mass Spectrom.*, (2009), **20**, 1425–34
- [40] Mischerikow N., van Nierop P., Li K.W., Bernstein H. G., Smit A.B., Heck A.J., Altelaar A.F., *Analyst*, (2010), **135**, 2643–52
- [41] Zhang J., Wang Y., Li S., *Anal. Chem.*, (2010), **82**, 7588–95
- [42] Frese C.K., Altelaar A.F., Hennrich M.L., Nolting D., Zeller M., Griep-Raming J., Heck A.J., Mohammed S., *J. Proteome Res.*, (2011), **10**, 2377-88
- [43] Perkins D.N., Pappin D.J., Creasy D.M., Cottrell J.S., *Electrophoresis*, (1999), **18**, 3551-67
- [44] Colinge J., Masselot A., Giron M., Dessingy T., Magnin J., *Proteomics*, (2003), **8**, 1454-63
- [45] Liang X., Hajivandi M., Veach D., Wisniewski D., Clarkson B., Resh M.D., Pope R.M., *Proteomics*, (2006), **6**, 4554-64
- [46] Lee A.Y., Paweletz C.P., Pollock R.M., Settlage R.E., Cruz J.C., Secrist J.P., Miller T.A., Stanton M.G., Kral A.M., Ozerova N.D., Meng F., Yates N.A., Richon V., Hendrickson R.C., *J. Proteome. Res.*, (2008), **7**, 5177-86

Bibliography

- [47] Song D., Chaerkady R., Tan A.C., Garcia-Garcia E., Nalli A., Suarez-Gauthier A., Lopez-Rios F., Zhang, X.F., Solomon A., Tong J., Read M., Fritz C., Jimeno A., Pandey A., Hidalgo M., *Mol. Cancer Ther.*, (2008), **7**, 3275-84
- [48] Domon B., Aebersold R., *Nat. Biotechnol.*, (2010), **28**, 710.
- [49] Berth M., Moser F.M., Kolbe M., Bernhardt J., *Appl. Microbiol. Biotechnol.*, (2007), **76**, 1223-43
- [50] Larbi N.B., Jefferies C., *Methods Mol Biol.*, (2009), **517**, 105-32.
- [51] Timms J.F., Cramer R., *Proteomics*, (2008), **8**, 4886-97
- [52] Viswanathan S., Unlü M., Minden J.S., *Nat. Protoc.*, (2006), **1**, 1351-8.
- [53] Gygi S.P., Corthals G., Zhang Y., Rochon Y., Aebersold, R., *Proc. Natl. Acad. Sci. U.S.A.*, (2000), **17**, 9390-5
- [54] Ong S.E., Pandey A., *Biomol. Eng.*, (2001), **18**, 195-205
- [55] Lilley K.S., Razzaq A., Dupree P., *Curr. Opin. Chem. Biol.*, 2002, **6**, 46-50
- [56] Ong S.E., Mann M., *Nat. Protoc.*, (2006), **1**, 2650-60
- [57] Ong S.E., Mann M., *Methods Mol Biol.*, (2007), **359**, 37-52.
- [58] Ong S.E., Blagoev B., Kratchmarova I., Kristensen D.B., Steen H., Pandey A., Mann M., *Mol. Cell. Proteomics*, (2002), **1**, 376-386
- [59] Ong S.E., Kratchmarova I., Mann M., *J. Proteome Res.*, (2003), **2**, 173-81
- [60] Shiiio Y., Aebersold R., *Nat. Protoc.*, (2006), **1**, 139-45
- [61] Wiese S., Reidegeld K.A., Meyer H.E., Warscheid B., *Proteomics*, (2007), **7**, 340-50
- [62] Hsu J.L., Huang S.Y., Chow N.H., Chen S.H., *Anal. Chem.*, (2003), **24**, 6843-52
- [63] Karp N.A., Huber W., Sadowski P.G., Charles P.D., Hester S.V., Lilley K.S., *Mol. Cell. Proteomics*, (2010), **9**, 1885-97

- [64] Mahoney D.W., Therneau T.M., Heppelmann C.J., Higgins L., Benson L.M., Zenka R.M., Jagtap P., Nelsestuen G.L., Bergen H.R., Oberg A.L., *J. Proteome Res.*, (2011), **10**, 4325-33
- [65] Boersema P.J., Raijmakers R., Lemeer S., Mohammed S., Heck A.J., *Nat. Protoc.*, (2009), **4**, 484-94
- [66] Boersema P.J., Aye T.T., van Veen T.A., Heck A.J., Mohammed S., *Proteomics*, (2008), **22**, 4624-32
- [67] Hsu J.L., Huang S.Y., Chen S.H., *Electrophoresis*, (2006), **18**, 3652-60
- [68] Patel V.J., Thalassinou K., Slade S.E., Connolly J.B., Crombie A., Murrell J.C., Scrivens J.H., *J. Proteome Res.*, (2009), **8**, 3752-59
- [69] Bantscheff M., Schirle M., Sweetman G., Rick J., Kuster B., *Anal. Bioanal. Chem.* (2007), **389**, 1017-31
- [70] Silva C., Denny, R., Dorschel C., *Anal. Chem.*, (2005), **7**, 2187-200
- [71] Chelius D., Bondarenko P.V., *J. Proteome Res.*, (2002), **1**, 317-23
- [72] Kobe B., Kemp B.E., *Nature*, (1999), 402, 373-6
- [73] Cravatt B.F., Wright A.T., Kozarich J.W., *Annu. Rev. Biochem.*, (2008), **77**, 383-6
- [74] Evans M.J., Cravatt B.F., *Chem. Rev.*, (2006), **106**, 3279-301
- [75] Shi H., Liu K., Xu A., Yao S.Q., *Chem. Commun.(Camb.)*, (2009), **33**, 5030-2
- [76] Saghatelian A., Jessani N., Joseph A., Humphrey M., Cravatt B.F., *Proc. Natl. Acad. Sci. USA*, (2004), **101**, 10000-5
- [77] Sieber S.A., Niessen S., Hoover H.S., Cravatt B.F., *Nat. Chem. Biol.*, (2006), **2**, 274-81
- [78] Chan E.W., Chattopadhyaya S., Panicker R.C., Huang X., Yao S.Q., *J. Am. Chem. Soc.*, (2004), **126**, 14435-46
- [79] Salisbury C.M., Cravatt B.F., *Proc. Natl. Acad. Sci. USA*, (2007), **104**, 1171-6

Bibliography

- [80] Ovaa H., van Swieten P.F., Kessler B.M., Leeuwenburgh M.A., Fiebigler E., van den Nieuwendijk A.M., Galardy P.J., van der Marel G.A., Ploegh H.L., Overkleeft H.S., *Angew. Chem. Int. Ed. Engl.*, (2003), **42**, 3626-9
- [81] Patricelli M.P., Giang D.K., Stamp L.M., Burbaum J., *J. Proteomics* (2001), **1**, 1067-71
- [82] Greenbaum D., Baruch A., Hayrapetian L., Darula Z., Burlingame A., *Mol. Cell. Proteomics*, (2002), **1**, 60-8
- [83] Kidd D., Liu Y., Cravatt B.F., *Biochemistry*, (2001), **40**, 4005-15
- [84] Jessani N., Liu Y., Humphrey M., Cravatt B.F., *Proc. Natl. Acad. Sci. U.S.A.*, (2002), **99**, 10335-40
- [85] Jessani N., Niessen S., Wei B.Q., Nicolau M., Humphrey M., Ji Y., Han W., Noh D.Y., Yates J.R., Jeffrey S.S., Cravatt B.F., *Nat. Methods*, (2005), **2**, 691-7
- [86] Sieber S.A., Niessen S., Hoover H.S., Cravatt B.F., *Nat. Chem. Biol.* (2006), **2**, 274-81
- [87] Alexander J.P., Cravatt B.F., *J. Am. Chem. Soc.*, (2006), **128**, 9699-704
- [88] Adam G.C., Burbaum J.J., Kozarich J.W., Patricelli M.P., Cravatt B.F., *J. Am. Chem. Soc.*, (2004), **126**, 1363-8
- [89] Okerberg E.S., Wu J., Zhang B., Samii B., Blackford K., Winn D.T., Shreder K.R., Burbaum J.J., Patricelli M.P., *Proc. Natl. Acad. Sci. USA* (2005), **102**, 4996-5001
- [90] Rolén U., Kobzeva V., Gasparjan N., Ovaa H, Winberg G, Kissel'jov F, Masucci M.G., *Mol. Carcinog.*, (2006), **45**, 260-9
- [91] Speers A.E., Cravatt B.F., *J. Am. Chem. Soc.*, (2005), **127**, 10018-9
- [92] Fauq A.H., Kache R., Kahn M.A., Vega I.E., *Bioconjug. Chem.* (2006), **17**, 248-254

- [93] van der Veken P., Dirksen E.H.C., Ruijter R., Elgersma R.C., Heck A.J.R., Rijkers D.T.S., Slijper M., Liskamp R.M.J, *ChemBioChem* (2005), **6**, 2271-80
- [94] Verhelst S.H., Fonović M., Bogyo M., *Angew. Chem. Int. Ed.*, (2007), **46**, 1284-6
- [95] Greenbaum D., Medzihradzky K.F., Burlingame A., Bogyo M., *Chem. Biol.*, (2000), **7**, 569-81
- [96] Chiang K. P., Niessen S., Saghatelian A., Cravatt B. F., *Chem. Biol.* , (2006), **13**, 1041-50
- [97] Long J.Z., Li W., Booker L., Burston J.J., Kinsey S.G., Schlosburg J.E., Pavón F.J., Serrano A.M., Selley D.E., Parsons L.H., Lichtman A.H., Cravatt B.F., *Nat.Chem. Biol.*, (2009), **5**, 37-44
- [98] Edgington L. E., Berger A. B., Blum G., Albrow V. E., Paulick M.G., Lineberry N., Bogyo M., *Nat. Med.*, (2009), **15**, 967-73
- [99] Verdoes M., Florea B.I., Menendez-Benito V., Maynard C.J., Witte M.D., van der Linden W.A., van den Nieuwendijk A.M., Hofmann T., Berkers C.R., van Leeuwen F.W., Groothuis T.A., Leeuwenburgh M.A., Ovaa H., Neefjes J.J., Filippov D.V., van der Marel G.A., Dantuma N.P., Overkleeft H.S., *Chem. Biol*, (2006), **13**, 1217-26.
- [100] Willems L.I., van der Linden W.A., Li N., Li K.Y., Liu N., Hoogendoorn S., van der Marel G.A., Florea B.I., Overkleeft H.S., *Acc. Chem. Res.* 2011, **9**, 718-29
- [101] Saxon E., Bertozzi C.R., *Science* (2000), **287**, 2007-10
- [102] Wang Q., Chan T.R., Hilgraf R., Fokin V.V., Sharpless K.B., Finn M.G., *J. Am. Chem. Soc.*, (2003), **125**, 3192-3
- [103] Agard N.J., Baskin J.M., Prescher J.A., Lo A., Bertozzi C.R. *ACS Chem. Biol.*, (2006), **1**, 644-8

Bibliography

- [104] Speers A.E., Adam G.C., Cravatt, B.F., *J. Am. Chem. Soc.*, (2003), **125**, 4686-7
- [105] Hong V., Presolski S.I., Ma C., Finn M.G., *Angew. Chem. Int. Ed.*, (2009), **48**, 9879-83
- [106] Agard N.J., Prescher J.A., Bertozzi C.R., *J. Am. Chem. Soc.* (2004), **126**, 15046-7
- [107] Bantscheff M., Drewes G., *Bioorg. Med. Chem.* (2012), **20**, 1973-8
- [108] Carlson E., *ACS Chem. Biol.*, (2010), **5**, 639-53
- [109] Katayama H., Oda Y., *J. Chromatogr. B Analyt. Technol. Biomed. Life Sci.*, (2007), **855**, 21-7
- [110] Raida M., *Curr. Opin. Chem. Biol.*, (2011), **15**, 570-5
- [111] Bain J., Plater L., Elliott M., Shpiro N., Hastie C.J., McLauchlan H., Klevernic I., Arthur J.S., Alessi D.R., Cohen P. *Biochem. J.*, (2007), **408**, 297-315
- [112] Fedorov O., Marsden B., Pogacic V., Rellos P., Muller S., Bullock A.N., Schwaller J., Sundstro M., Knapp S., *Proc. Natl. Acad. Sci. U.S.A.* (2007), **104**, 20523-8
- [113] Fliri A.F., Loging W.T., Thadeio P.F., Volkmann R.A., *Nat. Chem. Biol.*, (2005), **1**, 389-97
- [114] Lounkine E., Keiser M. J., Whitebread S., Mikhailov D., Hamon J., Jenkins J. L., Lavan P., Weber E., Doak A.K., Cote S., Shoichet B.K., Urban L., *Nature*, (2012), **486**, 361-7
- [115] Bach S., Blondel M., Meijer L., Bach, S., Blondel, M. and Meijer, L., (2006), CRC Press, Taylor & Francis, chapter 5, 103-119.
- [116] Yue E., Smith P.J., (2006), CRC Press, Boca Raton, 103-119
- [117] Margarucci L., Monti M.C., Tosco A., Riccio R., Casapullo A., *Angew. Chem. Int. Ed. Engl.*, (2010), **49**, 3960-3

- [118] Margarucci L., Monti M.C., Fontanella B., Riccio R., Casapullo A., *Mol. BioSyst.*, (2011), **7**, 480-5
- [119] Margarucci L., Monti M.C., Mencarelli A., Cassiano C., Fiorucci S., Riccio R., Zampella A., Casapullo A., *Mol. BioSyst.*, (2012), **8**, 1412-7
- [120] Lomenick B., Olsen R.W., Huang J., *ACS Chem. Biol.*, (2012), **6**, 34-46
- [121] Cassiano C., Monti M.C., Festa C., Zampella A., Riccio R., Casapullo A., *ChemBioChem*, (2012), **13**, 1953-8
- [122] Shimizu N., Sugimoto K., Tang J., Nishi T., Sato I., Hiramoto M., Aizawa S., Hatakeyama M., Ohba R., Hatori H., Yoshikawa T., Suzuki F., Oomori A., Tanaka H., Kawaguchi H., Watanabe H., Handa H., *Nat. Biotechnol.*, (2000), **18**, 877-81
- [123] Tamura T., Terada T., Tanaka A., *Bioconjug. Chem.*, (2003), **14**, 1222-30
- [124] O'Carra P., Barry S., Griffin T., *FEBS Lett.*, (1974), **43**, 169-75
- [125] Yamamoto K., Yamazaki A., Takeuchi M., Tanaka A., *Anal. Biochem.*, (2006), **352**, 15-23
- [126] Shiyama T., Furuya M., Yamazaki A., Terada T., Tanaka A., *Bioorg. Med. Chem.*, (2004), **12**, 2831-41
- [127] Kanoh N., Takayama H., Honda K., Moriya T., Teruya T., Simizu S., Osada H., Iwabuchi Y., *Bioconjug. Chem.*, (2010), **21**, 182-6
- [128] Yang Y, Hahne H, Kuster B, Verhelst S.H., *Mol cell. Proteomics*, (2013), **12**, 237-44
- [129] Bantscheff M., Scholten A., Heck A.J., *Drug Discov. Today*, (2009), **14**, 1021-6
- [130] Verdoes M., Florea B.I., Menendez-Benito V., Maynard C.J., Witte M.D., van der Linden W.A., van den Nieuwendijk A.M., Hofmann T., Berkers C.R., van Leeuwen F.W., Groothuis T.A., Leeuwenburgh M.A., Ovaa H., Neeffjes J.J., Filippov D.V., van der Marel G.A., Dantuma N.P., Overkleeft H.S., *Chem. Biol.*, (2006), **13**, 1217-26

Bibliography

- [131] Jung D.W., Williams D., Khersonsky S.M., Kang T.W., Heidary N., Chang Y.-T., Orlow S. J., *Mol. Biosyst.*, (2005), **1**, 85-92
- [132] Hwang H., Jeon H., Ock J., Hong S.H., Han Y.M., Kwon B.M., Lee W.H., Lee M.S., Suk K., *J. Neuroimmunol.*, (2011), **230**, 52-64
- [133] Margarucci L., Monti M.C., Cassiano C., Mozzicafreddo M., Angeletti M., Riccio R., Tosco A., Casapullo A., *Chem. Commun. (Camb.)*, (2013), **49**, 5844-46
- [134] Kaida D., Motoyoshi H., Tashiro E., Nojima T., Hagiwara M., Ishigami K., Watanabe H., Kitahara T., Yoshida T., Nakajima H., Tani T., Horinouchi S., Yoshida M., *Nat. Chem. Biol.*, (2007), **3**, 576-83
- [135] Bantscheff M., Eberhard D., Abraham Y., Bastuck S., Boesche M., Hobson S., Mathieson T., Perrin J., Raida M., Rau C., Reader V., Sweetman G., Bauer A., Bouwmeester T., Hopf C., Kruse U., Neubauer G., Ramsden N., Rick J., Kuster B., Drewes G., *Nat. Biotechnol.*, (2007), **25**, 1035-44
- [136] Daub H., Olsen J.V., Bairlein M., Gnad F., Oppermann F.S., Körner R., Greff Z., Kéri G., Stemmann O., Mann M., *Mol. Cell*, (2008), **31**, 438-48
- [137] Newman D. J., Cragg G. M., *J. Nat. Prod.*, (2007), **70**, 461-77.
- [138] Folmer F., Jaspars M., Dicato M., Diederich M., *Biochem. Pharmacol.*, (2008), **75**, 603-17
- [139] Blunt J.W., Copp B.R., Hu W.P., Munro, Northcote P.T., Prinsep M.R., *Nat. Prod. Rep.*, (2009), **26**, 170-244.
- [140] Kimura J., Ishizuka E., Nakao Y., Yoshida W.Y., Scheuer P.J., Kelly-Borges M., *Nat. Prod.*, (1998), **61**, 248-50
- [141] De Marino S., Festa C., D'Auria M.V., Bourguet-Kondracki M.L., Petek S., Debitus C., Andrs R.M., Terencio M.C., Pay M., Zampella A., *Tetrahedron*, (2009), **65**, 2905-09.
- [142] Carr G., Raszek M., Van Soest R., Matainaho T., Shopik M.L., Holmes C.F.B., Andersen R.J.J., *Nat. Prod.*, (2007), **70**, 1812-15

- [143] Fu X., Ferreira M.L.G, Schmitz F. J., Kelly M.J., *Nat. Prod.*, (1999), **62**, 1190-91
- [144] a) D.S. Shin, T.H. Lee, H.S. Lee, J. Shin, K.B. Oh, *FEMS Microbiol. Lett.*, (2007), **272**, 43-7, b) Lee H.S., Lee T.H., Yang S.H., Shin H.J., Shin J., Oh K.B., *Bioorg. Med. Chem. Lett.*, (2007), **17**, 2483-86.
- [145] Loukaci A., Le Saout I., Samadi M., Leclerc S., Damiens E., Meijer L., Debitus C., Guyot M., *Bioorg. Med. Chem.*, (2001), **9**, 3049-54.
- [146] Shevchenko A., Tomas H., Havlis J., Olsen J. V, Mann M., *Nat. Protoc.*, (2006), **6**, 2856-60
- [147] Hartl F.U., *Nature*, (1996), **381**, 571-80
- [148] Becker J., Craig E.A., *Eur. J. Biochem.*, (1994), **219**, 11-23
- [149] Habich C., Burkart V., *Cell. Mol. Life Sci.*, (2007), **64**, 742-51
- [150] Chen W., Syldath U., Bellmann K., Burkart V., Kolb H., *J. Immunol.* (1999), **162**, 3212-19
- [151] Dadvar P., O'Flaherty M., Scholten A., Rumpel K., Heck A.J.R., *Mol.BioSyst.*, (2009), **5**, 472-82
- [152] Buchner J., Grallert H., Jakob U., *Methods Enzymol.*, (1998), **290**, 323-38
- [153] Buchner J., Schmidt M., Fuchs M., Jaenicke R., Rudolph R., Schmid F.X., Kiefhaber T., *Biochemistry*, (1991), **30**, 1586-91
- [154] Itoh H., Komatsuda K.A., Wakui H., Miura A.B., Tashima Y., *J. Biol. Chem.*, (1999), **274**, 35147-51
- [155] Nagumo Y., Kakeka H., Shoji M., Hayashi Y., Dohmae N., Osada H., *Biochem.J.*, (2005), **387**, 835-40
- [156] Ziegler S., Pries V., Hedberg C., Waldmann H., *Angew. Chem. Int. Ed.*, (2013), **52**, 2744-92
- [157] Kamel H.N., Kim Y.B., Rimoldi J.M., Fronczek F.R., Ferreira D., *J Nat Prod.*, (2009), **72**, 1492-6

Bibliography

- [158] Schumacher M., Cerella C., Eifes S., Chateauvieux S., Morceau F., Jaspars M., Dicato M., Diederich M., *Biochem. Pharm.*, (2010), **79**, 610-22
- [159] Ayala Y.M., Pantano S., D'Ambrogio A., Buratti E., Brindisi A., Marchetti C., Romano M., Baralle F.E., *J Mol Biol.*, (2005), **348**, 575-88
- [160] Ou S.H., Wu F., Harrich D., García-Martínez L.F., Gaynor R.B., *J Virol.*, (1995), **69**, 3584-96
- [161] Buratti E., Baralle F.E., *Front Biosci.*, (2008), **13**, 867-78
- [162] Buratti E., Baralle F.E., *J Biol Chem.*, (2001), **276**, 36337-43
- [163] Cohen T., Lee V.M., Trojanowski J.Q., *Trends Mol Med.*, **17**, 659-67
- [164] Sreedharan J., Blair I.P., Tripathi V.B., Hu X., Vance C., Rogelj B., Ackerley S., Durnall J.C., Williams K.L., Buratti E., Baralle F., de Bellerocche J., Mitchell J.D., Leigh P.N., Al-Chalabi A., Miller C.C., Nicholson G., Shaw C.E., *Science*, (2008), **319**, 1668-72
- [165] Guo W., Chen Y., Zhou X., Kar A., Ray P., Chen X., Rao E.J., Yang M., Ye H., Zhu L., Liu J., Xu M., Yang Y., Wang C., Zhang D., Bigio E.H., Mesulam M., Shen Y., Xu Q., Fushimi K., Wu J.Y., *Nat Struct Mol Biol.*, (2011), **18**, 822-30
- [166] Zhang X.L., Xu Y.F., Cook C., Gendron T.F., Roettges P., Link C.D., Lin W.L., Tong J., Castanedes-Casey M., Ash P., Gass J., Rangachari V., Buratti E., Baralle F., Golde T.E., Dickson D.W., Petrucelli L., *Proc. Natl. Acad. Sci. U.S.A.*, (2009), **106**, 7607-12
- [167] Caragounis A., Price K.A., Soon C.P., Filiz G., Masters C.L., Li Q.X., Crouch P.J., White A.R., *Free Radic Biol Med.*, (2010), **48**, 1152-61
- [168] Zhang H.X., Tanji K., Yoshida H., Hayakari M., Shibata T., Mori F., Uchida K., Wakabayashi K., *Exp Neurol.*, (2010), **222**, 296-303
- [169] Anderson P., Kedersha N., *Trends Biochem Sci.*, (2008), **33**, 141-50
- [170] Anderson P., Kedersha N., *Nat Rev Mol Cell Biol.*, (2009), **10**, 430-6

- [171] Liu-Yesucevitz L., Bilgutay A., Zhang Y.J., Vanderweyde T., Citro A., Mehta T., Zaarur N., McKee A., Bowser R., Sherman M., Petrucelli L., Wolozin B., *PLoS ONE*, (2010), **5**, e13250
- [172] Cohen T.J., Hwang A.W., Unger T., Trojanowski J.Q., Lee V.M., *The EMBO Journal* , (2012), **31**, 1241-52
- [173] Huang Y.C., Lin K.F., He R.Y., Tu P.H., Koubek J., Hsu Y.C., Huang J.J., *PLoS ONE*, (2013), **8**, e64002
- [174] Ou S.H., Wu F., Harrich D., García-Martínez L.F. , Gaynor R.B., *J Virol.*, (1995), **69**, 3584-96
- [175] Cassel J.A., Blass B.E., Reitz A.B., Pawlyk A.C., *J Biomol. Screen*, (2010), **15**, 1099-106
- [176] Neumann M., Sampathu D.M., Kwong L.K., Truax A.C., Micsenyi M.C, Chou T.T., Bruce J., Schuck T., Grossman M., Clark C.M., McCluskey L.F., Miller B.L., Masliah E Mackenzie., I.R., Feldman H., Feiden W., Kretzschmar H.A., Trojanowski J.Q., Lee V.M., *Science*, (2006), **314**, 130-3
- [177] Parker S.J., Meyerowitz J., James J.L., Liddell J.R., Crouch P.J., Kanninen K.M. , *Neurochem. Int.*, (2012), **60**, 415-24
- [178] van Eersel J., Ke Y.D., Gladbach A., Bi M., Götz J. , Kril J.J., Ittner L.M., *PLoS ONE*, (2011), **6**, e22850
- [179] Caragounis A., Price K.A., Soon C.P., Filiz G., Masters C.L., Li Q.X., Crouch P.J., White A.R., *Free Radic Biol Med.*, (2010), **48**, 1152-61
- [180] Speers A.E., Cravatt B.F., *Chem. Biol.*, (2004), **11**, 535-46
- [181] Zheng T., Jiang H., Wu P., *Bioconjug. Chem.* (2013), **24**, 859–64
- [182] Huisgen R., Padwa, A., ed. Wiley., (1984), **1**, 1-176
- [183] Kolb H.C., Finn M.G., Sharpless K.B., (2001), *Angew. Chem. Int. Ed.*, **40**, 2004-21
- [184] Cimino G., De Stefano S., Minale L., *Experientia*, (1974), **30**, 846-7

Bibliography

- [185] Cimino G., De Stefano S., Minale L., Trivellane E., *J. Chem. Soc. Perkin 1.*, (1977), **13**, 1587-93
- [186] Marshall L.A., Winkler J.D., Griswold D.E., Bolognese B., Roshak A., Sung C.M., Webb E.F., Jacobs R., *J. Pharmacol. Exp. Ther.*, (1994), **268**, 709-17.
- [187] De Stefano D., Tommonaro G., Malik S.A., Iodice C., De Rosa S., Maiuri M.C., Carnuccio R., *PLoS ONE*, (2012), **7**, e33031
- [188] Xie Y., Liu L., Huang X., Guo Y., Lou L., *J Pharmacol Exp Ther*, (2005), **314**, 1210-17
- [189] Monti M.C., Casapullo A., Riccio R., Gomez-Paloma L., *Rapid Commun Mass Spectrom*, (2005), **19**, 303-8
- [190] Margarucci L., Monti M.C., Chini M.G., Tosco A., Riccio R., Bifulco G., Casapullo A., *Chembiochem*, (2012), **13**, 2259-64
- [191] Ekkebus R., van Kasteren S.I., Kulathu Y., Scholten A., Berlin I., Geurink P., de Jong A., Goerdayal S., Neefjes J., Heck A.J.R., Komander D., Ovaa H., *J.Am.Chem.Soc.*, (2013), **135**, 2867-70
- [192] Banerjee S.S., Aher N., Patil R., Khandare J., *J Drug Deliv.*, (2012) **2012**, 103973-90
- [193] Beauchamp G.K., Keast R.S., Morel D., Lin J., Pika J., Han Q., Lee C.H., Smith A.B., Breslin P.A., *Nature*, (2005), **7055**, 45-6
- [194] Li W., Sperry J.B., Crowe A., Trojanowski J.Q., Smith A.B., Lee V.M., *J. Neurochem.*, (2009), **4**, 1339-51
- [195] Elnagar A.Y., Sylvester P.W., El Sayed K.A., *Planta Med.*, (2011), **10**, 1013-19
- [196] Daccache A., Lion C., Sibille N., Gerard M., Slomianny C., Lippens G., Cotelle P., *Neurochem. Int.*, (2011), **6**, 700-7
- [197] Monti M.C., Margarucci L., Tosco A., Riccio R., Casapullo A., *Food Funct.*, (2011), **2**, 423-28

- [198] Monti M.C., Margarucci L., Riccio R., Casapullo A., *J. Nat. Prod.*, (2012), **9**, 1584-88
- [199] Taylor S.S., Yang J., Wu J., Haste N.M., Radzio-Andzelm E., Anand G., *Biochim. Biophys. Acta*, (2004), **697**, 259-69
- [200] Hofmann F., *J. Biol. Chem.*, (2005), **280**, 1-4
- [201] Anderson T.R., *Mol. Cell. Endocrinol.*, (1982), **28**, 373-85
- [202] Bloch A., Dutschman G., Maue R., *Biochem. Biophys. Res. Commun.*, (1974), **59**, 955-59
- [203] Anderson T.R., *Mol. Cell. Endocrinol.*, (1982), **28**, 373-85
- [204] Cech S.Y., Ignarro L.J., *Science*, (1977), **198**, 1063-65
- [205] Gaion R.M., Krishna G., *Biochem. Biophys. Res. Commun.*, (1979), **86**, 105-11
- [206] Newton R.P., Salih S.G., Salvage B.J., Kingston E.E., *Biochem. J.*, (1984), **221**, 665-73
- [207] Newton R.P., Kingston E.E., Hakeem N.A., Salih S.G., Beynon J.H., Moyse C.D., *Biochem. J.*, (1986), **236**, 431-39
- [208] Burhenne H., Beste K.Y., Spangler C.M., Voigt U., Kaefer V., Seifert R., *N-S Arch Pharmacol*, (2011), **383**, 33
- [209] Desch M., Schinner E., Kees F., Hofmann F., Seifert R., Schlossmann, *FEBS Lett*, (2010), **584**, 3979-84
- [210] Zong X., Krause S., Chen C.C., Krüger J., Gruner C., Cao-Ehlker X., Fenske S., Wahl-Schott C., Biel M., *J. Biol. Chem.*, (2012), 287, 26506-12
- [211] Bond A.E., Dudley E., Tuytten R., Lemièrre F., Smith C.J., Esmans E.L., Newton R.P., *Rapid Commun. Mass Spectrom.*, (2007), 21, 2685-92.
- [212] Hammerschmidt A., Chatterji B., Zeiser J., Schröder A., Genieser H.G., Pich A., Kaefer V., Schwede F., Wolter S., Seifert R., *PLoS One*, (2012), **7**, e39848
- [213] Scholten A., Poh M.K., van Veen T.A., van Breukelen B., Vos M.A., Heck A.J., *J. Proteome Res.*, (2006), **5**, 1435-47
- [214] Margarucci L., Roest M., Preisinger C., Bleijerveld O.B., van Holten T.C., Heck A.J.R., Scholten A., *Mol. Biosyst.*, (2011), **7**, 2311-9

Bibliography

- [215] Aye T.T., Mohammed S., van den Toorn H.W., van Veen T.A., van der Heyden M.A., Scholten A., Heck A.J., *Mol. Cell Proteomics.*, (2009), **8**, 1016-28.
- [216] Cassiano C., Esposito R, Tosco A., Zampella A., D'Auria M.V., Riccio R., CasapulloA., Monti M.C, (2013), *Chem. Commun. (Camb.)*, **50**, 406-8
- [217] Kaiser E., Colescott R.L., Bossinger C.D, Cook P.I., *Anal. Biochem.* (1970), **34**, 595-8
- [218] Bradford M.M., *Anal. Biochem.*, (1976), **72**, 248-54
- [219] Mosmann T., *J. Immunol. Meth.*, (1983), **65**, 55-63

List of Abbreviations

4-AH-cCMP	N4-(6-Aminohexyl)cytidine-3',5'-cyclic monophosphate
1D/2D SDS PAGE	Sodium Dodecyl Sulphate - PolyAcrylamide Gel Electrophoresis
ABPP	Activity Based Protein Profile
ADP	Adenosine Diphosphate
ATP	Adenosine Triphosphate
ACN	Acetonitrile
AKAP	A-Kinase Anchoring Protein
cCMP	Cytidine-3',5'-cyclic monophosphate
CID	Collision Induced Dissociation
cAMP	Cyclic Adenosine Monophosphate
CDI	1,1'-carbonyldiimidazole
cGMP	Cyclic Guanosine Monophosphate
DMSO	Dimethyl Sulfoxide
ETD	Electron Transfer Dissociation
EDC	1-ethyl-3-(3-dimethylaminopropyl) carbodiimide
DTNB	5,5'-dithiobis-(2-nitrobenzoic acid)
GDP	Guanosine diphosphate
HCD	Higher-energy collisional dissociation
HPLC	High-performance liquid chromatography
HSP60	Heat ShockProtein 60
HSP70	Heat ShockProtein 70
HSP90	Heat ShockProtein 90
HET	Heteronemin
HuR	Hu-antigen R

List of Abbreviations

ICAT	Isotope Coated Affinity Tag
IC ₅₀	Half Maximal Inhibitory Concentration
iTRAQ	Isobaric Tag for Relative and Absolute Quantitation
ITC	Isothermal Titration Calorimetry
K _d	Dissociation Constant
K _a	Association Constant
LC-MS	Liquid Chromatography Coupled Mass Spectrometry
LC-MSMS	Liquid Chromatography Coupled Tandem Mass Spectrometry
LIT	Linear Ion Trap
Lys-C	Endoproteinase <i>Lys-C</i>
MS	Mass Spectrometry
MALDI	Matrix Assisted Laser Desorption Ionization
MTT	3-(4,5-Dimethylthiazol-2-yl)-2,5-diphenyltetrazolium bromid
NaBH ₄	Sodium Borohydride NO Nitric Oxide
NMR	Nuclear Magnetic Resonance
NHS	N-Hydroxysuccinimide
OLC	Olecanthal
OLC	Olecanthal azide
PEG	Poly-Ethylene Glycol
PINA	4-pentyn-1-amine
PKA	Protein Kinase A
PMF	Peptide Mass Fingerprint
PRX1	Peroxiredoxin 1

List of Abbreviations

PTM	Post Translational Modification
PKG	Protein Kinase G
PLA ₂	Phospholipase A ₂
PSMs	Peptide Spectral Matches
Q-Tof	Quadrupole-Time of Flight
RU	Response Units
RP-HPLC	Reverse Phase- High Performance Liquid Chromatography
SDS	Sodium Dodecyl Sulphate
SILAC	Stable Isotope Labeling with Aminoacids in Cell Culture
SLD	Scalaradial
SLD-Az	Scalaradial azide
SPR	Surface Plasmon Resonance
SUV	Suvanine
SUV-AL	Suvanine Aldehyde
TBTA	Tris-[(1-benzyl-1H-1,2,3-triazol-4- yl) methyl]amine
TDP 43	Tar-DNA-Binding Protein 43
TIOS	2-(2-amino-ethyl-disulfanyl)-ethyl-amine
TFA	Trifluoroacetic Acid
TRX-AZ	11-Azido-3,6,9-trioxaundecan-1-amine

Cassiano C., Margarucci M., Esposito R., Riccio R., Tosco A., Casapullo A., Monti M.C. “In cell Scalarial Interactome Profiling Using a Bio-Orthogonal Clickable Probe” *Submitted*

Cassiano C., Esposito R., Tosco A., Zampella A., D'Auria M.V., Riccio R., Casapullo A., Monti M.C. *Chem Commun (Camb)*, (2014), **50**, 406-8.

Margarucci L., Monti M.C., Cassiano C., Mozzicafreddo M., Angeletti M., Riccio R., Tosco A., Casapullo A., *Chem Commun (Camb)*, (2013) , **49**, 5844-6. May 24.

Cassiano C., Monti M.C., Festa C., Zampella A., Riccio R., Casapullo A., *Chembiochem*, (2012) **13**, 1953-8.

Margarucci L., Monti M.C., Mencarelli A, Cassiano C., Fiorucci S., Riccio R, Zampella A., Casapullo A., *Mol Biosyst.*, (2012), **8**, 1412-7.

Conference proceedings

Cassiano C., Monti M.C., Zampella A., Riccio R., Casapullo A., **Marine targetomics as a powerful tool in drug development**, 4th MS-J-DAY, Potenza (Italy) 14 November 2013

Margarucci L., Monti M.C., **Cassiano C.**, Riccio R., Casapullo A., **Marine drugs target discovery by chemical proteomics**, XXXIV Convegno della Divisione di Chimica Organica, Pavia (Italy), 10-14 September 2012

List of publications

Cassiano C., Monti M.C., Zampella A., Riccio R., Casapullo A., **Marine natural products target discovery by chemical proteomics**, Chemistry and Biology in Action, Salerno (Italy), 5-6 November 2012

Cassiano C., Monti M.C., Zampella A., Riccio R., Casapullo A., **Marine natural products target discovery by chemical proteomics**, IV Edizione della Scuola delle Sostanze Naturali e di Chimica Biorganica “Luigi Minale”, Naples (Italy), 5-9 June 2011